UNIVERSIDADE DE SÃO PAULO
FACULDADE DE FILOSOFIA, CIÊNCIAS E LETRAS DE RIBEIRÃO PRETO
PROGRAMA DE PÓS-GRADUAÇÃO EM BIOLOGIA COMPARADA

Tooth attachment in Silesauridae: understanding the ankylo-thecodont ontogenetic phase in the evolution of archosaur thecodonty

Fixação dentária em Silesauridae: entendendo a fase ontogenética "anquilo-tecodonte" na evolução da tecodontia de Arcossauros

Gabriel Mestriner da Silva

Dissertação apresentada à Faculdade de Filosofia, Ciências e Letras de Ribeirão Preto da Universidade de São Paulo, como parte das exigências para obtenção do título de Mestre em Ciências, obtido no Programa de Pós-Graduação em Biologia Comparada

Ribeirão Preto - SP

2020

UNIVERSIDADE DE SÃO PAULO
FACULDADE DE FILOSOFIA, CIÊNCIAS E LETRAS DE RIBEIRÃO PRETO
PROGRAMA DE PÓS-GRADUAÇÃO EM BIOLOGIA COMPARADA

Tooth attachment in Silesauridae: understanding the ankylo-thecodont ontogenetic phase in the evolution of archosaur thecodonty

Fixação dentária em Silesauridae: entendendo a fase ontogenética “anquilo-tecodonte” na evolução da tecodontia de Arcossauros

Gabriel Mestriner da Silva

Dissertação apresentada à Faculdade de Filosofia, Ciências e Letras de Ribeirão Preto da Universidade de São Paulo, como parte das exigências para obtenção do título de Mestre em Ciências, obtido no Programa de Pós-Graduação em Biologia Comparada.

Orientador: Prof. Dr. Max Cardoso Langer

Ribeirão Preto - SP

2020

FICHA CATALOGRÁFICA

Mestriner, Gabriel

Tooth attachment in Silesauridae: understanding the ankylo-thecodont ontogenetic phase in the evolution of archosaur thecodonty, 2020.

92 páginas

Dissertação de Mestrado, apresentada à Faculdade de Filosofia, Ciências e Letras de Ribeirão Preto/USP. Área de concentração: Biologia Comparada.

Orientador: Langer, Max Cardoso.

1. Tooth attachment. 2. Tooth implantation. 3. Silesauridae. 4. Archosauria. 5. Dental histology.

Acknowledgements

First, I wish to show my gratitude to my supervisor Max Langer. Thank you for proportionating such a friendly and productive environment to work, and for always doing more than the expected of a supervisor. I am also very grateful for all the field works you gave me the opportunity to participate, as well the visits to scientific collections.

I want to thank my co-supervisor and friend Julio Marsola, for all the guidance and support that he always provided me. Thank you for improving so much the dissertation, and contributing on my background as a paleontologist and researcher.

Thanks to Sterling Nesbitt for supervising me on my BEPE, and for the support during the six months that I Spent in USA.

To Aaron Leblanc for having me at University of Alberta, and for everything he taught me about dental histology. Also, thanks for proportionating a great Canadian experience during the three weeks I spent in Edmonton. And cheers for Oilers!!

To Átila Da Rosa, for providing me materials for my research and for all his contributions with this work.

To Ana Maria Ribeiro and Jorge Ferigolo for providing such important specimen for the histologic work, and for having me in "Fundação zoobotânica" when I needed to study the dinosaur's collection.

Thanks to The São Paulo Research Foundation (FAPESP) for the financial support through the following grants: Master (2018/24031-6) and Research Internships Abroad (BEPE) (2019/07510-0).

To the Program of Comparative Biology, Faculdade de Filosofia, Ciências e Letras de Ribeirão Preto.

Thanks to Vera Cassia Cicilini de Lucca for always being so considerate, patient, and for all assistance in resolving bureaucratic situations.

To Elisabete Dassie, for all her assistance with bureaucratic issues related to FAPESP documents.

I want to thank researchers, collection managers, and curators who provided access to the collections under their care, namely: André Silveira (Universidade Federal do Rio Grande do Sul, RS), Cecilia Apaldetti (Universidad Nacional de San Juan, Argentina), César Schultz (Universidade Federal do Rio Grande do Sul, RS), Claudio Revuelta (Universidad Nacional de la Rioja, Argentina), Fernando Abdala (Instituto Miguel Lillo, Argentina), Fernando Novas (Museo Argentino de Ciencias Naturales Bernardino Rivadavia, Argentina), Flávio Pretto (Universidade Federal de Santa Maria, RS), Gabriela Cisterna (Universidad Nacional de La Rioja, Argentina), Leonardo Haerter (Universidade Luterana do Brasil, RS), Leonardo Kerber (Centro de Apoio à Pesquisa Paleontológica da Quarta Colônia, RS), Martín Ezcurra (Museo Argentino de Ciencias Naturales Bernardino Rivadavia, Argentina), Michael Caldwell (University of Alberta, Canada), Michelle Stocker (Virginia

Polytechnic Institute and State University, EUA), Pablo Ortíz (Instituto Miguel Lillo, Argentina), Pedro Hernández (Universidade Luterana do Brasil, RS), Rodrigo Müller (Centro de Apoio à Pesquisa Paleontológica da Quarta Colônia, RS), Ricardo Martínez (Instituto y Museo de Ciencias Naturales de la Universidad Nacional de San Juan, Argentina), Sergio Cabreira (Universidade Luterana do Brasil, RS) and Vicki Yarborough (Virginia Polytechnic Institute and State University, EUA).

I am grateful to the cleaning staff of the Biology Department building where the USP Paleontology laboratory in Ribeirão Preto is located. Thanks for always providing a clean and organized work environment.

Thanks also to Gabriel Baréa for suggestions and improvement in the edition of the pictures, and Ben Kligman, for sharing experiences and helping with the 3D printer at Virginia Tech.

I could not fail to my lovable lab friends, who have always helped me in the most diverse ways throughout the master's degree: Ana Laura Paiva, Bruna Farina, Fellipe Muniz, Gabriel Ferreira (Fumaça), Guilherme Hermanson (Squirtle), Giovanne Cidade (Gigio), Gustavo Darlim, Julian Gonçalves, Mario Bronzati (Roque), Paulo Ricardo, Sílvio Onari (Oncinha); Thiago Fachini (Schumi), Wafa Alhalabi. Thank you guys for all the daily conversations, laughs and good moments. A special thanks to Francisco Neto (Xico), for staying by my side in the most difficult moments, and João Pedro Kirmse, for the partnership in visiting the collections in Rio Grande do Sul and Argentina, providing these trips with a much more enjoyable experience.

I also would like to express my thanks to my girlfriend Luana Liaw (Lulu). Thank you for all the encouragement, support and motivation you gave me during the final stage of my master's.

I wish to acknowledge the constant love, support and encouragement of my family: Andressa Zaccaro, Daniel Felix, Dulce Mestriner, Gilberto Mestriner, José Mário Mestriner, Manoelina da Silva, Marcela Granzote e Nelson Barbosa.

Finally, and most importantly, I want to thank my mom Fernanda Mestriner. Thank you for the unconditional support in all the difficult moments of my academic trajectory. This work would not have been possible without your input.

Dedication

In memory of my grandfather Miguel Alexandre Signori (Vô Miguel), with all love and gratitude for everything he has done for me throughout my life. I wish I can come to be worthy of the effort dedicated by you in all aspects.

Resumo

Gabriel, M. **Fixação dentária em Silesauridae: entendendo a fase ontogenética "anquilo-tecodonte" na evolução da tecodontia de Arcossauros. 2020. 92p.** Dissertação (Mestrado) – Faculdade de Filosofia, Ciências e Letras de Ribeirão Preto, Universidade de São Paulo, Ribeirão Preto, 2020.

Contrária a tradicional visão, em que a dentição anquilo-tecodonte é recuperada como um traço sinapomórfico de Silesauridae, novos dados histológicos mostram que essa condição meramente representa o último estágio de desenvolvimento dos dentes no grupo. Esses dinossauromorfos não possuem nem a "gonfose permanente" de crocodilos/dinossauros, tampouco a "rápida anquilose" plesiomórfica para amniotas. Ao invés disso, todos os silessaurídeos amostrados mostram "anquilose atrasada", condição na qual os dentes passam por um estágio inicial de gonfose, seguido por uma anquilose final. Isso sugere que, como já documentado para sinápsidas, a fixação dentária em Archosauria pode ter seguido um padrão evolutivo pedomórfico, com a gonfose de crocodilos/dinossauros representando a manutenção de um estágio ontogenético inicial em que o osso alveolar não calcifica o ligamento periodontal entre a raiz do dente e o alvéolo. A "anquilose atrasada" de Silesauridae resulta na aceitação da "gonfose permanente" de dinossauros e crocodilos como convergentemente adquirida, ou, menos provável, que a condição de silessaurídeos represente uma reversão sinapomórfica. Além disso, se Silesauridae for agrupado dentro de Ornitischia, a "gonfose permanente" poderia até mesmo ser convergente entre as duas principais linhagens de dinossauros. Em todo o caso, a transição em um único passo, de uma dentição anquilo-tecodonte para uma tecodonte, parece cada vez mais como uma simplificação de uma história evolutiva muito mais complexa. De fato, características envolvendo fixação dentária devem ser avaliadas com maior detalhe

quando codificadas em estudos filogenéticos de arcossauros. Um importante aspecto emergente está relacionado com o fato da gonfose ser possivelmente sinapomórfica para dinossauros, e como tal, uma característica-chave que pode ter auxiliado no domínio deste grupo na Terra ao longo de 150 milhões de anos.

Abstract

Gabriel, M. **Tooth attachment in Silesauridae: understanding the ankylo-thecodont ontogenetic phase in the evolution of archosaur thecodonty**. 2020. 92p. Dissertation (Master) – Faculdade de Filosofia, Ciências e Letras de Ribeirão Preto, Universidade de São Paulo, Ribeirão Preto, 2020.

Contrary to the traditional view in which ankylo-thecodonty is recovered as a synapomorphic trait of Silesauridae, new histological data show that it merely represents the last stage of tooth development within the group. Those dinosauromorphs have neither the crocodilian/dinosaur "permanent gomphosis" nor the "rapid ankylosis" that is plesiomorphic for amniotes. Instead, all sampled silesaurids show "delayed ankylosis", a condition in which teeth pass through an initial gomphosis stage followed by final ankylosis. This suggests that, as already documented for synapsids, tooth fixation in Archosauria might have followed a paedomorphic evolutionary pattern, with the crocodile/dinosaur gomphosis representing the maintenance of an early ontogenetic stage, in which the alveolar bone does not calcify the periodontal ligament between the tooth root and the alveolus. "Delayed ankylosis" in Silesauridae results in accepting the dinosaur and crocodile "permanent gomphosis" as convergently acquired or, less likely, that the silesaurid condition represents a synapomorphic reversal. Moreover, if Silesauridae is nested within Ornitischia, "permanent gomphosis" could even be convergent between the two main dinosaurs lineages. In any case, a ankylo-thecodonty to thecodonty one-step transition appears even more as the oversimplification of a much more complex evolutionary history. In fact, characteristics involving tooth attachment must be evaluated in more detail when they are codified in archosaur phylogenies. An important emerging aspect of gomphosis as synapomorphic for dinosaurs, is that it may represent one of the key features that allowed their thriving on Earth for more than 150 million years.

Summary

1. GENERAL CONTEXTUALIZATION OF THE THEME 1

1.1 Origin of dinosaurs **1**

1.2 Silesauridae **2**

1.3 Evolutionary implications of tooth attachment in Silesauridae **4**

2. GENERAL STRUCTURE OF THE DISSERTATION 7

3. GOALS 7

4. CONCLUSIONS 8

5. REFERENCES 9

ANNEX 15

Tooth attachment in Silesauridae: understanding the ankylo-thecodont ontogenetic phase in the evolution of archosaur thecodonty 16

Introduction **18**

Institutional abbreviations **21**

Material and Methods **21**

Material **21**

Methods: **21**

Results 23

Eucoelophysis baldwini **23**

Osteohistology: **23**

Santa Maria Formation silesaurid – UFSM 1579 ..... **26**

Osteohistology: **27**

Sacisaurus agudoensis **31**

Osteohistology: **31**

Asilisaurus kongwe **32**

Osteohistolgy: **33**

Discussion 34

Evolutionary implication of the tooth attachment system in Silesauridae **39**

Conclusion 41

Acknowledgements **42**

References **43**

Table 1. ..... **47**

Figures 48

SUPPLEMENTARY ONLINE MATERIAL 71

1. GENERAL CONTEXTUALIZATION OF THE THEME

1.1 Origin of dinosaurs

Dinosaurs, which would become the dominant Mesozoic megafauna, arose in the late Triassic period (Langer et al., 2010). Further than their well-supported origin in southern Gondwana (Marsola et al., 2018), questions pervade the relationships of various early forms (Langer, 2014). In addition, a recently resurfaced hypothesis of dinosaur relationships contradicts the traditionally agreed upon topology of Ornitischia as sister-group to Saurischia (Baron et al., 2017). Even though the traditional scheme (Seeley 1888) was soon recovered in a reply (Langer et al., 2017), it shows that controversy still persists on the minutiae of dinosaur origins.

Few aspects of early dinosaur relationships are known for sure (Langer, 2014). The issue of which morphological traits characterize the group continues to be discussed (Novas, 1996; Langer & Benton, 2006; Sereno, 2007b; Langer, 2014). Much of what was considered synapomorphic to dinosaurs has been the target of criticisms with the discovery related forms. Dinosauromorpha was coined by Benton (1985) to include Ornitosuchids, dinosaurs and birds (Sereno, 1991; Langer et al., 2013). Currently, the group is understood as including *Lagerpeton chanarensis*, *Lagosuchus talampayensis*, *Lewisuchus admixtus*, Dinosauria, and all descendants of their most recent common ancestor (Sereno, 1991; Langer et al., 2013). Dinosauriformes was proposed by Novas (1992) to represent a less-inclusive group within Dinosauromorpha, starting with the most recent common ancestor of *Lagosuchus talampayensis* (sensu Agnolìn & Ezcurra, 2019) and Dinosauria (Sereno & Arcucci ,1994).

Those non-dinosaur Dinosauromorpha are key point to define the dinosaurian diagnostic traits (Langer, 2014), as various previously-considered dinosaur apomorphies

now also known in non-dinosaurian forms (Langer & Benton, 2006). For example, the increase of the number of sacral vertebrae, the dorsally expanded cranial margin of the first primordial sacral rib, the ischium with the presence of a reduced medioventral lamina and with a proximal dorsolateral sulcus, are features presents in dinosaurs that were once thought as diagnostic for them, but later found in forms outside of Dinosauria (Novas, 1996; Langer & Benton 2006; Yates, 2007; Langer et al., 2010).

Therefore, it is clear that a clearer definition of the dinosaurian sister-groups is pivotal to shed light on the morphology and adaptations of all major subgroups of Dinosauria (Benton, et al., 2014), as well on their origin and irradiation.

1.2 Silesauridae

Silesauridae is a clade coined and phylogenetically defined by Langer et al. (2010) as the group of archosaurs more related to *Silesaurus opolensis* Dzik, 2003 than to *Lagosuchus talampayensis* Romer, 1971, and *Heterodontosaurus tucki* Crompton & Charig, 1962. Forms in this group include *Ignotosaurus fragilis* Martínez et al., 2012, *Diodorus scytobrachion* Kammerer & Nesbitt, 2011, *Sacisaurus agudoensis* Ferigolo & Langer, 2007, *Silesaurus opolensis* Dzik, 2003, *Eucoelophysis baldwini* Sullivan & Lucas, 1999, *Asilisaurus kongwe* Nesbitt et al., 2010, *Lutungutali sitwensis* Peecook et al., 2013, *Pisanosaurus mertii* Casamiquela, 1967, *Kwanasaurus williamparkeri* Martz & Small, 2019), and possibly *Lewisuchus admixtus* Romer, 1972.

According to Nesbitt et al. (2010), the diagnosis of Silesauridae include the joint presence of the following unique combination of characters: rugose ridge on the anterolateral edges of the supraocciptal; notch ventral to femoral head; straight transverse groove on the proximal surface of the femur; and ilium with a straight ventral emargination of the acetabulum (see Langer et al., 2013). Furthermore, all silesaurids

with more complete preservation have an elongation of the neck and forearms (Nesbit *et al*., 2010), which suggest at least facultative quadrupedality (Langer, 2014).

The phylogenetic relationship of silesaurids among Dinosauriformes is, however, still controversial. Usually considered as the sister-group of Dinosauria (Benton & Walker 2011; Langer et al., 2010; Nesbitt, 2011; Bittencourt et al., 2015; Baron et al., 2017; Langer et al., 2017; Nesbitt et al., 2017), but also recovered as paraphyletic and/or in the ornithischian lineage (Ferigolo & Langer, 2007; Langer & Ferigolo, 2013; Cabreira et al., 2016; Müller & Garcia, 2020). In fact, the shape of silesaurid teeth (sub-triangular crowns, with a constricted root) and its peculiar toothless lower jaw tip, which was probably covered by a keratinous "beak", forms the basis of their proposed affinity to ornithischians, which also bears that toothless beak, formed by a predentary bone (Langer, 2014). Although showing these similarities in general shape (Ferigolo & Langer 2007), the homology of both structures has been contested, mainly because the silesaurid beack is formed by a pair of bones that are not fully detached from the dentary (Langer, 2014), unlike the ornithischian predentary, which is single separated from the dentary (Ferigolo & Langer, 2007).

Phylogenetic studies frequently score putative dinosaurs synapomorphies as absent in Silesaurids (Ezcurra 2006; Langer & Benton 2006; Irmis et al., 2007; Brusatte et al., 2010; Nesbitt et al., 2010; Nesbitt, 2011). These include an expanded upper temporal fossa, epipophyses on proximal cervical vertebrae, and an asymmetrical fourth trochanter (Langer, 2014). The internal relationships of silesaurids also remain uncertain as well as the inclusiveness of the group (Agnolín & Rozadilla, 2018). *Asilisaurus kongwe*, *Lewisuchus admixtus*, and *Eucoelophysis baldwini* are nested out of the group in some phylogenetics analyses (Langer et al., 2017). In other hypothesis, *Eucoelophysis*

baldwini is recovered as sister group of all silesaurids, whereas *Asilisaurus kongwe* and *Lewisuchus admixtus* are nested out of Silesauridae (Bittencourt et al. 2015).

Therefore, the position of silesaurids among Dinosauriformes is an important aspect to be taken into account when assessing the early evolution of dinosaurs. As an example, the status of putative apomorphies of dinosaur skull is dependent on the position of Silesauridae. If silesaurids are not considered dinosaurs, some of its cranial traits (e.g., frontal participating in the supratemporal fossa), are disregarded as dinosaur apomorphies (Langer et al. 2010). If the position of Silesauridae as an early ornithischian is accepted, on the other hand, that trait continues potentially representing a dinosaur synapomorphy. In fact, a best understanding of morphological traits of Silesauridae and a refined analysis of their potential synapomorphies could clarify its internal relationships and, consequently, further define their position among Dinosauriformes.

1.3 Evolutionary implications of tooth attachment in Silesauridae

Tooth attachment and implantation are important characters used for interpreting phylogenetic relations and dietary preference among vertebrates (LeBlanc et al.,2017). Whereas tooth implantation categorizes teeth by their spatial relationships in the jaws, tooth attachment distinguishes those that are completely fused to the jaw, i.e., ankylosis type of fixation, from those anchored by a periodontal ligament, i.e., gomphosis type of fixation (LeBlanc & Reisz, 2013; LeBlanc et al., 2017; LeBlanc et al., 2018). In general, three types of implantation are recognized: acrodonty, pleurodonty, and thecodonty. Acrodonty occurs when the teeth are attached at their bases to the apices of the jaws, pleurodonty when the teeth are attached at their bases and to a single wall of the jaw, and the latter when the teeth are set into deep sockets in the jaw (LeBlanc & Reisz, 2013; LeBlanc et al., 2017).

The tooth root is coated in cementum, providing an attachment site for the periodontal ligament. The periodontal ligament is anchored to the alveolar bone that forms the tooth socket, and the cementum layers can be acellular or cellular, providing sites of attachment for periodontal ligament fibers, known as Sharpey's fibers (LeBlanc & Reisz, 2013, Fong et al., 2016). Among extant amniotes, only mammals and crocodilians are considered truly thecodont, because they possess those complex histological properties. However, a remarkably conservative evolutionary history across Amniota has been shown for this trait (LeBlanc et al., 2017), with the tooth attachment tissues (involving the presence of alveolar bone, periodontal ligament, and acellular and cellular cement) being histologically and developmentally identical across early synapsids (LeBlanc et al., 2016), mammals (LeBlanc et al., 2018), crocodilians (LeBlanc et al., 2017), non-avian dinosaurs (LeBlanc et al., 2016a), toothed birds (Dumont et al., 2016), and other eureptiles (Caldwell, 2003; Maxwell et al., 2011; LeBlanc & Reisz, 2013). In this way, current consensus considers the three tooth attachment tissues (i.e., cellular cementum, alveolar bone, and periodontal ligament) as symplesiomorphic for the major amniote clades (Caldwell et al., 2003; Budney et al., 2006; Maxwell et al., 2011; LeBlanc and Reisz., 2013; Sassoon et al., 2015; García and Zurriaguz, 2016; LeBlanc et al., 2017; LeBlanc et al., 2018).

Similarity and phylogenetic congruence in the presence of these types of tooth attachment tissues across amniote groups strongly support the hypothesis that this system is plesiomorphic for Dinosauria (Fong et al., 2016; García and Zurriaguz, 2016; LeBlanc et al., 2016; LeBlanc et al., 2017). In the last few years, a lot of works involving tooth development, histology and enamel microstructure in Dinosaurs have been performed. This has clarified the implications for dental evolution in diverse groups, including the non-Iguanodontia ornithopod *Changchunsaurus* (Chen et al., 2018), the hadrosaurids *Hypacrosaurus*, *Corythosaurus*, and *Prosaurolophus* (LeBlanc et al., 2016, LeBlanc et

al., 2017), the ceratopsid *Triceratops* (LeBlanc et al., 2017), the esrly theropod *Coelophysis* (Hwang, 2005; Fong et al., 2016), the tyrannosaurids *Albertosaurus* (Hwang, 2005) and *Gorgosaurus,* among others.

In extreme cases, the alveolar bone and the cementum might be so extensive that they completely enclose the periodontal ligament, forming a dental ankylosis where the tooth is fused to the jaw. This so-called ankylo-thecodont tooth attachment configuration encompasses all the plesiomorphic tissues found in amniotes (cementum, alveolar bone, and periodontal ligament), but the periodontal ligament is completely calcified (Caldwell et al., 2003; Maxwell et al., 2011; LeBlanc & Reisz, 2013; Fong et al., 2016; LeBlanc et al, 2017; LeBlanc et al., 2018). New discoveries have suggested that the ankylo-thecodont condition is retained in many archosauromorphs groups (e.g., rhynchosaurs, *Prolacerta*, *Proterosuchus*, *Sarmatosuchus*) including Silesauridae (Modesto & Sues, 2004; Ferigolo & Langer 2007; Nesbitt et al., 2010; Nesbitt, 2011; Kammerer et al., 2011; Langer et al., 2013; Ezcurra, 2016; Ezcurra et al., 2019; Martz & Small, 2019). Indeed. an ankylo-thecodonty dentition has been suggested as synapomorphic for Silesauridae (character 174 of Nesbitt, 2011; Ferigolo & Langer 2007; Nesbitt et al., 2010; Nesbitt, 2011; Kammerer et al., 2011; Langer et al., 2013; Ezcurra, 2016; Ezcurra et al., 2019; Martz & Small., 2019; Nesbitt et al., 2019), supporting the nesting *Silesaurus opolensis*, *Sacisaurus agudoensis*, *Asilisaurus kongwe*, the Hayden Quarry specimens (Nesbitt et al., 2010; Nesbitt, 2011), *Eucoelophysis baldwini*, and *Lewisuchus admixtus* (Ezcurra et al., 2020) within a monophyletic Silesauridae (Benton & Walker 2011; Langer et al., 2010; Nesbitt, 2011; Bittencourt et al., 2015; Baron et al., 2017; Langer et al., 2017; Nesbitt et al., 2017).

In this sense, although a lot of information regarding tooth attachment in non-dinosaur Dinosauromorpha entered the literature, this was actually never evaluated on the basis of osteohystological studies.

2. GENERAL STRUCTURE OF THE DISSERTATION

This document is integrated by an annex that corresponds to the development of the goals of the dissertation presented below. This annex is presented in article format, according to the rules of the scientific journal "The Anatomical Record", to which the paper is being submitted. Preceding the annex, the general conclusions of the Master Dissertation are presented, whereas more specific points, such as discussion and methodology, integrate the body of the annex.

3. GOALS

Four central goals justified this study:

(1) assess tooth attachment in Silesauridae, providing a comprehensive characterization of the so-called ankylo-thecodont dentition, based on data from different species.

(2) describe the histological properties of the tissues that attach the teeth to the jaw in silesaurids, assessing the Silesauridae homologues of cementum, alveolar bone, and periodontal ligament.

(3) more clearly differentiate Silesauridae ankylo-thecodonty from the dinosaur/crocodile gomphosis.

(4) evaluate the evolutionary implications of the Silesauridae tooth attachment for the diversification of the dinosaur line of archosaurs.

4. CONCLUSIONS

From the annex work, the main conclusions of this dissertation are:

1. The tooth attachment pattern identified for silesaurids challenges the traditional view in which an “ankylo-thecodont” dentition is regarded as synapomorphic for the group. In fact, the four different phases of a standard sequence of dental ontogeny were identified for the sampled species: eruption, gomphosis, “mineralization”, and ankylosis. As such, our data show that ankylo-thecodonty represents just the last stage of their tooth ontogeny, in which teeth pass through a gomphosis stage followed by final ankylosis.

2. The simple mapping of “ankylosis” and “gomphosis” as alternative states is too simplistic to reconstruct ancestral characters for Dinosauromorpha across phylogenies, because silesaurids, and potentially other unsampled groups, can exhibit both stages in the same taxon/individual/jaw. In this way, Silesauridae has neither the crocodilian/dinosaur “permanent gomphosis” nor the “rapid ankylosis” that is plesiomorphic for amniotes.

3. Differences between silesaurid ankylosis and dinosaur/crocodile gomphosis cannot be associated to increasing teeth complexity, but to differences on time and sequence of dental ontogeny (heterochronic events). Therefore, crocodile/dinosaur gomphosis represents the maintenance of an early ontogenetic stage, in which alveolar bone does not calcify the periodontal ligament between the tooth root and the adjacent alveolus, whereas Silesauridae presents a delay on the alveolar bone calcification of the periodontal ligament (delayed ankylosis).

4. An ankylo-thecodonty to thecodonty transition appears as an oversimplification of a more complex evolutionary history, and features involving tooth attachment must be evaluated accurately when these are codified through archosaur phylogenetic datasets.

5. REFERENCES

Agnolin FL, Ezcurra MD. (2019). The validity of Lagosuchus talampayensis Romer, 1971 (Archosauria, Dinosauriformes), from the late triassic of Argentina. Breviora, 565(1), 1-21.

Agnolín FL, Rozadilla S. 2018. Phylogenetic reassessment of Pisanosaurus mertii Casamiquela, 1967, a basal dinosauriform from the Late Triassic of Argentina. Journal of Systematic Palaeontology, 16(10), 853-879.

Baron MG, Norman DB, Barrett PM. 2017. A new hypothesis of dinosaur relationships and early dinosaur evolution. Nature, 543(7646), 501-506.

Benton MJ, Walker AD. 1985. Palaeoecology, taphonomy, and dating of Permo-Triassic reptiles from Elgin. Palaeontology, 28(Part 2), 207-234.

Benton MJ, Walker AD. 2011. Saltopus, a dinosauriform from the Upper Triassic of Scotland. Earth and Environmental Science Transactions of the Royal Society of Edinburgh, 101(3-4), 285-299.

Benton, MJ, Forth J, Langer MC. 2014. Models for the rise of the dinosaurs. Current Biology, 24(2), R87-R95.

Bittencourt JS, Arcucci AB, Marsicano CA, Langer MC. 2015. Osteology of the Middle Triassic archosaur Lewisuchus admixtus Romer (Chañares Formation, Argentina), its inclusivity, and relationships amongst early dinosauromorphs. Journal of Systematic Palaeontology, 13(3), 189-219.

Brusatte SL, Nesbitt SJ, Irmis RB, Butler RJ, Benton MJ, Norell MA. 2010. The origin and early radiation of dinosaurs. Earth-Science Reviews, 101(1-2), 68-100.

Budney L. A., M. W. Caldwell, and A. Albino. 2006. Tooth socket histology in the Cretaceous snake Dinilysia, with a review of amniote dental attachment tissues. Journal of Vertebrate Paleontology 26:138–145.

Cabreira SF, Kellner AWA, Dias-da-Silva S, da Silva LR, Bronzati M, Marsola JC, Müller RT, Bittencourt JS, Batista BJ, Raugust T, Carrilho, R, Brodt A. 2016. A unique Late Triassic dinosauromorph assemblage reveals dinosaur ancestral anatomy and diet. Current Biology, 26(22), 3090-3095.

Caldwell MW, Budney LA, Lamoureux DO. 2003. Histology of tooth attachment tissues in the Late Cretaceous mosasaurid Platecarpus. Journal of Vertebrate Paleontology 23:622–630.

Casamiquela RM. 1967. Un Nuevo dinosaurio ornitisquio triasico (Pisanosaurus mertii; Ornithopoda) de la formacion Ischigualasto, Argentina. Ameghiniana, v. 5, n. 2, p. 47-64, 1967

Chen J, LeBlanc ARH, Jin L, Huang T, Reisz RR. 2018. Tooth development, histology, and enamel microstructure in Changchunsaurus parvus: Implications for dental evolution in ornithopod dinosaurs. PLoS ONE 13(11): e0205206.

Crompton, AW, Charig AJ. 1962. A new ornithischian from the Upper Triassic of South Africa. Nature, 196(4859), 1074-1077.

Dumont M, Tafforeau P, Bertin T, Bhullar BA, Field D, Schulp A, Louchart A. (2016). Synchrotron imaging of dentition provides insights into the biology of Hesperornis and Ichthyornis, the “last” toothed birds. BMC evolutionary biology, 16(1), 178. Dzik, J. (2003).

Dzik J. 2003. A beaked herbivorous archosaur with dinosaur affinities from the early Late Triassic of Poland. Journal of Vertebrate Paleontology, 23(3), 556-574.

Ezcurra MD. 2006. A review of the systematic position of the dinosauriform archosaur Eucoelophysis baldwini Sullivan & Lucas, 1999 from the Upper Triassic of New Mexico, USA. Geodiversitas, 28(4), 649-684.

Ezcurra MD. 2016. The phylogenetic relationships of basal archosauromorphs, with an emphasis on the systematics of proterosuchian archosauriforms. PeerJ, 4, e1778.

Ezcurra MD., Nesbitt SJ, Fiorelli LE, Desojo JB. 2019. New specimen sheds light on the anatomy and taxonomy of the early Late Triassic dinosauriforms from the Chañares Formation, NW Argentina. The Anatomical Record, 303(5), 1393-1438.

Ezcurra MD, Nesbitt SJ, Fiorelli LE, Desojo JB. 2020. New specimen sheds light on the anatomy and taxonomy of the early Late Triassic dinosauriforms from the Chañares Formation, NW Argentina. The Anatomical Record, 303(5), 1393-1438.

Ferigolo J, Langer MC. 2007. A Late Triassic dinosauriform from south Brazil and the origin of the ornithischian predentary bone. Historical Biology, 19(1), 23-33.

Fong RK, LeBlanc ARH, Berman DS, Reisz RR. 2016. Dental histology of Coelophysis bauri and the evolution of tooth attachment tissues in early dinosaurs: dinosaur dental histology. Journal of Morphology 277:916–924.

García RA, Zurriaguz V. 2016. Histology of teeth and tooth attachment in titanosaurs (Dinosauria; Sauropoda). Cretaceous Research, 57, 248-256.

Hwang SH. 2005. Phylogenetic patterns of enamel microstructure in dinosaur teeth. Journal of Morphology, 266(2), 208-240.

Irmis RB, Nesbitt SJ, Padian K, Smith ND, Turner AH, Woody D, Downs A. 2007. A Late Triassic dinosauromorph assemblage from New Mexico and the rise of dinosaurs. Science, 317(5836), 358-361.

Langer MC, Benton MJ. 2006. Early dinosaurs: a phylogenetic study. Journal of Systematic Palaeontology, 4(4), 309-358

Langer MC, Ezcurra MD, Bittencourt JS, Novas FE. 2010. The origin and early evolution of dinosaurs. Biological Reviews, 85(1), 55-110.

Langer MC, Ferigolo J. 2013. The Late Triassic dinosauromorph *Sacisaurus agudoensis* (Caturrita Formation; Rio Grande do Sul, Brazil): anatomy and affinities. Geological Society, London, Special Publications, 379(1), 353-392.

Langer MC, Nesbitt SJ, Bittencourt JS, Irmis RB. 2013. Non-dinosaurian dinosauromorpha. Geological Society, London, Special Publications, 379(1), 157-186.

Langer MC. 2014. The origins of Dinosauria: much ado about nothing. Palaeontology, 57(3), 469-478.

Langer MC, Ezcurra MD, Rauhut OW, Benton MJ, Knoll F, McPhee BW, Novas FE., Pol D, Brusatte SL. 2017. Untangling the dinosaur family tree. Nature, 551(7678), E1-E3.

LeBlanc ARH, Reisz RR. 2013. Periodontal ligament, cementum, and alveolar bone in the oldest herbivorous tetrapods, and their evolutionary significance. PLoS ONE 8:e74697.

LeBlanc ARH, Reisz RR, Brink KS, Abdala F. 2016. Mineralized periodontia in extinct relatives of mammals shed light on the evolutionary history of mineral homeostasis in periodontal tissue maintenance. Journal of Clinical Periodontology 4.

LeBlanc ARH, Brink KS, Cullen TM, Reisz RR. 2017. Evolutionary implications of tooth attachment versus tooth implantation: a case study using dinosaur, crocodilian, and mammal teeth. J. Vertebr. Paleontol. 37, e1354006.

LeBlanc ARH, Brink KS, Whitney MR, Abdala F, Reisz RR. 2018. Dental ontogeny in extinct synapsids reveals a complex evolutionary history of the mammalian tooth attachment system. Proc. R. Soc. B 285: 20181792.

Kammerer CF, Nesbitt SJ, Shubin NH. 2011. The first silesaurid dinosauriform from the Late Triassic of Morocco. Acta Palaeontologica Polonica, 57(2), 277-284.

Marsola JC, Ferreira GS, Langer MC, Button D J, Butler RJ. 2018. Increases in sampling support the southern Gondwanan hypothesis for the origin of dinosaurs. Palaeontology, 62(3), 473-482.

Martínez RN, Apaldetti C, Alcober OA, Colombi CE, Sereno PC, Fernandez E, Malnis PS, Correa GA, Abelin D. 2012. Vertebrate succession in the Ischigualasto Formation. Journal of Vertebrate Paleontology, 32(sup1), 10-30.

Martz JW, Small BJ. 2019. Non-dinosaurian dinosauromorphs from the Chinle Formation (Upper Triassic) of the Eagle Basin, northern Colorado: Dromomeron romeri (Lagerpetidae) and a new taxon, Kwanasaurus williamparkeri (Silesauridae). PeerJ, 7, e7551.

Maxwell, EE, Caldwell MW, Lamoureux, DO. 2011. The structure and phylogenetic distribution of amniote plicidentine. Journal of Vertebrate Paleontology, 31(3), 553-561.

Modesto SP, Sues HD. 2004. The skull of the early Triassic archosauromorph reptile Prolacerta broomi and its phylogenetic significance. Zoological Journal, 140 (3), 335-351.

Müller RT, Garcia MS. (2020) A paraphyletic 'Silesauridae' as an alternative hypothesis for the initial radiation of ornithischian dinosaurs. Biol. Lett. 16:20200417.

Nesbitt SJ, Sidor CA, Irmis RB, Angielczyk KD, Smith RM, Tsuji LA. 2010. Ecologically distinct dinosaurian sister group shows early diversification of Ornithodira. Nature, 464(7285), 95.

Nesbitt SJ. 2011. The early evolution of archosaurs: relationships and the origin of major clades. Bulletin of the American Museum of Natural History, 2011(352), 1-292.

Nesbitt SJ, Butler RJ, Ezcurra MD, Barrett PM, Stocker MR, Angielczyk KD, Smith RMH, Sidor CA, Niedzwiedzki G, Sennikov AG, Charig AJ. 2017. The earliest bird-line archosaurs and the assembly of the dinosaur body plan. Nature, 544(7651), 484-487.

Nesbitt SJ, Langer MC, Ezcurra MD. 2019. The anatomy of Asilisaurus kongwe, a dinosauriform from the Lifua Member of the Manda Beds (~ Middle Triassic) of Africa. The Anatomical Record, 303(4), 813-873.

Novas FE. 1992. La evolución de los dinosaurios carnívoros. In: Sanz, J. L. & Buscalioni, A. (eds) Los dinosaurios y su entorno biotico. Actas II Curso de Paleontologíca en Cuenca. Ayuntamiento de Cuenca, Spain, 125–163.

Novas FE (1996). Dinosaur monophyly. Journal of vertebrate Paleontology, 16(4), 723-741.Novas, F. E. (1992). The evolution of carnivorous dinosaurs. The Dinosaurs and Their

Environment Biotic: Proceedings of the Second Year of Paleontology in Cuenca. Institute" Juan Valdez", Cuenca, Argentina, 126-163.

Romer AS. (1971). The Chañares (Argentina) Triassic reptile fauna. XIV. Lewisuchus admixtus, gen. et sp. nov., a further thecodont from the Chañares beds. Breviora 390, 1–13.

Peecook BR, Steyer JS, Tabor NJ, Smith RM. 2018. Updated geology and vertebrate paleontology pf the Triassic Ntawere Formation of Northeastern Zambia, with special emphasis on the archosauromorphs. Journal of Vertebrate Paleontology, 37(sup1), 8-38.

Sassoon J, Foffa D, Marek R. 2015. Dental ontogeny and replacement in Pliosauridae. Royal Society open science, 2(11), 150384.

Seeley HG. 1888. On the classification of the fossil animals commonly named Dinosauria. Proceedings of the Royal Society of London 43, 165–171.

Sereno PC. 1991. Basal archosaurs: phylogenetic relationships and functional implications. Memoir of the Society of Vertebrate Paleontology 2, 1–53.

Sereno PC, Arcucci AB. 1994. Dinosaurian precursors from the Middle Triassic of Argentina: Marasuchus lilloensis, gen. nov. Journal of Vertebrate Paleontology, 14(1), 53-73.

Sereno PC. 2007. The phylogenetic relationships of early dinosaurs: a comparative report. Historical Biology, 19(1), 145-155.

Sullivan RM, Lucas SG. 1999. Eucoelophysis baldwini a new theropod dinosaur from the Upper Triassic of New Mexico, and the status of the original types of Coelophysis. Journal of Vertebrate Paleontology, 19(1), 81-90.

Yates AM. 2007. Solving a dinosaurian puzzle: the identity of Aliwalia rex Galton. Historical Biology, 19(1), 93-123.

ANNEX

Tooth attachment in Silesauridae: understanding the ankylo-thecodont ontogenetic phase in the evolution of archosaur thecodonty

Being submitted to the journal "The Anatomical Record" as: Mestriner G, Leblanc ARH, Nesbitt SJ, Marsola JCA, da Rosa A, Ribeiro AM, Ferigolo J, Langer MC. Tooth attachment in Silesauridae: understanding the ankylo-thecodont ontogenetic phase in the evolution of archosaur thecodonty. *The Anatomical Record.*

Figures and Supplementary material at the end.

Tooth attachment in Silesauridae: understanding the ankylo-thecodont ontogenetic phase in the evolution of archosaur thecodonty

Gabriel Mestriner[1]; Aaron LeBlanc[2]; Sterling J. Nesbitt[3]; Júlio C. A. Marsola[4, 1]; Randall B. Irmis[5]; Átila da Rosa[6]; Ana Maria Ribeiro[7]; Jorge Ferigolo[7]; Max Langer[1]

[1]. Departamento de Biologia, Universidade de São Paulo, Avenida Bandeirantes 3900, Ribeirão Preto 14040-190, Brazil.

[2]. Department of Biological Sciences, University of Alberta, Edmonton, AB, Canada

[3]. Department of Geosciences, Virginia Tech, Blacksburg, Virginia, 24061, U.S.A.

[4].Programa de Pós-Graduação em Biologia Animal, Instituto de Biociências, Letras e Ciências Exatas – UNESP Campus de São José do Rio Preto

[5]. Utah Museum of Natural History and Department of Geology & Geophysics, University of Utah, 1390 E. Presidents Circle, Salt Lake City, UT 84112–0050, USA.

[6]. Laboratório de Estratigrafia e Paleobiologia, Departamento de Geociências, Universidade Federal de Santa Maria, Campus, Faixa de Camobi km 09, prédio 17, Santa Maria, Rio Grande do Sul, Brasil CEP 97105-900.

[7]. Museu de Ciências Naturais, Fundação Zoobotânica do rio Grande do Sul, Av. Salvador França, 1427, 90690-000 Porto Alegre, RS, Brasil.

Abstract – Contrary to the traditional view in which ankylo-thecodonty is recovered as a synapomorphic trait of Silesauridae, new histological data show that it merely represents the last stage of tooth development within the group. Those dinosauromorphs have neither the crocodilian/dinosaur "permanent gomphosis" nor the "rapid ankylosis" that is plesiomorphic for amniotes. Instead, all sampled silesaurids show "delayed ankylosis", a condition in which teeth pass through an initial gomphosis stage followed by final ankylosis. This suggests that, as already documented for synapsids, tooth fixation in Archosauria might have followed a paedomorphic evolutionary pattern, with the crocodile/dinosaur gomphosis representing the maintenance of an early ontogenetic stage, in which the alveolar bone does not calcify the periodontal ligament between the tooth root and the alveolus. "Delayed ankylosis" in Silesauridae results in accepting the dinosaur and crocodile "permanent gomphosis" as convergently acquired or, less likely, that the silesaurid condition represents a synapomorphic reversal. Moreover, if Silesauridae is nested within Ornitischia, "permanent gomphosis" could even be convergent between the two main dinosaurs lineages. In any case, a ankylo-thecodonty to thecodonty one-step transition appears even more as the oversimplification of a much more complex evolutionary history. In fact, characteristics involving tooth attachment must be evaluated in more detail when they are codified in archosaur phylogenies. An important emerging aspect of gomphosis as synapomorphic for dinosaurs, is that it may represent one of the key features that allowed their thriving on Earth for more than 150 million years.

Key words: Tooth attachment; Tooth implantation; Silesauridae; Archosauria; Dental histology.

Introduction

Evolutionary changes in tooth attachment and implantation have shed light on phylogenetic relationships and dietary preference among many amniote groups, providing valuable clues for paleoecological and palaeobiological characterizations (Zaher and Rieppel, 1999; Caldwell, 2003; LeBlanc et al., 2017; LeBlanc et al., 2018). Also, tooth implantation and attachment have been important features for interpreting evolutionary patterns in major tetrapod groups (LeBlanc & Reisz, 2013). Whereas tooth implantation categorizes teeth by their spatial relations in the jaws, tooth attachment distinguishes those that are fused to the jaw, i.e., ankylosis type of fixation, from those anchored by a periodontal ligament, i.e., gomphosis type of fixation (LeBlanc et al., 2017). Mammals and living crocodilians have received much attention because of their seemingly unique combination of thecodont implantation and permanent gomphosis (LeBlanc et al., 2017). The traditional view that this is a more "advanced" condition and that the associated attachment tissues have evolved independently in crocodilians and mammals was recently challenged. Instead, the current consensus considers the three tooth attachment tissues (i.e., cellular cementum, alveolar bone, and periodontal ligament) as symplesiomorphic features of the major amniote clades (Caldwell et al., 2003/ Budney et al., 2006; Maxwell et al., 2011; LeBlanc and Reisz., 2013; Sassoon et al., 2015; García and Zurriaguz, 2016; LeBlanc et al., 2017; LeBlanc et al., 2018).

Distinguishing thecodonty from the presence of a ligamentous tooth attachment is critical for understanding how attachment and tooth implantation are related and what they tell us about dental evolution in amniotes (LeBlanc et al., 2017). That said, the presence of extensive Sharpey's fiber networks in the hard tissues surrounding ankylosed teeth has revealed that the so-called "attachment bone" in fact encompass different tissues, which exhibit multiple growth directions and mineralizations prior to compete ankylosis. Furthermore, the Sharpey's fibers networks in the hard tissues surrounding ankylosed teeth are insertion points of a

periodontal ligament that had become completely calcified during dental ontogeny (Caldwell et al., 2003; LeBlanc and Reisz, 2013; LeBlanc et al., 2017; LeBlanc et al., 2018).

The tooth socket is formed by alveolar bone, which is a vascularized tissue, with the matrix composed of dense Haversian Bone in mammals, and wove-fiber matrix in crocodilians (LeBlanc & Reisz., 2013; LeBlanc et al., 2017; Leblanc et al., 2018). The tooth root is coated in cementum (which can be cellular or acelluar), providing an attachment area for the periodontal ligament, which is also anchored to the alveolar bone that forms the tooth socket (LeBlanc & Reisz, 2013). The periodontal ligament is composed of an unmineralized network of collagen fibers, and serves multiple purposes: e.g., provide a flexible attachment for the tooth to the alveolar bone, facilitate post-eruptive tooth movement, and serve as a sensory system to help in proper positioning of the jaws during mastication (LeBlanc & Reisz., 2013; LeBlanc et al., 2017).

The so-called ankylo-thecodont tooth attachment encompasses all the plesiomorphic amniote tissues (cementum, alveolar bone, and periodontal ligament), but the periodontal ligament gets completely calcified (Caldwell et al., 2003; Maxwell et al., 2011; LeBlanc & Reisz, 2013; Fong et al., 2016). The novelty of the archosaurian and mammalian tooth attachment is that the periodontal ligament remains (partially or completely) non-mineralized, connecting the root cementum to the alveolar bone and occupying a space between them that is retained during the entire tooth ontogeny (Caldwell et al., 2003; Maxwell et al., 2011; Leblanc et al., 2016; LeBlanc & Reisz, 2013; Fong et al., 2016; LeBlanc et al., 2016; LeBlanc et al., 2017; LeBlanc et al., 2018; Chen et al., 2018). Periodontal histology in archosaurs has shown that the dental tissues of dinosaurs, such as *Coelophysis bauri*, and modern crocodilians are nearly identical (Fong et al., 2016; LeBlanc et al., 2017). However, as shown for Synapsida (LeBlanc et al., 2018), the transition from ankylo-thecodonty to thecodonty might be much more complex than usually thought. In fact, although the dinosaur and crocodilian gomphosis

presumably have a common origin (Edmund, 1960; Nesbitt et al., 2010; Fong et al., 2016; LeBlanc et al., 2017; LeBlanc et al., 2018; Martz & Small., 2019), new discoveries have suggested that the ankylo-thecodont condition is retained in many archosauromorphs (e.g., rhynchosaurs, *Prolacerta*, *Proterosuchus*, *Sarmatosuchus*) including some on the line to dinosaurs, i.e, the Silesauridae (Modest & Sues, 2004; Ferigolo & Langer 2007; Nesbitt et al., 2010; Nesbitt et al., 2011; Kammerer et al., 2011; Langer et al., 2013; Ezcurra, 2016; Ezcurra et al., 2019; Martz & Small, 2019).

Silesaurids have a controversial phylogenetic position among Dinosauriformes; usually considered the sister-group of Dinosauria (Benton & Walker 2011; Langer et al., 2010; Nesbitt, 2011; Bittencourt et al., 2015; Baron et al., 2017; Langer et al., 2017; Nesbitt et al., 2017), but also recovered as paraphyletic and/or in the ornithischian lineage (Ferigolo & Langer, 2007; Langer & Ferigolo, 2013; Cabreira et al., 2016; Müller & Garcia, 2020). Accordingly, their inferred ankylo-thecodonty has been suggested as sinapomorphic for the group (character 174 of Nesbitt, 2011; Ferigolo & Langer 2007; Nesbitt et al., 2010; Nesbitt et al., 2011; Kammerer et al., 2011; Langer et al., 2013; Ezcurra, 2016; Ezcurra et al., 2019; Martz & Small., 2019; Nesbitt et al., 2020), supporting the former hypothesis. Hence, the better knowledge of their tooth attachment is pivotal to infer their relations, which is itself critical for understanding the origin of dinosaurs and the key features that allowed their evolutionary success (Brussate et al., 2008; Langer et al., 2010; Brussate et al., 2010; Langer et al., 2013; Benton et al., 2014). Indeed, although a lot of information regarding tooth attachment in non-dinosaur Dinosauromorpha entered the literature, this was actually never evaluated on the basis of osteohystological studies. Here, we assess this complex feature, providing a comprehensive characterization of the Silesauridae tooth attachment, based on data from different species. Further, we evaluate its evolutionary implications for the diversification of the dinosaur line of archosaurs.

Institutional abbreviations

MCN, Museu de Ciências Naurais, Fundação Zoobotânica do Rio Grande do Sul, Porto Alegre, Brazil; **NMT**, National Museum of Tanzania, Dar es Salam, Tanzania; **UFSM**, Universidade Federal de Santa Maria, Rio Grande do Sul, Brazil.

Material and Methods

Material

This study is based on osteohistological sections of tooth-bearing bones of four silesaurids: 1 - *Eucoelophysis baldwini* (GR 1072) from the Petrified Forest Formation, Norian of New Mexico (Sullivan & Lucas, 1999; Ezcurra 2006); 2 - *Sacisaurus agudoensis* (MCN PV 10095) from the Caturrita Formation, Norian of Brazil (Ferigolo & Langer, 2007; Marsola et al. 2018a); 3 - *Asilisaurus kongwe* (NMT RB 1086; NMTRB 1087) from the Lifua Member of the Mnada beds, Anisian of Tanzania (Nesbitt et al., 2010; Nesbitt et al., 2017; Peecook et al., 2018); 4 - UFSM 11579, newly recovered from the upper levels of the Alemoa Member (Santa Maria Formation) at Cerro da Alemoa site, Carnian of Brazil (Langer et al. 2018). All measurements taken for the specimens are available in Table 1. The incompleteness of the anterior and posterior ends of all specimens above (except for NMT RB 1086) hampers inferring the anatomical position of the teeth and/or alveoli, so that the numbers ascribed to them in the sessions below serve only for descriptive purposes.

Methods:

The specimens were thin sectioned at the histology lab of the University of Alberta. Moulds and casts were made prior the sectioning procedures. Moulds were made using *Blustar Silicones V-SIL 1062* and *Hi Pro Green* catalyst, and casts by pouring *Smooth-on-Smooth-Cast*

321 or 322 liquid plastic into the silicon moulds and placing them under pressure until they set (LeBlanc et al., 2018). All paleohistological sections followed the standard procedures employed for sectioning fossil material according to LeBlanc et al. (2018). The specimens were separately embedded in *Castolite AC* polyester resin in a plastic container and then peroxide catalyst was incorporated in a ratio of 10 MEKP drops for 30 ml of resin. Then the container was vacuumed for five minutes to evacuate all air bubbles. After that, the specimens were fully imbedded in *Castolite AC* polyester resin and left to set for 24 hours.

The samples were cut using the *Buehler Isomet 1000* water blade saw set to 200-300 rpm. After the cut, the surfaces were polished before being glued to the glass plates, using 600 and 1000 grit silicon carbide powder. After polishing, they were left to dry for 24 hours halted and mounted to plexiglass frosted slides using *Scotch-Weld SF-100* to stick the specimens to the slide. Once fixed, the samples were cut using the *Isomet 1000* at a trim thickness of approximately 0.7 mm. The isomet was set to cut at a distance of 99.3 mm, once it has been zeroed with the blade contacting the slide. After being cut, the specimens were grounded using the *Hillquist* grinding machine. The slides were slowly passed across the grinding cup and steadily bringing the slide closer to the grinding surface. The slide was constantly checked up in the microscope, until the needed histological details could be seen. Once the slide was nearing the desired thickness, the final grinding was done by hand with 600 and 1000-grit silicon carbide powder. During this process, the thickness was frequently checked under a cross-polarizing microscope and halted when the specimen shone entirely grey/white and black. The specimens were then polished with 1-micron aluminum oxide powder and a soft cloth, and left to dry for a day.

All the specimens were catalogued in a lab worksheet that indicates the dates and work done to the specimen, type of slide, plane of section, taxonomic information, locality from which the specimen was recovered, name of preparator, dates, adhesives used, location of slide,

and catalogue number. The section images were taken using a *Nikon DS-fi2* camera mounted to a *Nikon AZ-100* microscope using *Nikon NIS-Elements* imaging software (Basic Research package). The slides are available to examination in the follow institutions: NMT RB 1086, NMTRB 1087 (*A. kongwe*) and GR 1072 (*E. baldwini*) – Department of Geosciences, Virginia Tech University, Blacksburg-VA, USA; MCN PV 10095 (*S. agudoensis*) – Museu de Ciências Naturais, Fundação Zoobotânica do Rio Grande do Sul, Porto Alegre-RS, Brasil; UFSM 11579 – Departamento de Geociências, Universidade Federal de Santa Maria, Santa Maria-RS, Brasil.

Results

Eucoelophysis baldwini (Figs. 1-5)

The sampled bone corresponds to a right dentary fragment (GR 1072– Figure 1). Its anterior and posterior edges are damaged, but tooth implantation is pristine. The fragment preserves eight alveoli; the first, third, and eighth of which contain fully erupted tooth crowns (Figure 2A). Additionally, a replacement tooth is coming out of the fifth alveolus. The crown in the eighth alveolus has only its anteriormost part preserved. Alveoli 2, 4, 6, and 7 are empty. Due to taphonomic distortions, the bone is arched towards the lateral.

Osteohistology:

The dentine forms the bulk of the teeth, with the dental tubules extending across its entire thickness. The root of all functional teeth (first, third, and eighth alveoli – Figure 2A-D) shows two layers of globular dentine separating the orthodentine from the root cementum, which is positioned outer to the orthodentine layer (Fig. 3). In the former layer, the tubules end within a zone of poorly mineralized dentine, known as the globular zone, which corresponds to the granular layer of Tomes (Nanci, 2013; Fong et al., 2016). This is similar to the condition seen

in other tetrapods, including the neotheropod *C. bauri* (LeBlanc & Reisz., 2013; Fong et al., 2016). The first layer of globular dentine is thin (ca. 10 μm), and has a white aspect, whereas the second layer is thicker (ca. 24 μm) and darker. Such color difference could result from taphonomics alterations.

The acellular cementum is bright, its layer is positioned external to the globular dentine (Fig. 3) and is virtually as thin as the second layer of globular dentine (ca. 10 μm). The cellular cementum consists of a woven bone matrix, much thicker than the acellular layer (ca. 114 μm; Figs. 3-4). It contains cementocyte cells distributed with no recognizable pattern, and the cells present an oval to rounded aspect. The cellular cementum layer is divided in three growth bands (Fig. 3), which are recognized based on color differences: the inner layer is white, the middle one is orange, and the outer is dark orange. Again, color differences are probably associated to taphonomic events. Sharpey's fibers perforate the cellular cementum perpendicularly, radiating around the circumference of the root. These fibers are better seen under cross-polarized light (Fig. 4B), where it is possible to identify their bundles radiating within the cellular cementum, extending towards the alveolar bone, and coating the tooth roots.

The teeth in the first and eighth alveoli (Figs. 2B, D-E; 3B) show periodontal space (ca. 56 μm thick) between the cellular cementum and the alveolar bone, characterizing gomphosis (Fong et al., 2016; Leblanc et al., 2017; Leblanc et al., 2018). The periodontal space has a wave aspect around the root circumference, resulting from the position of the blood vessels. In this arrangement, the vessels are located at the intersection between the alveolar bone and cellular cementum. Each of these two tissues hosts half of the vessels, conferring the wave aspect to the periodontal space around the roots (Figs. 2E; 3B). The tooth in the third alveolus is ankylosed to the jaw (Figs. 2C, F), meaning that the periodontal space is mineralized, with the cellular cementum and the alveolar bone touching one another (Figs. 2F, 3, 4). In this case, the

vascular spaces are mostly displaced to the alveolar bone area, with a minor portion occupying the cellular cementum layer.

The alveolar bone is vascularized along its entire thickness, in all parts of the dentary (ca. 500 μm from tooth root to jaw bone). The cross section of the blood vessel is rounded, indicating that they are dorsoventrally directed. The area around some of these vascular channels has been remodeled, as indicated by the lamellar bone, formed by organized cells, around the circumference of the vessels (Fig. 5D; Reid, 1996; LeBlanc & Reisz, 2013; LeBlanc et al., 2017). As expected for archosaurs (LeBlanc & Reisz., 2013), the matrix of the alveolar bone is composed by woven bone, which is morphologically similar to those of the cellular cementum.

The area between each alveolus (Fig. 1 of Supplementary Material), i.e., interdental plate of LeBlanc et al. (2017), is formed by alveolar bone. The boundary between the alveolar bone of each of the adjacent alveoli is outlined by a reversal line; as is clear in the alveolar bone between the third and fourth alveoli (Fig. 1 of Supplementary Material). This reversal line is formed by lamellar bone and surrounded by many cementocytes. The boundary between the alveolar bone and the jaw bone is also outlined by a reversal line (Fig. 2 of Supplementary Material), indicating that it was resorbed and redeposited (Snyder et al., 2020). This line marks the farthest extent of bone resorption and subsequent redeposition of alveolar bone, between successive tooth replacement cycles (Fong et al., 2016).

The jaw bone tissue (ca. 750 μm from the alveolar bone to the outer dentary surface) consists of parallel-fibered bone (lamellar bone), in which the cells are flat, organized, and anteroposteriorlly arranged. Under cross-polarized light, the jaw and alveolar bones can be distinguished from one another by their different colors, in which the jaw bone is darker (Fig. 2 of Supplementary Material). The primary vascular channels of the jaw bone are anteroposteriorly long and mediolaterally thin (Fig. 2A). This shape in cross section indicates

that those vessels extend in an anteroposterior direction. The teeth of alveoli 1 and 3 show different degrees of contact between the alveolar bone and cellular cementum. The tooth of alveolus 1 has a completely unmineralized periodontal space, as seen around the entire root in two more apical cross sections (Fig. 3 of Supplementary Material), whereas the most basal section reveals some points where the periodontal space is being mineralized by the alveolar bone (Fig. 3 of Supplementary Material). Conversely, the tooth of alveolus 3 has the periodontal space totally mineralized around the root in the two more apical cross sections, but it has points in which the periodontal space is not mineralized in the more basal section (Fig. 4 of Supplementary Material).

The dentary has four empty alveoli (positions 2, 4, 6, and 7; Fig. 2A). The second, fourth, and sixth are ovoid and not taphonomically deformed. The seventh has the same anteroposteriorly elongated outline also seen in the fifth alveolus, being anteroposteriorlly longer (ca. 5 mm) than the other alveoli (ca. 2.5 μm). The replacement tooth erupting from the fifth alveolus (Figs. 2A; 9A) has an evident enamel layer. The most apical cross section (not included in Fig. 2) shows a remaining piece of the replaced tooth, which was not totally resorbed, surrounding the new tooth labially. The attachment tissues of that piece are intact, revealing a completely mineralized periodontal space, with the alveolar bone touching the cellular cementum, i.e., ankylosed (Fig. 5B), which is compatible with an old stage of tooth development.

Santa Maria Formation silesaurid – UFSM 1579 (Figures 6-12)

The sampled elements correspond to two jaw elements, a left maxilla and a right dentary. The maxilla contains four alveoli (Figs. 6-8). The anterior and posterior edges are lost, but the piece is generally well preserved. Following anteroposteriorly, the fully erupted crowns fill the first and third alveoli, whereas the second and fourth alveoli are empty. Besides, the bone still bears

tooth portions from old generations that were not completely resorbed. The dentary (Fig. 9) contains two fully erupted tooth crowns, two empty alveoli, one replacement tooth, and some remnants of dentine from older teeth generation. The anterior and posterior edges of the bone are damaged, but the preservation is informative as for tooth attachment. The preserved crowns occupy the first and the fourth alveoli, the second and fifth alveoli are empty, and the replacement tooth occupies the third alveolus (Fig. 10).

Osteohistology:

Dental tubules extend across the entire dentine thickness. The roots of the fully erupted functional teeth (Fig. 7A, 10A) have two layers of globular dentine (the inner with an average thickness of 8 μm and the outer of 12 μm) separating the orthodentine from the root cementum (e.g., Fig. 11). This is the same structure present in *C. bauri* (Fong et al., 2016), and corresponds to the granular layer of Tomes (Nanci, 2013; Fong et al., 2016). The acellular cementum forms a bright and thin band (ca. 13 μm in the maxilla and 11 μm in the dentary; Figs. 8, 11) around the roots, whereas the cellular cementum forms a thicker layer (ca. 100 μm in the maxilla and 91 μm in the dentary) of a woven bone matrix (Figs. 8A, 11B). The cellular cementum contains cementocytes distributed randomically, with shape varying from oval to round. Under cross-polarized light, it is possible to see numerous Sharpey's fibers traversing the full thickness of the cellular cementum and radiating around the circumference of the roots toward the alveolar bone (Figs. 8B, 11B, 12B). The alveolar bone in UFSM 1579 forms a thicker layer compared to that of cellular cementum (ca. 300 μm in the maxilla and 370 μm in the dentary) and is composed by a woven bone matrix, with cells arranged in no recognizable pattern. It is vascularized with circular vascular channels (Figs. 8, 12) that extend dorsoventrally. The osteocits have the same morphology and density seen in the cellular cementum. The area around the alveolar bone of both sampled fragments has been remodeled, as indicated by the

presence of lamellar bone surrounding the channels (Fig. 8A; Fig. 7 of Supplementary Material; Reid, 1996; LeBlanc & Reisz, 2013; LeBlanc et al., 2017). The contacts between the alveolar and the jaw bones are outlined by a distinct reversal line, marking the farthest extent of bone resorption among successive tooth replacement cycles (Fong et al., 2016). The jaw bone tissue (ca. 290 μm in the maxilla and 125 μm in the dentary) consists of parallel-fibered (lamellar) bone, in which the cells are flat, organized in an anteroposterior fashion. Its contact with the alveolar bone is clearly marked by different patterns of cell organization: arranged in rows in the jaw bone and with no clear pattern in the alveolar bone. The primary vascular channels extend anteroposteriorly, appearing as long and mediolaterally thin lines in cross section (Fig. 10A; Fig. 5 of Supplementary Material).

Two different layers of alveolar bone are seen on the labial side of the third tooth of the maxilla and the fourth tooth of the dentary, with each of their boundaries outlined by a distinct reversal line (Figs. 5, 8 of Supplementary Material). Such line indicates resorption and redeposition of the alveolar bone during successive tooth replacement cycles (Fong et al., 2016). The primary alveolar bone (Figs. 5, 8 of Supplementary Material) corresponds to the most recently deposited layer, belonging to the functional teeth. The secondary layer is a remnant of the previous tooth generation, which fell out during the replacement event, and marks the farthest extent of bone resorption (Fong et al., 2016; LeBlanc et al., 2017; Snyder et al., 2020). Indeed, blood vessels of the secondary alveolar bone are surrounded by layers of lamellar bone, indicating intense remodeling. Under cross-polarized light, it is possible to see Sharpey's fibers crossing both layers of alveolar bone (Fig. 5D). Accordingly, the boundary between the secondary layer of alveolar bone and the adjacent jaw bone is also outlined by a reversal line (Fig. 8B of Supplementary Material). The teeth occupying the first alveolus of the maxilla (Figs. 7B, D) and the fourth alveolus of the dentary (Figs.16D, G) are on the gomphosis stage, in which the periodontal space is completely unmineralized. The periodontal space varies

its thickness around the root circumference of the maxillary tooth, being ticker in the lingual (ca. 89 μm) than in the labial (ca. 36 μm) side, whereas the thickness is of about 11 μm in the dentary tooth. This size difference is associated to the ontogenetic stage of the teeth, in which a broader periodontal space represents an earlier stage, whereas the thinner periodontal space results from alveolar bone being deposited for a longer amount of time. The area around the periodontal space of both teeth has vascular channels giving a wave shape to the contact between the cellular cementum and the alveolar bone (Figs. 7D, 12A), each of which encloses half of the channels. The teeth occupying the third alveolus of the maxilla (Figs. 7C, E) and first alveolus of the dentary (Figs. 10B, E, 11) are on the ankylosis stage, with the periodontal space totally mineralized.

The empty alveoli of the maxilla and dentary have different outlines. The second of the maxilla is ovoid and irregular (Fig. 7A), indicating that the tooth was likely broken at the base, as seen in lizards and tetrapods with ankylosed teeth (LeBlanc & Reisz, 2013). Conversely, the fourth alveolus of the maxilla (Fig. 7A; Fig. 6B of Supplementary Material) and the second of the dentary (Fig. 10 of Supplementary Material) are rounded and regular, which seem to preserve their original anatomy, as observed in taxa with a gomphosis-type of tooth fixation, as dinosaurs, crocodilians, and mammals (LeBlanc & Reisz, 2013; LeBlanc et al., 2017; Leblanc et al., 2018). Besides, the second alveolus of the maxilla has signs of a resorption event in its labial side, as expected for teeth on a late ontogenetic stage. On the contrary, the alveolar bone in the fourth alveolus of the maxilla and second of the dentary forms a wavy outline around the tooth socket (i.e., the area of the periodontal space if the tooth was preserved), as seen in the first alveolus, which bears a tooth on the gomphosis stage. That wavy shape morphology is given by the blood vessels of the periodontal space, positioned between the alveolar bone and the cellular cementum.

Two remnants of dentine from previous tooth generation are seen surrounding the labial side of the second alveolus of the maxilla (Fig. 7 A; Fig. 6 of Supplementary Material). They have had their attachment tissues already resorbed and are formed only by alveolar bone. Surrounding the labial portion of the fourth alveolus of that same piece there is another dentine remnant, also lacking attachment tissues (Fig. 6 of Supplementary Material). The maxilla also preserved two teeth that are smaller (approximately ¼ the size) than the functional teeth. Their size suggests that they correspond to an early generation of teeth that was functional when this animal was younger, but were not completely resorbed (Fig. 7A; Figs. 6A-C of Supplementary Material). The first of those (Figs. 6A, C of Supplementary Material) is positioned anterolateraly to the first alveolus, whereas the second sits posterolateraly to the empty fourth alveolus (Fig. 6A-B of Supplementary Material). Although both teeth are incomplete, it is possible to see that they have a rounded cross-section (Fig. 7A) and that dentine is their only remaining tissue. The dentary is also bears one such small teeth (Fig. 10A; Fig. 8A of Supplementary Material). Positioned between the fourth and fifth alveoli, it is rounded in cross section and solely composed by dentine, as the other tissues have been already resorbed. As suggested for the maxilla, it likely corresponds to a tooth functional at an earlier stage of the animal ontogeny.

The erupting replacement tooth of the dentary has a “kidney” shape in a dorsal view. In a more apical cross-section, it is possible to see the enamel as the outer layer (Fig. 9A of Supplementary Material), which faints towards the base, as the attachment tissues appear (Fig. 9B of Supplementary Material). At this point, it is possible to identify the granular dentine, a thin layer of acellular cementum (ca. 6 μm), followed by a thicker layer of cellular cementum (ca. 36 μm), showing that those tissues were present even in an early stage of tooth development. The cellular cementum shows oval cells with no organized pattern. Surrounding the replacement tooth, there is a not fully resorbed piece of the replaced tooth. This piece is no

longer functional, but its attachment tissues are still evident. In this case, the tooth was ankylosed to the jaw, with the periodontal space totally mineralized by the alveolar bone (Figs. 10C, F), as expected for the fixation of a tooth in a later ontogenetic stage.

***Sacisaurus agudoensis* (Figure 13-15)**

One specimen of *S. agudoensis* (MCN PV 10095) was sectioned (Fig. 13). It comprises an incomplete right dentary containing one fully erupted tooth crown and eight empty alveoli. The anterior and posterior edges of the bone are missing, but the tooth and its attachment tissues are well preserved (Fig. 14). The preserved tooth occupies the eighth alveolus (Fig. 14).

Osteohistology:

The only preserved tooth is entirely made of dentine, with the tubules extending through its entire thickness. The acellular cementum forms a thin (ca. 9 μm) layer, positioned outer to the dentine. Under cross-polarized light, it appears as a bright band outlining the root (Fig. 15C). The cellular cementum (Figs. 15B, C) consists of a woven bone matrix and it is more than five times thicker than the acellular layer (ca. 57 μm). It contains many cementocyte cells distributed with no recognizable pattern. These cells can be either oval or rounded and cross-polarized light shows numerous Sharpey's fibers (Fig. 15C) across the entire thickness of the cellular cementum and alveolar bone layers. The cementum and the alveolar bone contact one another, with the complete mineralization of the periodontal space indicating the the toot is at the ankylosis stage (Fig. 14C). The resorption pit seen in the lingual side of the jaw (Fig. 13A) confirms that the tooth is on a late ontogenetic stage, even though there is no trace of the replacement tooth in the histologic sections.

The alveolar bone is formed by a woven bone matrix, which is vascularized by simple vascular channels. These vascular channels are simple and rounded in cross section, extending dorsoventrally (Fig. 15B) within the alveolar bone, near its contact with the cellular cementum. The alveolar bone layer is thicker (ca. 145 μm) than the cellular cementum layer (ca. 57 μm). As typical to woven fibered matrix (Fong et al. 2016), the osteocits distribution in the alveolar bone has no recognizable pattern, sharing shape and orientation with those in the cellular cementum. The boundary between the alveolar and jaw bones is outlined by a reversal line, which is very distinct under cross-polarized light (Fig. 15C). The jaw bone is approximately 142 μm thick and formed by parallel-fibered (lamellar) bone. The cells are longer anteroposteriorlly than lateromedially (Fig. 15B) and arranged in anteroposteriorly directed rows (Fig. 1 of Supplementary Material). Under cross-polarized light, the jaw bone is brighter than both the alveolar bone and cellular cementum (Fig. 15C). The primary vascular channels are longer anteroposteriorly and some of them branch in two (Fig. 15A, B). Damages in the material preclude assessing the margins of the empty alveoli to find out if they form regular or irregular outlines, which would respectively indicate gomphosis or ankylosis (LeBlanc & Reisz, 2013; LeBlanc et al., 2017; Leblanc et al., 2018).

***Asilisaurus kongwe* (Figure 16-21)**

Two specimens of *A. kongwe* (NMT RB 1086; NMTRB 1087; Figs. 16-17) have been sampled. Even though both specimens are fragmentary, many teeth bear information about their attachment. NMT RB 1086 is a partial right dentary, preserving its anterior tip, i.e., predentary equivalent of Ferigolo and Langer (2007; Langer and Ferigolo 2013), and the seven subsequent teeth, i.e., dentary teeth 1-7 (Fig. 18). NMTRB 1087 preserves eleven empty alveoli and eight tooth crowns. Because of its poor preservation, we could not differentiate the lingual from the labial surfaces NMTRB 1087 and consequently its side. The preserved teeth occupy alveoli 1,

2, 3, 5, 6, 7, 8, and 11 (Fig. 19). Due to damage, the contour of the root is incomplete in some teeth (e.g., teeth 1, 3, and 4 in NMT RB 1086, and teeth 2, 3, and 6 in NMT RB 1087).

Osteohistolgy:

Most of the teeth are entirely formed by dentine, with the dental tubules extending across their entire thickness. The roots have a thick layer (ca. 18 μm) of globular dentine separating the orthodentine from the root cementum (Fig. 20). This corresponds to the granular layer of Tomes (Nanci, 2013), as also seen in *C. bauri* (Fong et al., 2016). The globular dentine has a yellow aspect (Figs. 20A, B) that appears dark under cross-polarized light (Fig. 20C). The acellular cementum layer is thinner (ca. 10 μm), positioned outer to the globular dentine, and differentiated from it by its brighter color (Fig. 20B), even under cross-polarized light (Fig. 20C). The cellular cementum consists of woven bone matrix and is thicker than the acellular cementum (ca. 57 μm in NMT RB 1086 and ca. 91 μm in NMT RB 1087). The cells are small and distributed with no recognizable pattern. Under cross-polarized light, numerous Sharpey's fibers traverse the cellular cementum and alveolar bone zone around the whole circumference of the root (Fig. 20C). The contact between the cellular cementum and the alveolar bone are seen in all teeth, even if only in some portions (e.g., Figs. 18B, 21). In NMT RB 1086 (Fig. 18A), parts of the periodontal space of the tooth roots are clearly mineralized, but it is not clear if some other parts are not, or if they were taphonomically damaged. The fifth tooth of NMT RB 1086 is the only one that clearly shows parts where the cellular cementum and alveolar bone are contacting one another (evidencing ankylosis) and points where the periodontal space evidences gomphosis, characterizing the "mineralization" stage (Fig. 15G).

The alveolar bone layer is formed by woven tissue matrix and thicker (ca. 227 μm in NMT RB 1086 and ca. 182 μm in NMT RB 1087) than the cellular cementum. It is vascularized, with simple vascular channels that are either oval or circular in cross section. All

the vascular channels are located outer to the contact with the cellular cementum. The anterior margin of the seventh alveolus of NMT RB 1086 bears dentine remnants from the older tooth generation (Fig. 11 of Supplementary Material).

The jaw bone is approximately 227 μm thick in NMT RB 1086 and 409 μm thick in NMT RB 1087. It is formed by parallel-fibered (lammelar) bone, the matrix of which has an organized pattern of cell distribution. The boundary between the alveolar and jaw bones is outlined by an evident reversal line (Fig. 11 of Supplementary Material), corresponding to the oldest portion of the alveolar bone that had been deposited (Fong et al., 2016; Leblanc et al., 2017; Leblanc et al., 2018). The primary vascular channels of the jaw bone are anteroposteriorlly longer in cross section (Figs. 18, 19).

Discussion

Understanding ankylosis (i.e., complete calcification of the periodontal ligament) in silesaurids is important because this mode of tooth fixation is currently interpreted as synapmorphic for the group (Nesbitt et al., 2010, 2020; Nesbitt, 2011; Langer & Ferigolo 2013; Martz & Small 2019). Yet, our studied sample shows that both gomphosis and ankylosis are present in silesaruids, as well as an intermediate “mineralization” phase (LeBlanc et al., 2018), where the periodontal space is only partially calcified by the alveolar bone. In addition, the presence of Sharpey fibers in the cellular cementum and alveolar bone indicates that silesaurids bore the three tooth attachment tissues symplesiomorphic for Amniota: root cementum, alveolar bone, and periodontal ligament (Caldwell et al., 2003; Maxwell et al., 2011; Leblanc et al., 2017; Leblanc et al., 2018). The abundance of alveolar bone compared to cellular cementum indicates that this is the tissue responsible for entombing the periodontal ligament when the tooth is ankylosed.

In *E. baldwini*, it is possible to identify growth lines in the cellular cementum (Fig. 3), whereas in other silesaurids this band is not multilayered. Growth lines in ankylosed teeth (e.g., tooth in alveolus 3; Fig. 3A) evidence a preceding gomphosis phase, because they are only produced when periodontal space is present in the tooth (LeBlanc & Reisz., 2013; LeBlanc et al., 2018). This indicates that a certain amount of time was required until the tooth was fully ankylosed to the jaw. Sharpey's fibers were identified both in the cellular cementum and alveolar bone, as plesiomorphic for amniotes (Caldwell et al., 2003; Maxwell et al., 2011; Leblanc et al., 2016; Leblanc et al., 2017; Leblanc et al., 2018; Chen et al., 2018). They correspond to the mineralized portion of the periodontal ligament, anchored to the cellular cementum and/or alveolar bone (Caldwell et al., 2003; Leblanc & Reisz, 2013; LeBlanc et al., 2017; LeBlanc et al. 2018).

In amniotes with a gomphosis-type of tooth fixation (LeBlanc & Reisz, 2011), the periodontal space persists throughout tooth development (Fong et al., 2016; LeBlanc et al., 2017; LeBlanc et al., 2018). Among the studied silesaurids, this condition was identified in both *E. baldwini* (Fig. 2A-B, E) and UFSM 1579 (Figs. 11A-B, D; 16A, D, G), whereas most teeth of *A. kongwe* are on the "mineralization" stage (Fig. 18A-B). In all these forms, the non-mineralized periodontal space is identified by the wavy outline morphology around the tooth root (Fig. 3B; 11D; 18B).

Ankylosed teeth are also present in specimens with teeth on the gomphosis phase: e.g., *E. baldwini* (Fig. 2C, F) and UFSM 1579 (Figs. 11C, E; 16B, E). The blood vessels here are positioned either in the mineralized intersection of the alveolar bone with the cellular cementum (Figs. 11E; 16F) or restricted to the former (Figs. 4; 12; 17), as also seen in the only tooth preserved for *S. agudoensis*. It seems that the ankylosed teeth of *E. baldwini* also had a wavy outline before they were entombed by the alveolar bone, as reflected by the shape of the empty alveoli. Indeed, the wavy outline is seen in ankylosed teeth of *E. baldwini* (Fig. 2C, F)

and UFSM 1579 (Fig. 11A, B), but not in *S. Agudoensis*, where the outline seems to be more regular (Fig. 15B). The empty alveoli of *A. kongwe* are damaged and do not allow a clear interpretation of its morphology.

As plesiomorphic for amniotes (LeBlanc & Reisz., 2013; LeBlanc et al., 2018), but unlike crocodiles and theropod dinosaurs (Fong et al., 2016; LeBlanc et al., 2017), alveolar bone is the thickest and more abundant tissue in the tooth socket of all silesaurids analyzed here. Ankylosis in Silesauridae occurs via the apposition of alveolar bone, as in various synapsid groups studied by LeBlanc et al. (2018). More precisely, it occurs with the alveolar bone calcifying centripetally towards the cellular cementum, causing the complete entombment of the periodontal space. This calcification pattern differs from that of other amniotes with an ankylosis type of fixation, such as mosasaurs, in which the cellular cementum is the thickest tissue and grows toward the alveolar bone layer (Caldwell et al., 2003).

The woven bone matrix with several reversal lines, as seen in *E. baldwini*, UFSM 1579, and *A. kongwe* (Figs. 2, and 11 of Supplementary Material), indicates that this tissue was resorbed and redeposited quickly (LeBlanc et al., 2017). The same pattern is seen in early theropods, mammals, and crocodiles (Budney et al., 2006; LeBlanc & Reisz, 2013; Fong et al., 2016; LeBlanc et al., 2017). UFSM 1579 has a secondary layer of alveolar bone in some areas (Figs. 5, 8 of Supplementary Material), which remained from the previous tooth generation. Blood vessels at this layer are surrounded by lamellar bone, indicating intense remodeling. Secondary osteons around blood vessels (Fong et al., 2018; LeBlanc et al., 2017; LeBlanc et al., 2018) are seen in the interdental plates of *E. baldwini* (Fig. 1 of Supplementary Material) and also in the alveolar bone of UFSM 1579 (Fig. 8B). A reversal line around these vascular spaces indicates extensive resorption of the surrounding hard tissues occurring before alveolar bone deposition (Reid, 1996; LeBlanc & Reisz, 2013; LeBlanc et al., 2017).

Some empty alveoli of *E. baldwini* (2, 4, and 6; Fig. 2A) and UFSM 1579 (maxillary alveoli 2 and 4; lower jaw alveoli 2; Figs. 7A, 10A), have a regular outline, indicating that the teeth have fallen out, and were not broken at their bases. This suggests a gomphosis mode of attachment (LeBlanc et al., 2017; Leblanc et al., 2018), approaching that of animals that lose their teeth with the decay of the periodontal ligament (LeBlanc & Reisz, 2013). Other teeth have the irregular cracked outline of a broken base (e.g., first maxillary alveolus of UFSM 1579; Fig. 7A). This is common to animals with an ankylosis mode of fixation, as found in some lizards and other tetrapods with a mineralized connection between the tooth root and the alveolar bone (LeBlanc & Reisz, 2013). Because the outline morphology of empty alveoli helps inferring tooth attachment, the many empty alveoli of *S. agudoensis* suggests a post-mortem tooth loss scenario (Fig. 14A). In this way, although its only preserved tooth is ankylosed and damages in the areas surrounding empty alveoli preclude getting trustworthy data on alveoli outline, it seems that gomphosis was also present in some tooth development phase of *S. agudoensis*.

Summarizing the above information, the specimens studied here can be interpreted as follows: *E. baldwini* – alveoli 3 and 8 ankylosed, alveoli 1, 2, 4, and 6 with gomphosis; UFSM 1579 – maxillary alveoli 2 and 3 and dentary alveolus 1 ankylosed; maxillary alveoli 1 and 4 and dentary alveoli 2 and 4 with gomphosis. Such a detailed account is not feasible for *S. agudoensis* and *A. kongwe*, but it is clear that both gomphosis and ankylosis were present. In addition, the "intermediate" stage, characterized by an incomplete ankylosis of tooth root to the socket (LeBlanc et al., 2018), was found in both *E. baldwini* (Fig. 3C and 4C of supplementary material) and *A. kongwe* (Fig. 20A). In the former taxon, the most apical section of the tooth in alveolus 1 is on the gomphosis stage (Fig. 2B), whereas that of alveolus 3 is on the ankylosis stage (Fig. 2C). This means that the process of mineralization progresses in different rates throughout the tooth length.

Different stages of tooth development are present in our silesaurid samples; from erupting replacement teeth, teeth under resorption, to remains of old tooth generations. In alveolus 5 of *E. baldwini* (Fig. 5) and in alveolus 3 of the UFSM 1579 lower jaw (Fig. 10C), the old tooth pieces inform on tooth fixation at later ontogeny stages, which is ankylosis in all cases (Figs. 5B, 10F, 22B, C). The replacement tooth in both species is already in the functional position, with an enamel layer surrounding the dentine (Figs. 5A; 9A2 of Supplementary Material). However, a more basal cross-section of the UFSM 1579 younger tooth already shows attachment tissues, i.e., acellular and cellular cementum (Fig. 9B3 of Supplementary Material), instead of enamel. A similar arrangement of old tooth pieces is present in the neotheropod *C. bauri* (Fig. 22A). However, unlike in *E. baldwini* and UFSM 1579, the old tooth generation of *C. bauri* still have unmineralized periodontal space, with no contact between the cementum and the alveolar bone, i.e., gomphosis, enduring until the last stage of tooth development (Fig. 22). *Asilisaurus kongwe* also has an old generation tooth near a functional tooth, but only its dentine is preserved, with all attachment tissues already resorbed (Fig. 11 of Supplementary Material). This is also the case for both maxilla and dentary of UFSM 1579, in which such teeth are smaller than the functional teeth in dorsal view ("lt" in Figs. 6A, B, C and 8A of Supplementary Material).

In our silesaurid sample, replacement events have been documented only in *E. baldwni* and UFSM 1579. In the former, functional teeth occupying alveoli 1 and 3 are being lingually resorbed (Fig. 2A), but no evidence of this process is seen in more ventral cross sections of these elements (Fig. 3-4 of Supplementary Material). The replacement tooth in its alveolus 5 is anteroposteriorly elongated, showing enamel, but no attachment tissues. Alveolar bone is present both labialy and lingualy, representing the initial stage of the socket development in this tooth. The replacement tooth in the third alveolus of UFSM 1579 lower jaw has dentine and thin layers of acellular and cellular cementum in a more basal cross-section (Fig. 9B of

Supplementary Material). The condition in these silesaurids differs from that of mammals, crocodilians, and dinosaurs, in which the cellular cementum is only deposited when the tooth is already functional (LeBlanc & Reisz, 2013). The newly formed teeth develop within resorption pits along the lingual side of the dentary, as more typical for amniotes (Edmund, 1960; Zaher and Rieppel, 1999; Richman and Handrigan, 2011), including some dinosaurs (Fong et al., 2016). Such pits can be seen in the lingual side of the *S. agudoensis* jaw (Fig. 13), as well as in various other silesaurids (Langer & Ferigolo, 2013; Martz & Small, 2019; Nesbitt et al., 2020), theropods (Fong et al., 2016; Leblanc et al., 2017) and ornithischians (LeBlanc et al., 2017; Chen et al., 2018). The location of the developing replacement teeth in Silesauridae suggests that the position of the odontogenetic organ (dental lamina) is the same as in most of amniotes including dinosaurs, i.e., close to the gum line (Edmund, 1960; Wu et al., 2013; Fong et al., 2016), differing only from that of crocodilians (Martin and Stewart, 1999; Fong et al. 2016; LeBlanc et al., 2017).

Evolutionary implication of the tooth attachment system in Silesauridae

Four different phases of a standard sequence of dental ontogeny were identified in the sampled silesaurids: eruption, gomphosis, “mineralization”, and ankylosis. This sequence was also described for synapsids and recognized as an intermediate condition between full gomphosis and full ankylosis (LeBlanc et al., 2018). The silesaurid pattern identified here challenges the traditional view in which an “ankylo-thecodont” dentition is regarded as synapomorphic for the group (Nesbitt et al., 2010; Nesbitt, 2011; Kammerer et al., 2012; Martz & Small, 2019), showing that ankylosis is only a late stage of tooth ontogeny (Fig. 23). As pointed by LeBlanc et al (2018) for Synapsida, the simple mapping of “ankylosis” and “gomphosis” as alternative states is too simplistic to reconstruct ancestral characters for Dinosauromorpha across phylogenies, because silesaurids may have both stages in the same taxon/individual/jaw and

this may also apply to other still not sampled early members of the group. According to the three character states conceived by LeBlanc et al. (2018), Silesauridae has neither the crocodilian/dinosaur "permanent gomphosis" nor the "rapid ankylosis" that is plesiomorphic for amniotes. Instead, all sampled silesaurids present "delayed ankylosis", in which teeth pass through a gomphosis stage followed by final ankylosis (Fig. 23).

The explanation for the differences in tooth attachment across Synapsida were proposed to reflect a neotenic delay in the onset of ankylosis or to progenesis/truncation of that stage of dental ontogeny, resulting in the stereotypic mammalian permanent gomphosis (LeBlanc et al., 2018). The results found for Silesauridae indicate that an equivalent process might also have happened within Archosauria. Accordingly, differences between silesaurid ankylosis and dinosaur/crocodile gomphosis cannot be considered an increase in tooth complexity (LeBlanc et al., 2017), but to differences on time and sequence of dental ontogeny (Fig. 23). Therefore, crocodile/dinosaur gomphosis represents the maintenance of an early ontogenetic stage, in which alveolar bone does not calcify the periodontal ligament between the tooth root and the adjacent alveolus (LeBlanc et al., 2018)

The phylogenetic position of Silesauridae among Dinosauriformes is still controversial. Although usually considered the sister-group of Dinosauria (Langer & Benton 2006; Ezcurra, 2006; Langer et al., 2010, 2017; Nesbitt et al., 2010, 2017; Nesbitt, 2011; Bittencourt et al., 2015; Baron et al., 2017), another hypothesis places de group on the ornitischian lineage (Ferigolo & Langer, 2007; Langer & Ferigolo, 2013; Cabreira et al., 2016; Müller & Garcia, 2020). In any case, understanding tooth fixation in Silesauridae as a case of "delayed ankylosis" results in accepting dinosaur and crocodile "permanent gomphosis" as acquired convergently, or less likely that the silesaurid condition represents a synapomorphic reversal. Furthermore, if Silesauridae is nested within Ornitischia, "permanent gomphosis" could even be convergent between those dinosaurs and saurischians. In any case, the intermediate condition identified in

silesaurids is likely to occur also in other early archosaurs and dinosauromorphs, so undermining the status of their tooth attachment (the so-called ankylothecodonty; Nesbitt et al., 2010) as synapomorphic for the group. Clearly, further histologic approaches on tooth attachment are required for such taxa, as well as for early dinosaurs, to properly tackle this question.

Conclusion

Histology of the tooth attachment system of various silesaurids challenges the idea of a simple "ankylothecodont" dentition. Instead, tooth attachment in the group involves four phases of dental ontogeny: eruption, gomphosis, "mineralization", and ankylosis. As such, instead of the traditional view in which ankylosis is recovered as a synapomorphic trait of Silesauridae, our data shows that it represents just the last stage of their tooth ontogeny. A broader study of dental tissues is necessary to shed light on the evolution of tooth attachment within dinosauromorphs, including the significance of the "delayed ankylosis" stage seen in Silesauridae. In fact, an ankylo-thecodonty to thecodonty transition appears even more as an oversimplification of a more complex evolutionary history, and features involving tooth attachment must be evaluated accurately when these are codified through archosaur phylogeny. An important emerging aspect is if gomphosis may be synapomorphic to dinosaurs, perhaps representing one of the key characteristics that allowed their thriving on Earth for more than 150 million years (Brussate et al., 2008, 2010; Langer et al., 2010, 2013; Benton et al., 2014; Marsola et al., 2018b).

Acknowledgements

We thank researchers, collection managers, and curators who provided access to the collections under their care, namely: André Silveira, Cecilia Apaldetti, César Schultz, Claudio Revuelta, Fernando Abdala, Fernando Novas, Flávio Pretto, Gabriela Cisterna, Leonardo Haerter, Leonardo Kerber, Martín Ezcurra, Michael Caldwell, Michelle Stocker, Pablo Ortíz, Pedro Hernández, Rodrigo Müller, Ricardo Martínez, Sergio Cabreira, and Vicki Yarborough. Thanks also to Gabriel Baréa for suggestions and improvement in the edition of the pictures. This research was supported by the following grants: FAPESP 2018/24031-6 and 2019/07510-0 to GM; CAPES 88887.468538/2019-00 to JCAM.

References

Baron MG, Norman DB, Barrett PM. 2017. A new hypothesis of dinosaur relationships and early dinosaur evolution. Nature, 543(7646), 501-506.

Benton MJ, Walker AD. 2011. Saltopus, a dinosauriform from the Upper Triassic of Scotland. Earth and Environmental Science Transactions of the Royal Society of Edinburgh, 101(3-4), 285-299.

Benton, MJ, Forth J, Langer MC. 2014. Models for the rise of the dinosaurs. Current Biology, 24(2), R87-R95.

Bittencourt JS, Arcucci AB, Marsicano CA, Langer MC. 2015. Osteology of the Middle Triassic archosaur Lewisuchus admixtus Romer (Chañares Formation, Argentina), its inclusivity, and relationships amongst early dinosauromorphs. Journal of Systematic Palaeontology, 13(3), 189-219.

Brusatte SL, Benton MJ, Ruta M, Lloyd GT. 2008. Superiority, competition, and opportunism in the evolutionary radiation of dinosaurs. Science, 321(5895), 1485-1488.

Brusatte SL, Nesbitt SJ, Irmis RB, Butler RJ, Benton MJ, Norell MA. 2010. The origin and early radiation of dinosaurs. Earth-Science Reviews, 101(1-2), 68-100.

Budney L. A., M. W. Caldwell, and A. Albino. 2006. Tooth socket histology in the Cretaceous snake Dinilysia, with a review of amniote dental attachment tissues. Journal of Vertebrate Paleontology 26:138–145.

Cabreira SF, Kellner AWA, Dias-da-Silva S, da Silva LR, Bronzati M, Marsola JC, Müller RT, Bittencourt JS, Batista BJ, Raugust T, Carrilho, R, Brodt A. 2016. A unique Late Triassic dinosauromorph assemblage reveals dinosaur ancestral anatomy and diet. Current Biology, 26(22), 3090-3095.

Caldwell MW, Budney LA, Lamoureux DO. 2003. Histology of tooth attachment tissues in the Late Cretaceous mosasaurid Platecarpus. Journal of Vertebrate Paleontology 23:622–630.

Chen J, LeBlanc ARH, Jin L, Huang T, Reisz RR. 2018. Tooth development, histology, and enamel microstructure in Changchunsaurus parvus: Implications for dental evolution in ornithopod dinosaurs. PLoS ONE 13(11): e0205206.

Edmund AG. 1960. Tooth replacement phenomena in the lower vertebrates. Royal Ontario Museum, Life Sciences Division, Contribution 52:1–190.

Ezcurra MD. 2016. The phylogenetic relationships of basal archosauromorphs, with an emphasis on the systematics of proterosuchian archosauriforms. PeerJ, 4, e1778.

Ezcurra MD., Nesbitt SJ, Fiorelli LE, Desojo JB. 2019. New specimen sheds light on the anatomy and taxonomy of the early Late Triassic dinosauriforms from the Chañares Formation, NW Argentina. The Anatomical Record, 303(5), 1393-1438.

Ferigolo J, Langer MC. 2007. A Late Triassic dinosauriform from south Brazil and the origin of the ornithischian predentary bone. Historical Biology, 19(1), 23-33.

Fong RK, LeBlanc ARH, Berman DS, Reisz RR. 2016. Dental histology of Coelophysis bauri and the evolution of tooth attachment tissues in early dinosaurs: dinosaur dental histology. Journal of Morphology 277:916–924.

García RA, Zurriaguz V. 2016. Histology of teeth and tooth attachment in titanosaurs (Dinosauria; Sauropoda). Cretaceous Research, 57, 248-256.

Kammerer CF, Nesbitt SJ, Shubin NH. 2011. The first silesaurid dinosauriform from the Late Triassic of Morocco. Acta Palaeontologica Polonica, 57(2), 277-284.

Langer MC, Ezcurra MD, Bittencourt JS, Novas FE. 2010. The origin and early evolution of dinosaurs. Biological Reviews, 85(1), 55-110.

Langer MC, Ferigolo J. 2013. The Late Triassic dinosauromorph *Sacisaurus agudoensis* (Caturrita Formation; Rio Grande do Sul, Brazil): anatomy and affinities. Geological Society, London, Special Publications, 379(1), 353-392.

Langer MC, Ramezani J, Da Rosa AS. 2018. U-Pb age constraints on dinosaur rise from South Brazil.. Gondwana Research, 57, 133-140.

Langer MC, Nesbitt SJ, Bittencourt JS, Irmis RB. 2013. Non-dinosaurian dinosauromorpha. Geological Society, London, Special Publications, 379(1), 157-186.

Langer MC, Ezcurra MD, Rauhut OW, Benton MJ, Knoll F, McPhee BW, Novas FE., Pol D, Brusatte SL. 2017. Untangling the dinosaur family tree. Nature, 551(7678), E1-E3.

LeBlanc ARH, Reisz RR. 2013. Periodontal ligament, cementum, and alveolar bone in the oldest herbivorous tetrapods, and their evolutionary significance. PLoS ONE 8:e74697.

LeBlanc ARH, Reisz RR, Brink KS, Abdala F. 2016. Mineralized periodontia in extinct relatives of mammals shed light on the evolutionary history of mineral homeostasis in periodontal tissue maintenance. Journal of Clinical Periodontology 4.

LeBlanc ARH, Brink KS, Cullen TM, Reisz RR. 2017. Evolutionary implications of tooth attachment versus tooth implantation: a case study using dinosaur, crocodilian, and mammal teeth. J. Vertebr. Paleontol. 37, e1354006.

LeBlanc ARH, Brink KS, Whitney MR, Abdala F, Reisz RR. 2018. Dental ontogeny in extinct synapsids reveals a complex evolutionary history of the mammalian tooth attachment system. Proc. R. Soc. B 285: 20181792.

Martin LD, Stewart JD. 1999. Implantation and replacement of bird teeth. Smithsonian Contributions to Paleobiology, 89, 295-300.

Marsola JC, Bittencourt JS, Da Rosa AS, Martinelli AG, Ribeiro AM, Ferigolo J, Langer MC. 2018a. New sauropodomorph and cynodont remains from the late triassic Sacisaurus site in Southern Brazil and its stratigraphic position in the Norian Caturrita Formation. Acta Palaeontologica Polonica 63 (4): 653-669.

Marsola JC, Ferreira GS, Langer MC, Button D J, Butler RJ. 2018b. Increases in sampling support the southern Gondwanan hypothesis for the origin of dinosaurs. Palaeontology, 62(3), 473-482.

Martz JW, Small BJ. 2019. Non-dinosaurian dinosauromorphs from the Chinle Formation (Upper Triassic) of the Eagle Basin, northern Colorado: Dromomeron romeri (Lagerpetidae) and a new taxon, Kwanasaurus williamparkeri (Silesauridae). PeerJ, 7, e7551.

Maxwell, EE, Caldwell MW, Lamoureux, DO. (2011). The structure and phylogenetic distribution of amniote plicidentine. Journal of Vertebrate Paleontology, 31(3), 553-561.

Modesto SP, Sues HD. 2004. The skull of the early Triassic archosauromorph reptile Prolacerta broomi and its phylogenetic significance. Zoological Journal, 140 (3), 335-351.

Müller RT, Garcia MS. (2020) A paraphyletic 'Silesauridae' as an alternative hypothesis for the initial radiation of ornithischian dinosaurs. Biol. Lett. 16:20200417.

Nanci A. 2013. Ten Cate's Oral Histology: Development, Structure, and Function. Amsterdam: Elsevier. 379p.

Nesbitt SJ, Sidor CA, Irmis RB, Angielczyk KD, Smith RM, Tsuji LA. 2010. Ecologically distinct dinosaurian sister group shows early diversification of Ornithodira. Nature, 464(7285), 95.

Nesbitt SJ. 2011. The early evolution of archosaurs: relationships and the origin of major clades. Bulletin of the American Museum of Natural History, 2011(352), 1-292.

Nesbitt SJ, Butler RJ, Ezcurra MD, Barrett PM, Stocker MR, Angielczyk KD, Smith RMH, Sidor CA, Niedzwiedzki G, Sennikov AG, Charig AJ. 2017. The earliest bird-line archosaurs and the assembly of the dinosaur body plan. Nature, 544(7651), 484-487.

Nesbitt SJ, Langer MC, Ezcurra MD. 2020. The anatomy of Asilisaurus kongwe, a dinosauriform from the Lifua Member of the Manda Beds (~ Middle Triassic) of Africa. The Anatomical Record, 303(4), 813-873.

Peecook BR, Steyer JS, Tabor NJ, Smith RM. 2018. Updated geology and vertebrate paleontology pf the Triassic Ntawere Formation of Northeastern Zambia, with special emphasis on the archosauromorphs. Journal of Vertebrate Paleontology, 37(sup1), 8-38.

Reid REH. 1996. Bone histology of the Cleveland-Lloyd dinosaurs and of dinosaurs in general, part 1: Introduction: Introduction to bone tissues. Brigham Young University, Geological Studies 41: 25–71.

Richman JM, Handrigan GR. 2011. Reptilian tooth development. genesis, 49(4), 247-260.

Sassoon J, Foffa D, Marek R. 2015. Dental ontogeny and replacement in Pliosauridae. Royal Society open science, 2(11), 150384.

Snyder AJ, LeBlanc ARH, Jun C, Bevitt JJ, Reisz RR. 2020. Thecodont tooth attachment and replacement in bolosaurid parareptiles. PeerJ, 8, e9168.

Sullivan RM, Lucas SG. 1999. Eucoelophysis baldwini a new theropod dinosaur from the Upper Triassic of New Mexico, and the status of the original types of Coelophysis. Journal of Vertebrate Paleontology, 19(1), 81-90.

Wu P, Wu X, Jiang TX, Elsey RM, Temple BL, Divers SJ, Glenn TC, Yuan K, Chen, M, Widelitz RB, Chuong CM. 2013. Specialized stem cell niche enables repetitive renewal of alligator teeth. Proceedings of the National Academy of Sciences, 110(22), E2009-E2018.

Zaher H, Rieppel O. 1999. Tooth implantation and replacement in squamates, with special reference to mosasaur lizards and snakes. American Museum Novitates 3271:1–19.

Table 1. Measurements taken from the specimens. AB = alveolar bone; AC = acellular cementum. CC = cellular cementum. GD1 = first layer of granular dentine. GD2 = second layer of granular dentine. JB = jaw bone

Specie/osteohistology information	**GD1**	**GD2**	**AC**	**CC**	**AB**	**JB**
Eucoelophysis baldwini	10 µm	24 µm	10 µm	114 µm	500 µm	750 µm
UFSM 11579 – maxilla	NA	NA	13 µm	100 µm	300 µm	290 µm
UFSM 1579 – dentary	8 µm	12 µm	11 µm	91 µm	370 µm	125 µm
Sacisaurus agudoensis	NA	NA	9 µm	57 µm	145 µm	142 µm
***Asilisaurus konwge* 1086**	18 µm	NA	10 µm	57 µm	227 µm	227 µm
***Asilisaurus kongwe* 1087**	18 µm	NA	10 µm	91 µm	182 µm	409 µm

Figures

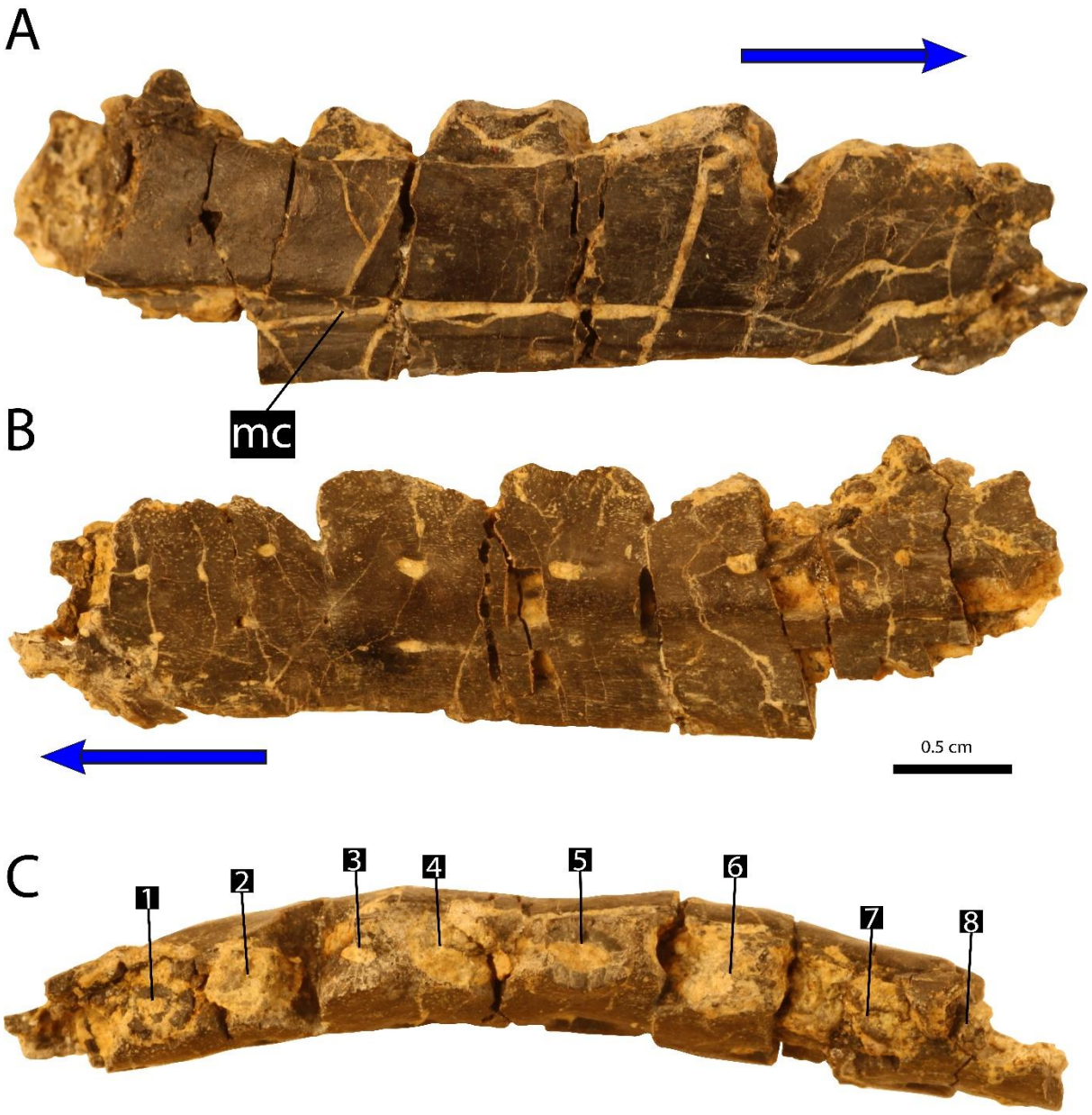

Figure 1. *Eucoelophysis baldwini* (GR 1072) right dentary fragment in lingual (A), labial (B) and dorsal (C) views prior to sectioning. Abbreviations: mc = Meckelian canal. Big blue arrow indicates the anterior direction; numbers indicate the alveoli position.

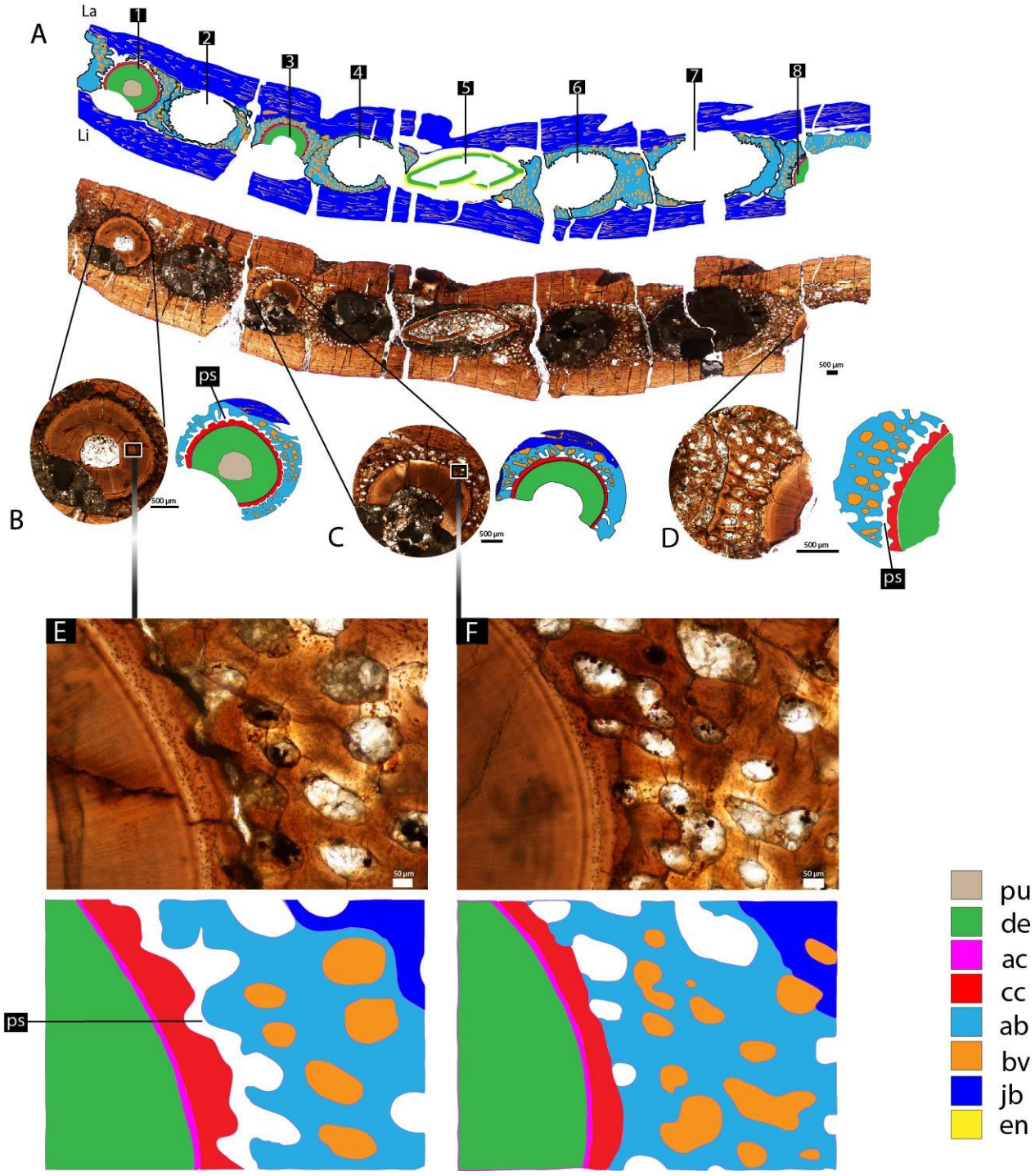

Figure 2. *Eucoelophysis baldwini* (GR 1072) right dentary, dental tissues in coronal section at root level, with diagrammatic illustrations. **A.** General view. **B-D.** Teeth of the first, third, and eighth alveoli. **E.** Detail of "B", showing unmineralized periodontal space. **F.** Detail of "C" showing the contact between the alveolar bone and the cellular cementum. Abbreviations: AC = acellular cementum; AB = alveolar bone; BV = blood vessel; CC = cellular cementum; de = dentine; en = enamel; jb = jaw bone; La = labial side; Li = lingual side; ps = periodontal space; pu = Pulp. Numbers indicate alveoli position.

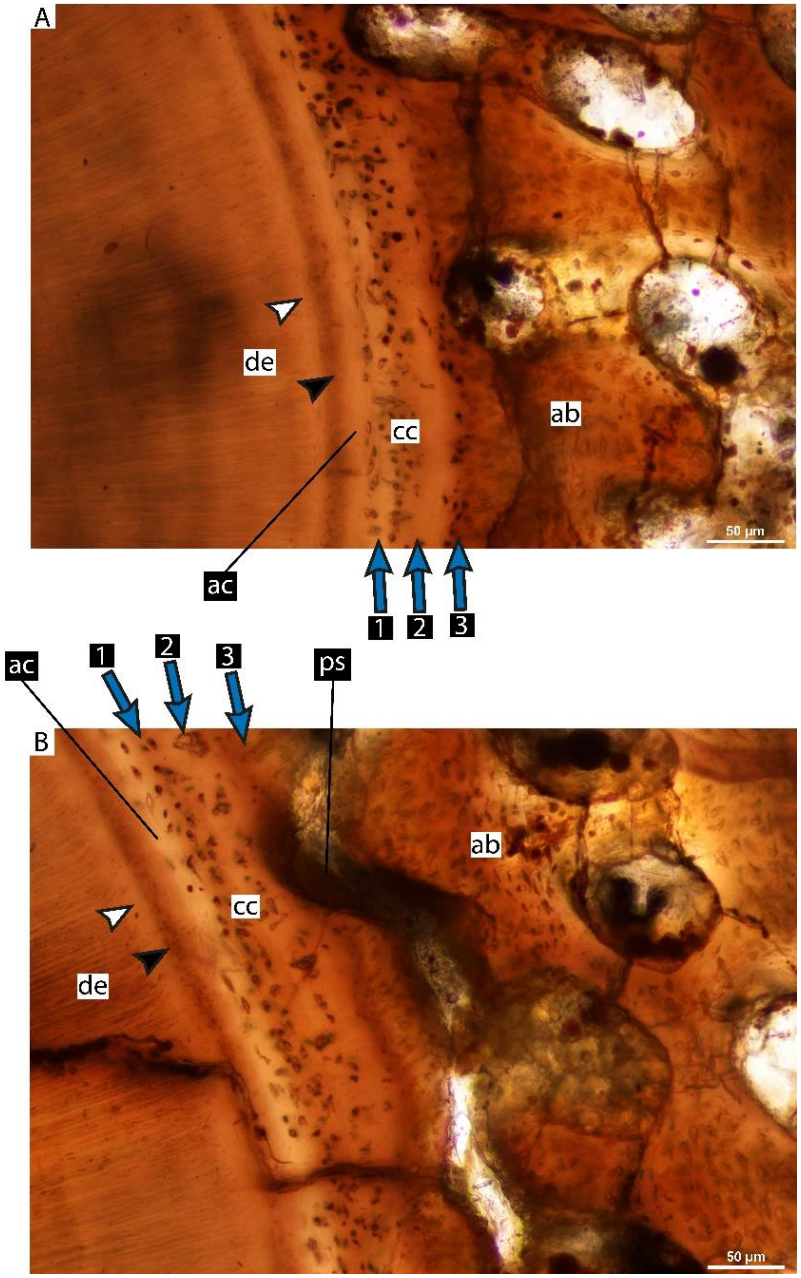

Figure 3. *Eucoelophysis baldwini* (GR 1072) right dentary, dental tissues in coronal section. **A.** Detail of the tooth in the third alveolus, showing the contact between the cellular cementum and alveolar bone (mineralized periodontal space). **B.** Detail of the tooth in the first alveolus, showing unmineralized periodontal space. Abbreviations: as in Fig. 2. White and black arrows indicate first and second layer of globular dentine, blue arrows indicate first, second, and third layers of cellular cementum.

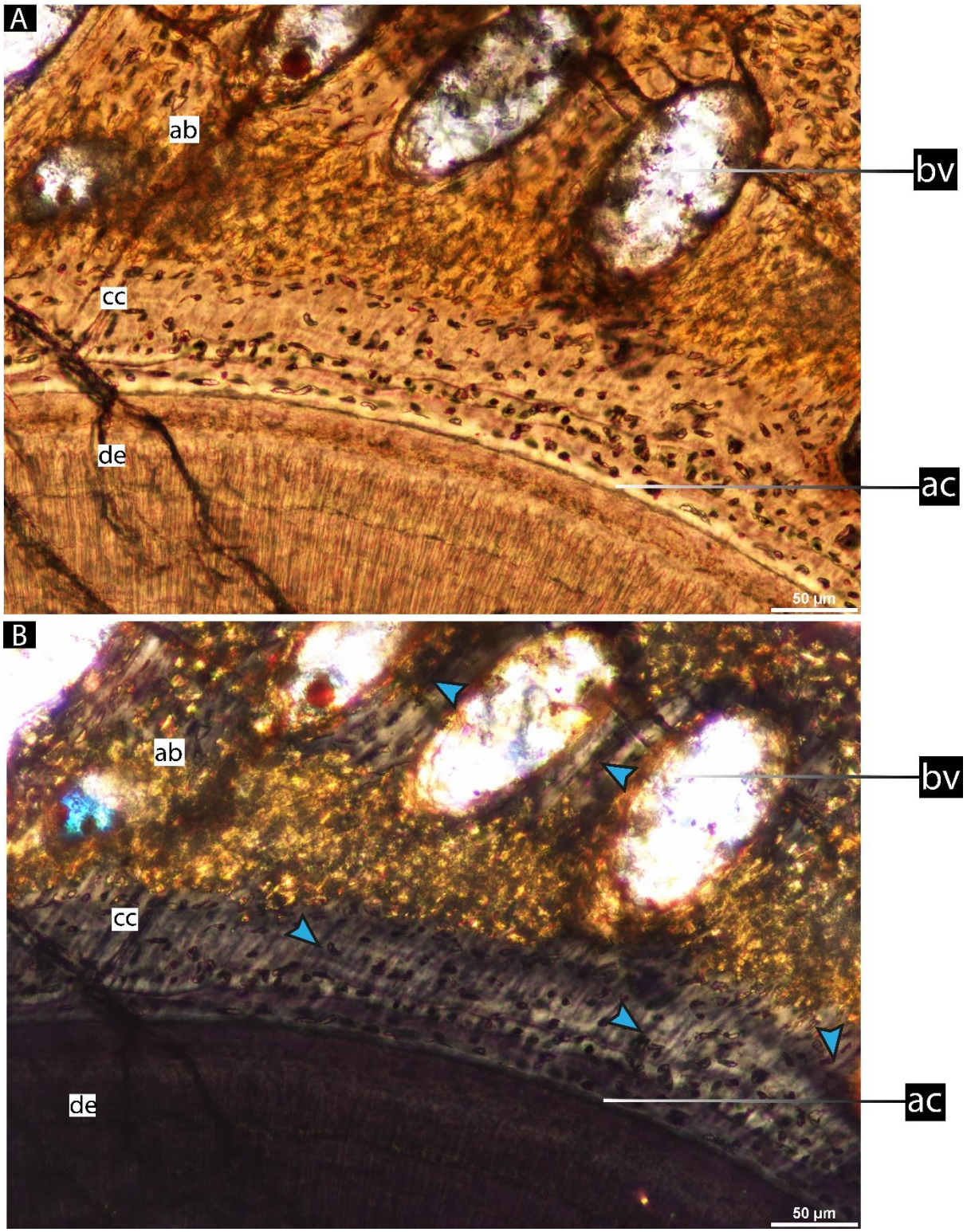

Figure 4. *Eucoelophysis baldwini* (GR 1072) right dentary, dental tissues in coronal section at root level. **A.** Details of the tooth positioned in the third alveolus, showing the alveolar bone and cellular cementum contact, and a periodontal space completely mineralized. **B.** "A" under cross-polarized light, showing Sharpey's fibers across de cellular cementum and alveolar bone layers (blue arrows). Abbreviations: as in Fig. 2.

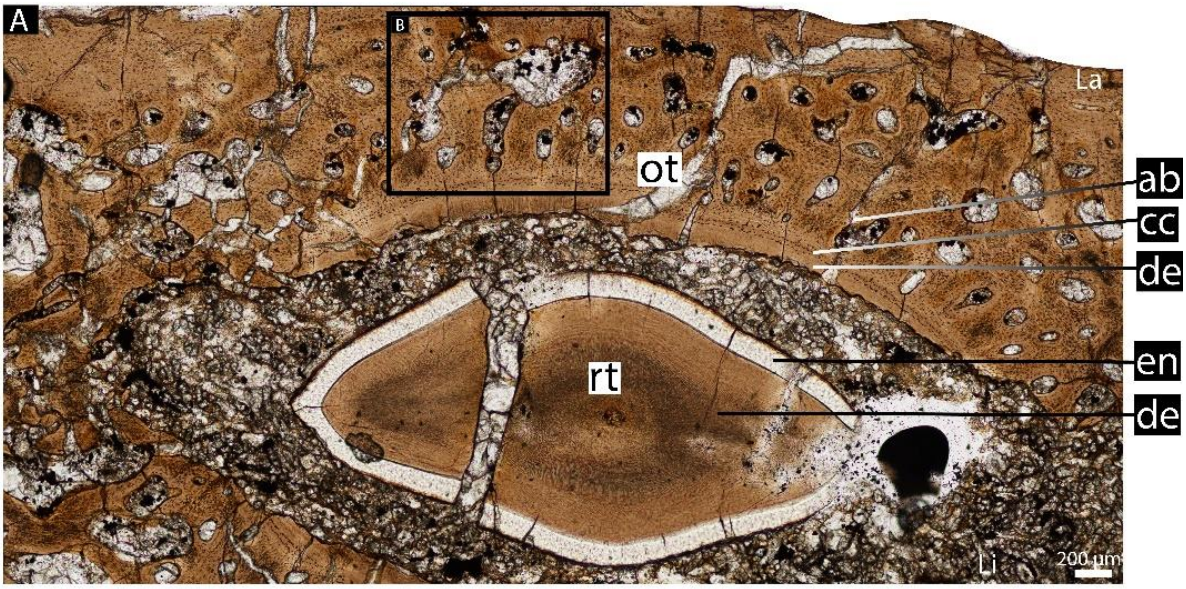

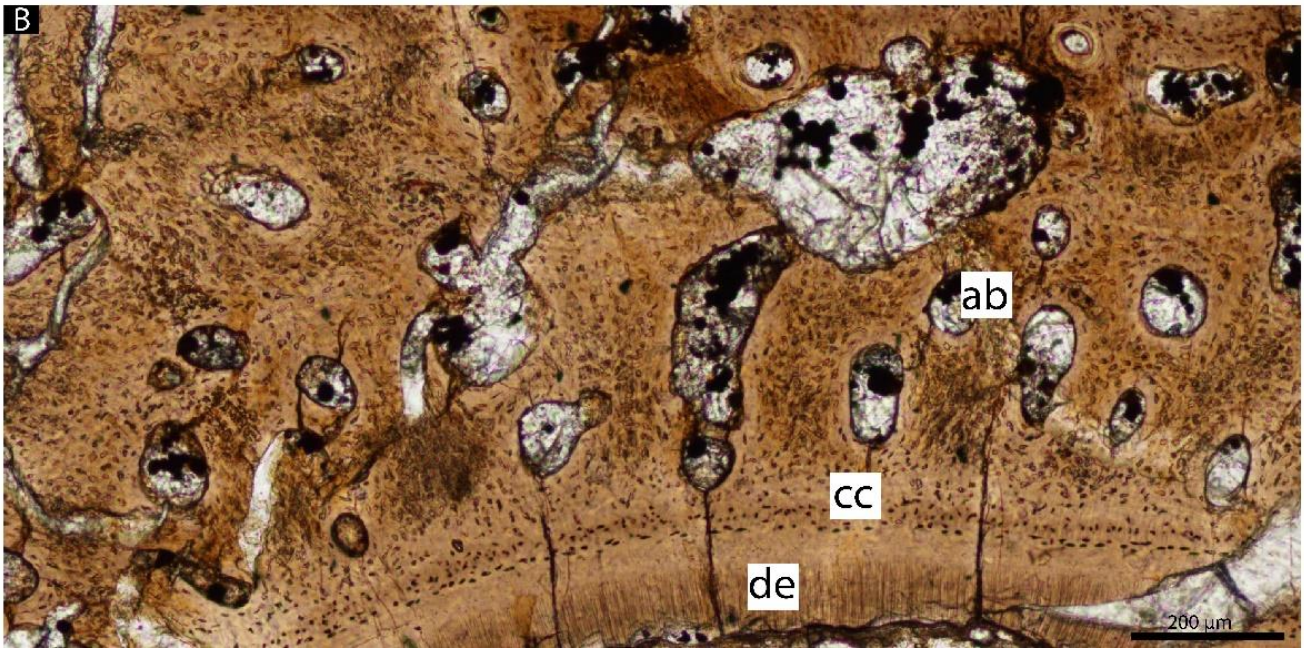

Figure 5. *Eucoelophysis baldwini* (GR 1072) right dentary, dental tissues in coronal section at root level. Replacement tooth and old tooth generation (fifth alveolus). **A**. replacement tooth and remnant of previous tooth generation. **B.** Old generation tooth showing tooth attachment details. Note the contact between the cellular cementum and the alveolar bone, completely mineralizing the periodontal space (ankylosis). Abbreviations: as in Fig. 2, plus: ot = old tooth generation; rt = replacement tooth.

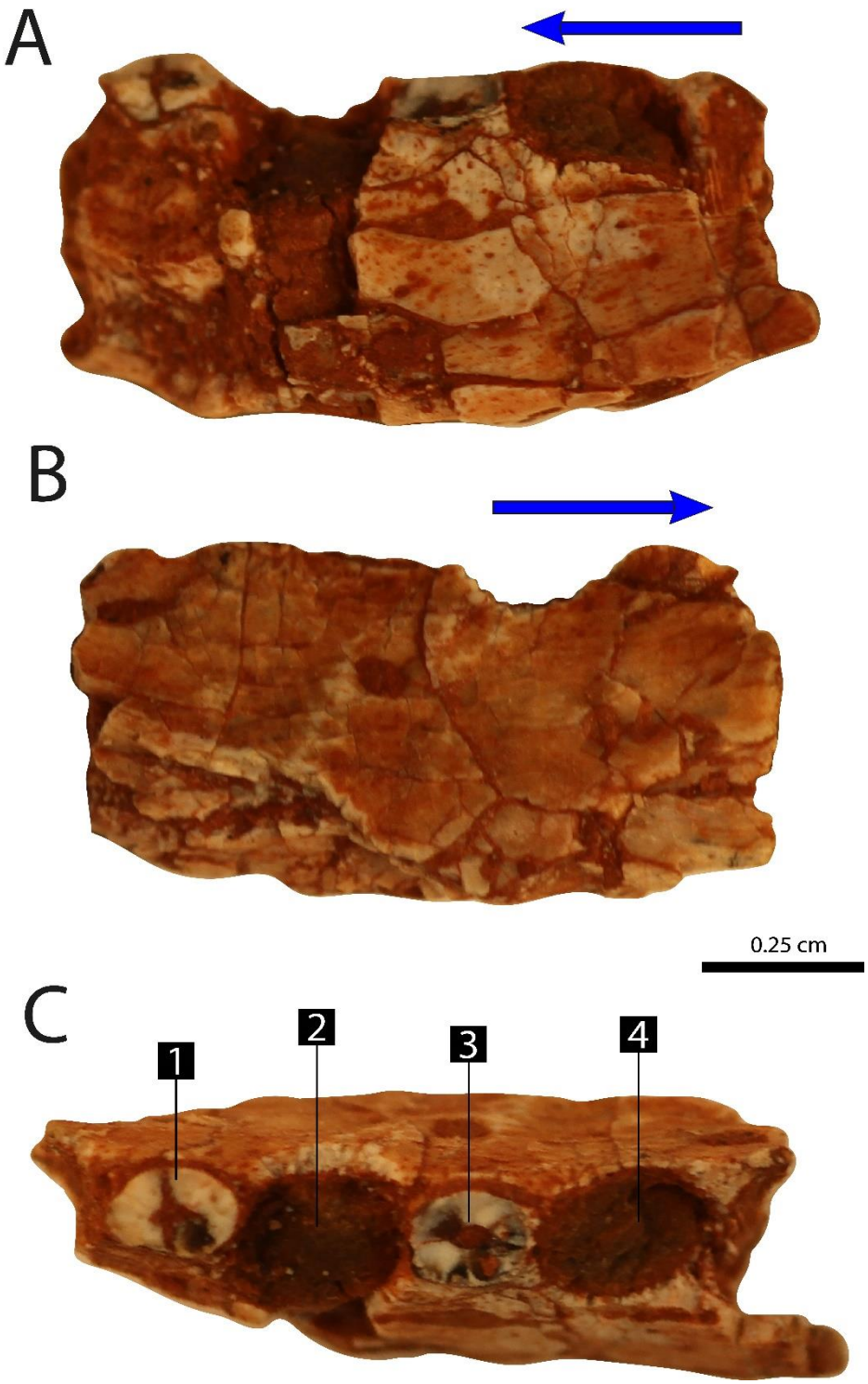

Figure 6. UFSM 1579 left maxilla fragment in a lingual (A), labial (B), and dorsal (C) views prior to sectioning. Blue arrow indicates anterior direction; numbers indicate alveoli positions.

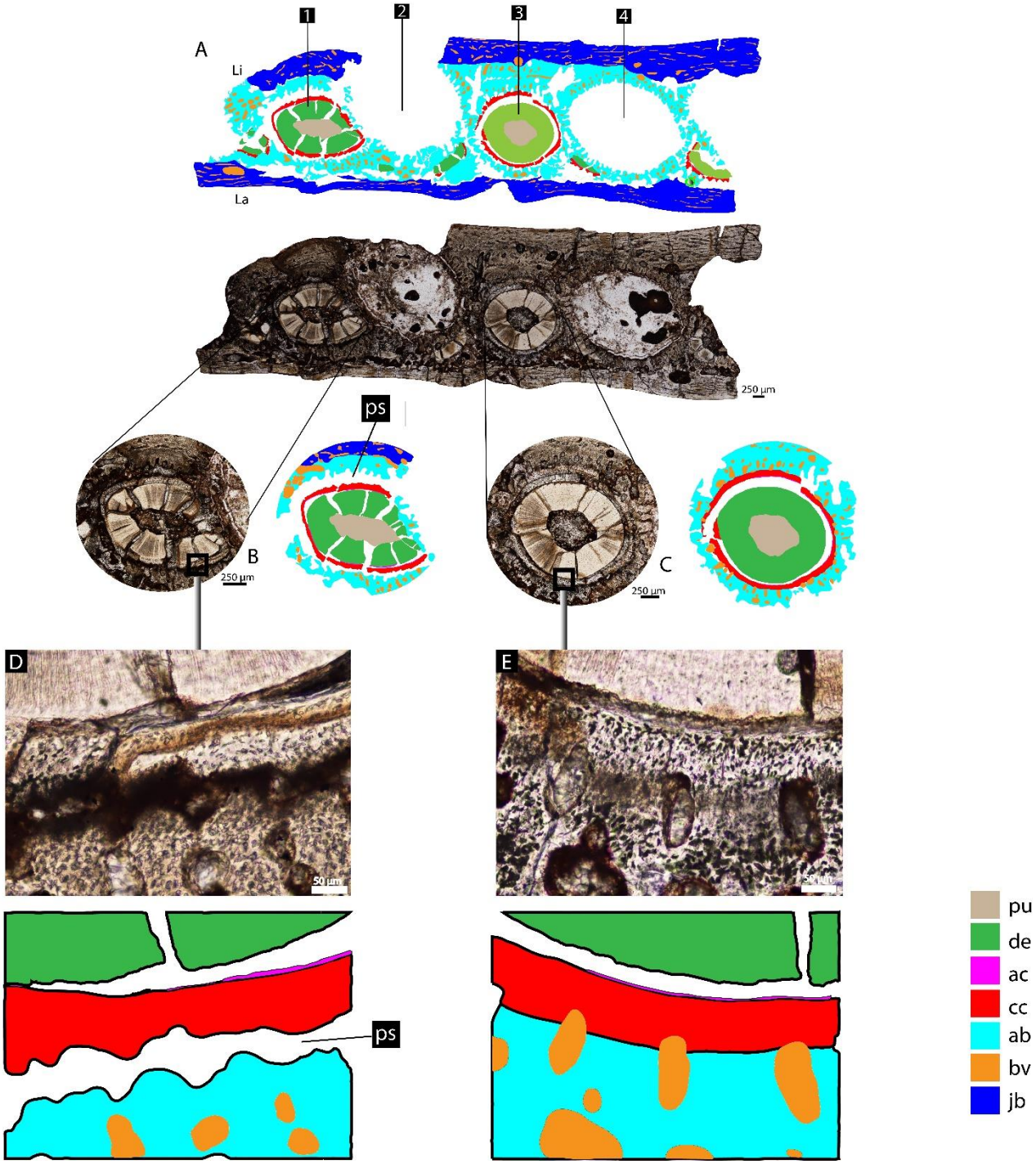

Figure 7. UFSM 1579 left maxilla, dental tissues in coronal section at root level, with diagrammatic illustrations. **A.** General view. **B-C.** Teeth of the first and third alveoli. **D.** Detail of "B", showing unmineralized periodontal space. **E.** Detail of "C" showing the contact between the alveolar bone and the cellular cementum. Abbreviations: as in Fig. 2.

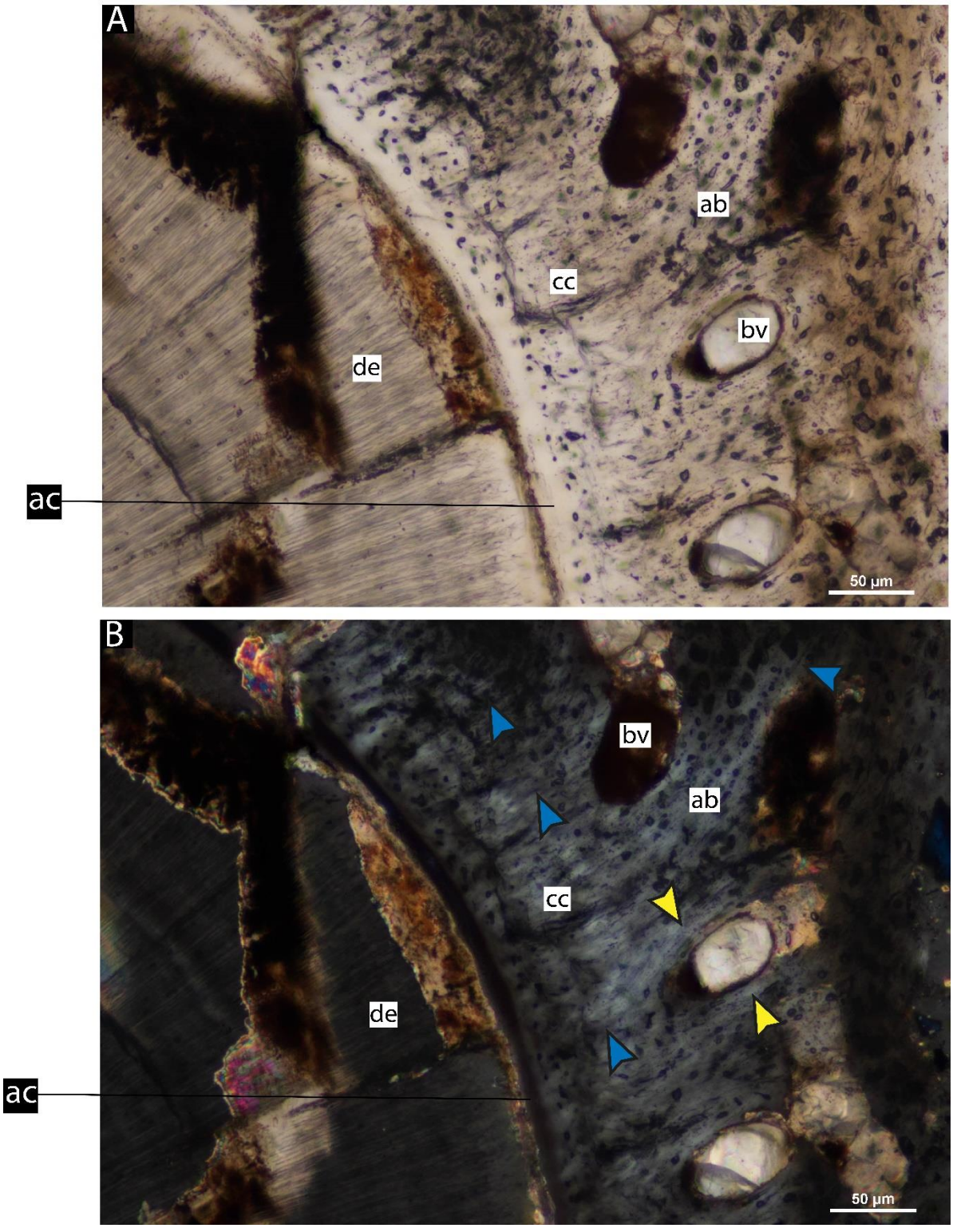

Figure 8. UFSM 1579 left maxilla, dental tissues in coronal section at root level. **A** Details of the tooth positioned in the third alveolus, showing the alveolar bone and cellular cementum contact (mineralized periodontal space). **B.** "A" under cross-polarized light, showing Sharpey's fibers across de cellular cementum and alveolar bone layers (blue arrows). Abbreviations: as in Fig.2. Yellow arrows indicate lamellar bone.

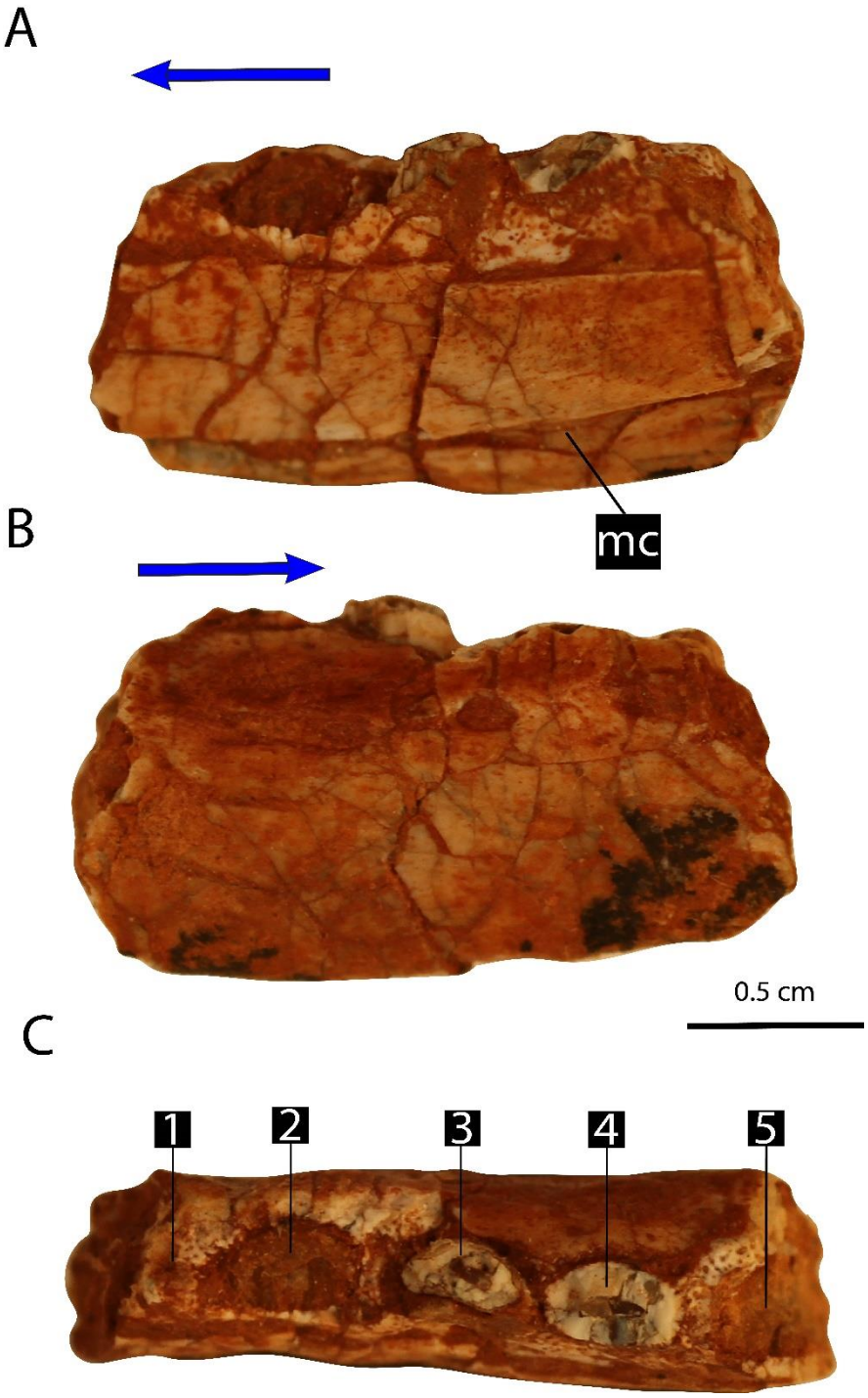

Figure 9. UFSM 1579 right dentary fragment in a lingual (A), labial (B), and dorsal (C) views prior to sectioning. Symbols as in Fig. 6.

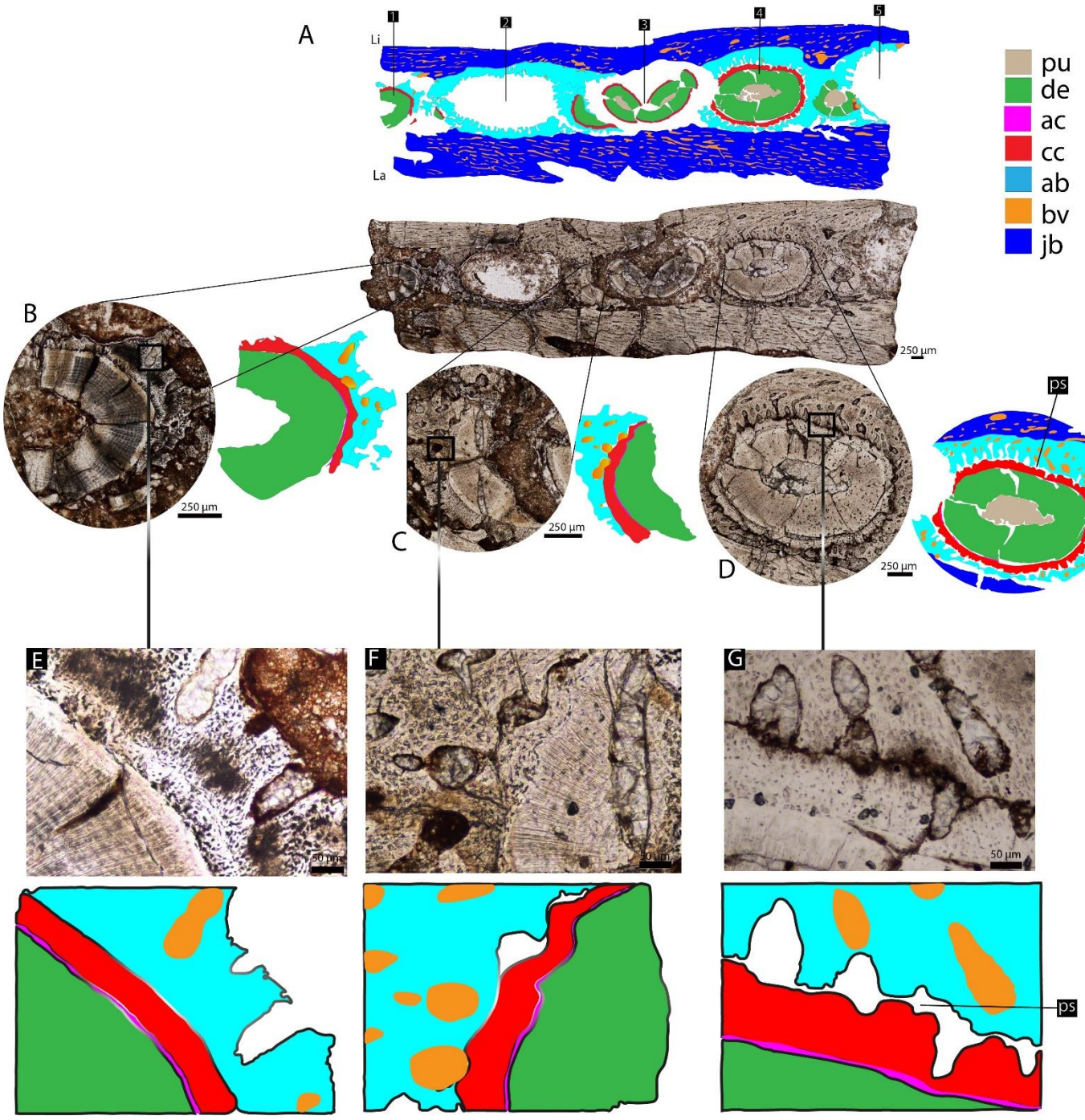

Figure 10. UFSM 1579 right dentary, dental tissues in coronal section at root level, with diagrammatic illustrations. **A.** General view. **B.** Tooth of the first alveolus. **C.** Old generation tooth of the third alveolus. **D.** Tooth of the fourth alveolus. **E-F.** Detail of "B" and "C", showing the contact between the alveolar bone and the cellular cementum. **G.** Detail of "D" showing unmineralized periodontal space. Symbols and abbreviations: as in Fig.2.

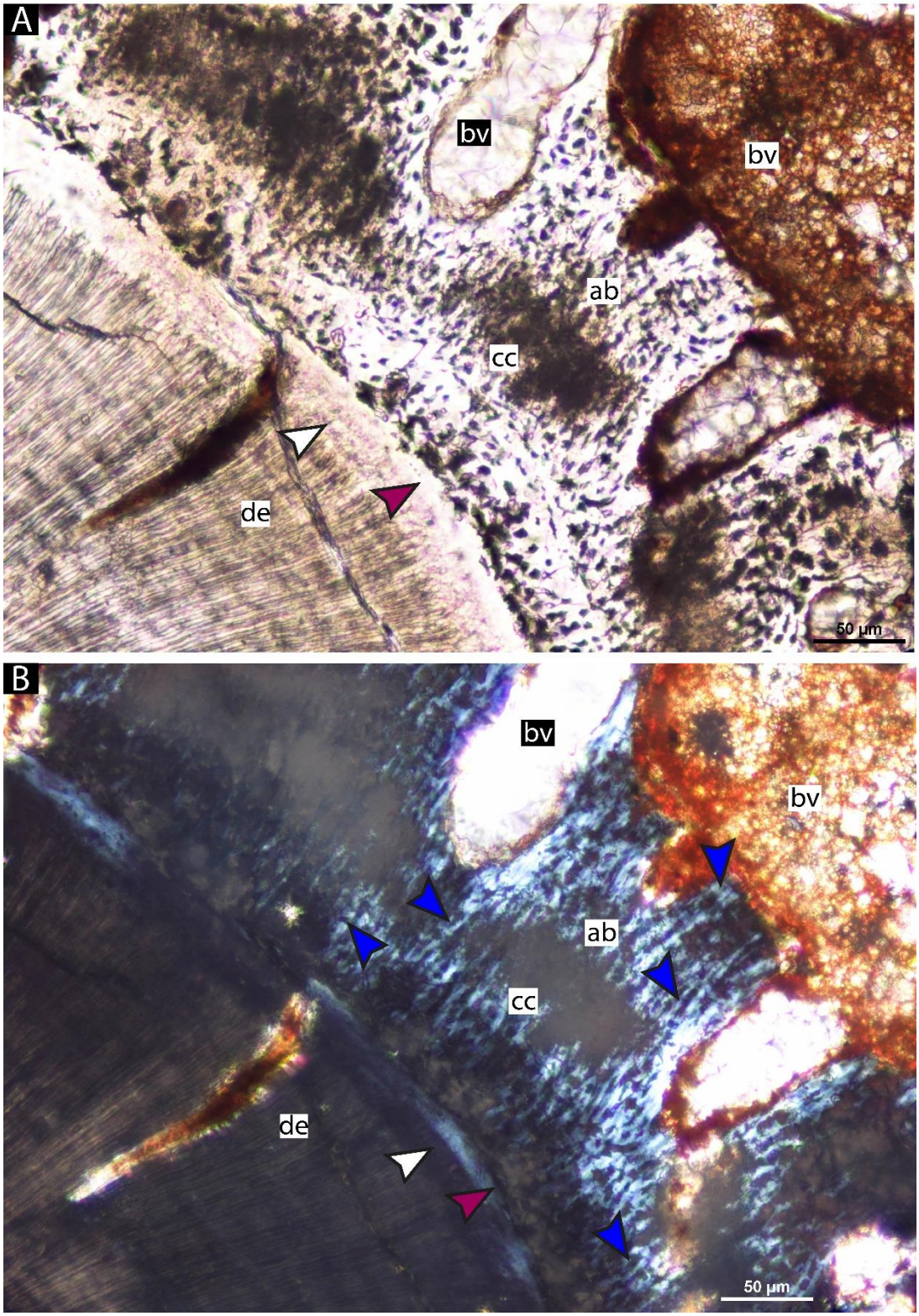

Figure 11 UFSM 1579 right dentary, dental tissues in coronal section at root level. **A.** Details of the tooth positioned in the first alveolus, showing the alveolar bone and cellular cementum contact (mineralized periodontal space). **B.** "A" under cross-polarized light, showing Sharpey's fibers across de cellular cementum and alveolar bone layers (blue arrows). Abbreviations: as in Fig.2. White arrow indicates the granular layer of dentine; purple arrow indicates the acellular cementum.

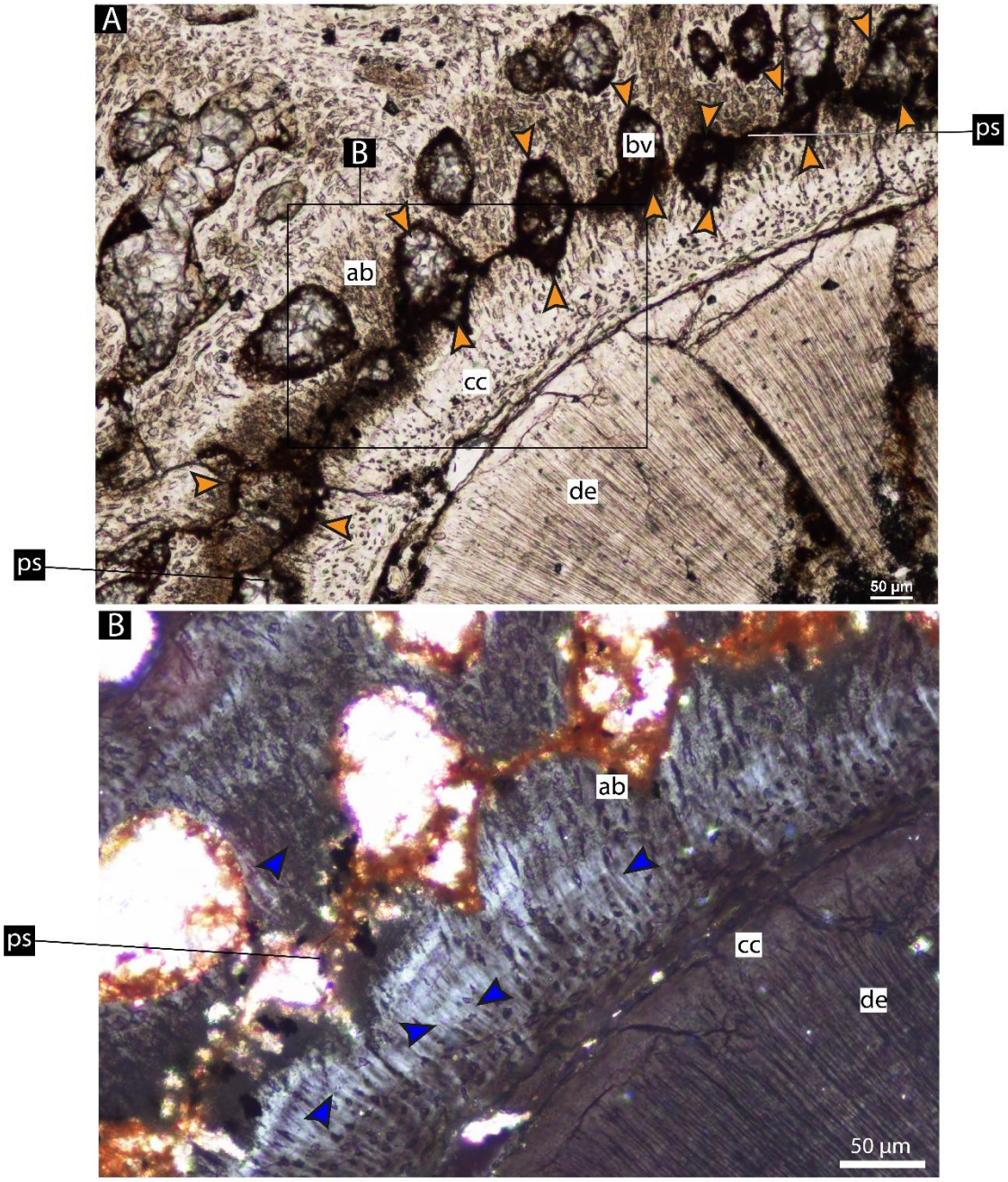

Figure 12. UFSM 1579 right dentary, dental tissues in coronal section at root level. Tooth in the fourth alveolus position. **A.** Tooth attachment details showing the "wave shape" of the periodontal space resulting from the position of the blood vessels. **B.** "A" under cross polarized light, showing Sharpey's fibers across de cellular cementum and alveolar bone layers (blue arrows). Abbreviations: as in Fig.2. Orange arrows indicate blood vessels.

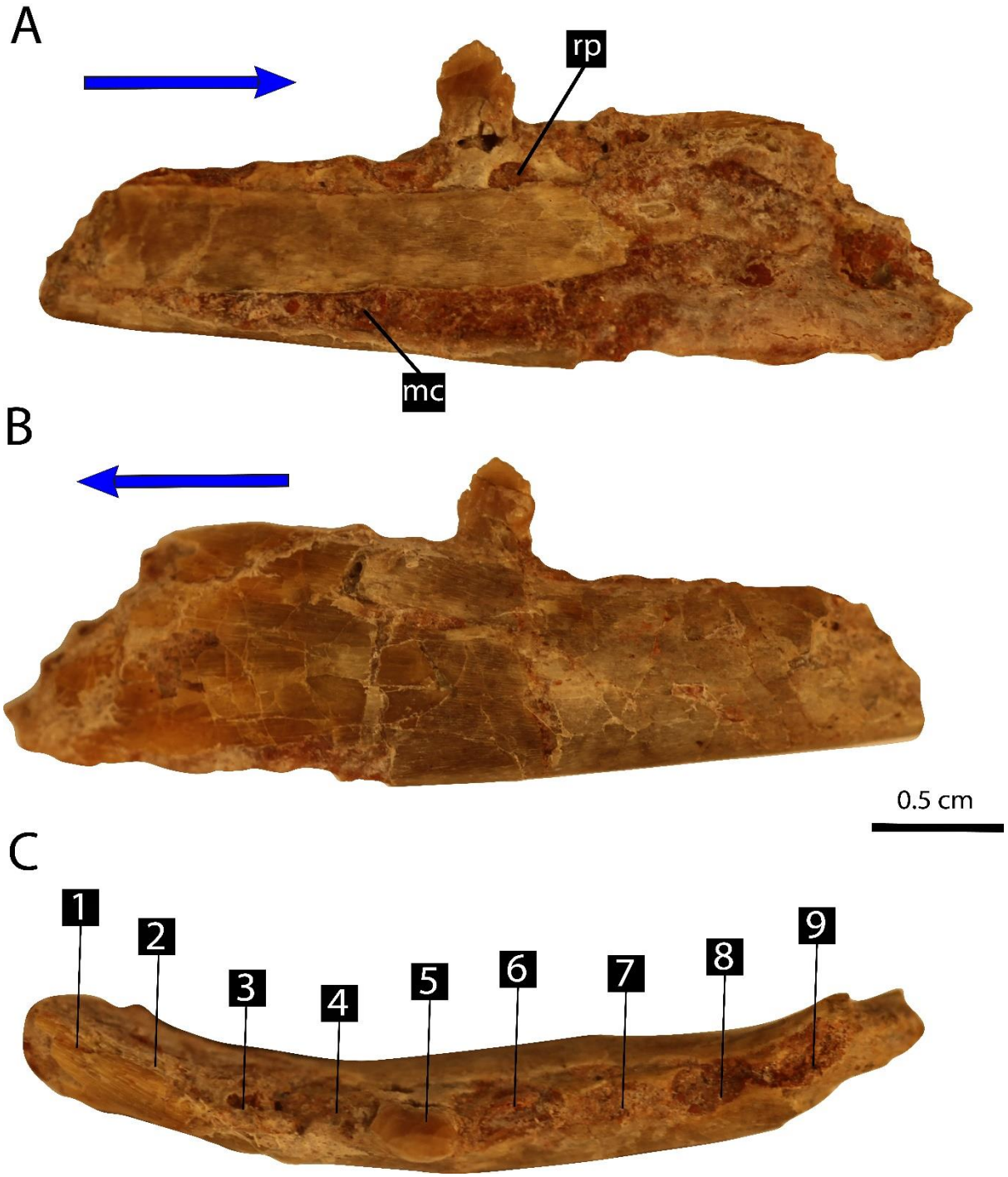

Figure 13. *Sacisaurus agudoensis* (MCN PV 10095) left dentary fragment in lingual (A), labial (B), and dorsal (C) views prior to sectioning. Abbreviation: rp = resorption pit. Symbols as in Fig. 6.

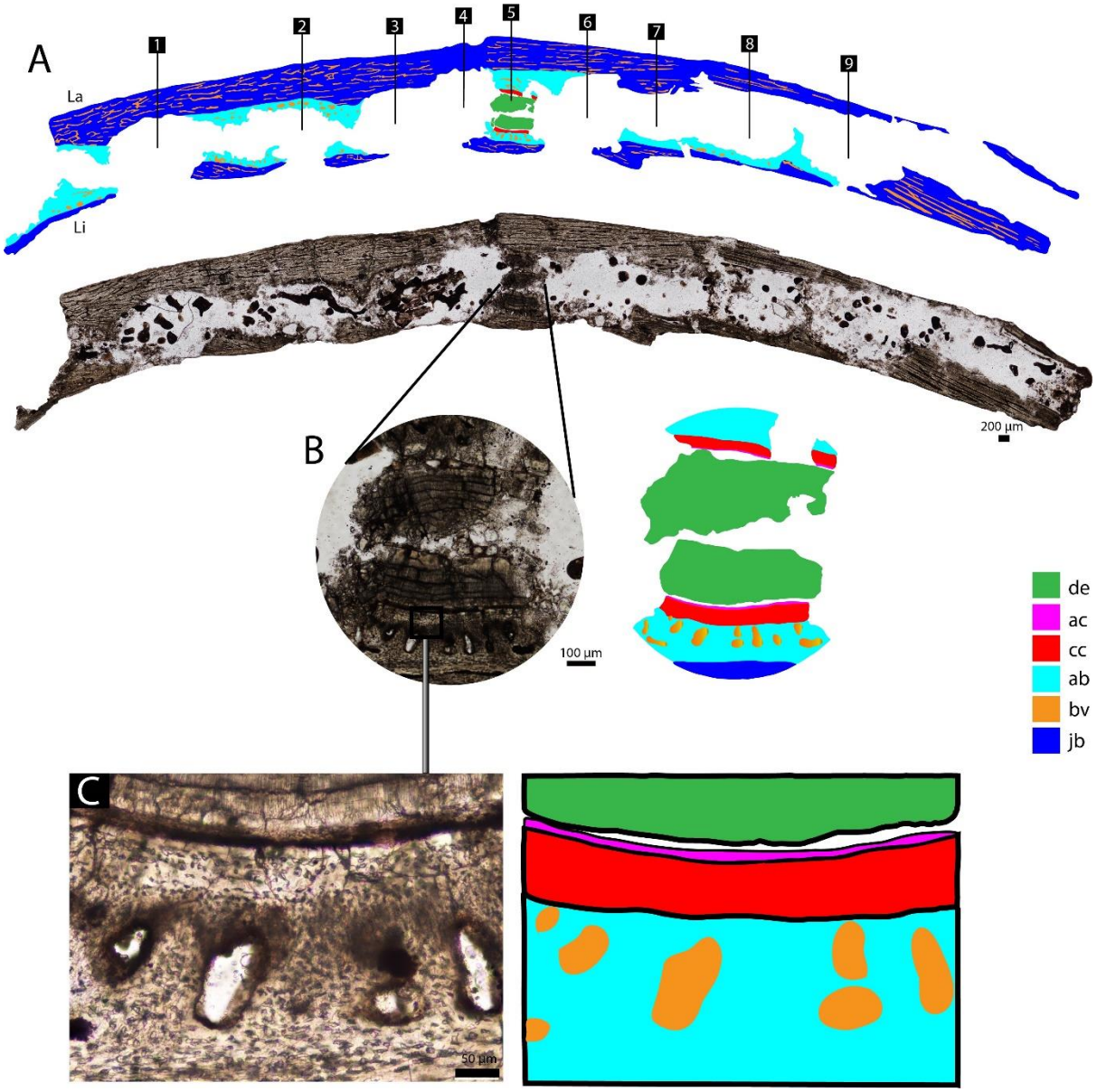

Figure 14. *Sacisaurus agudoensis* (MCN PV 10095) left dentary, dental tissues in coronal section at root level, with diagrammatic illustrations. **A.** General view. **B.** Tooth of the eighth alveolus. **C.** Detail of "B", showing the contact between the alveolar bone and the cellular cementum. Abbreviations: as in Fig. 2.

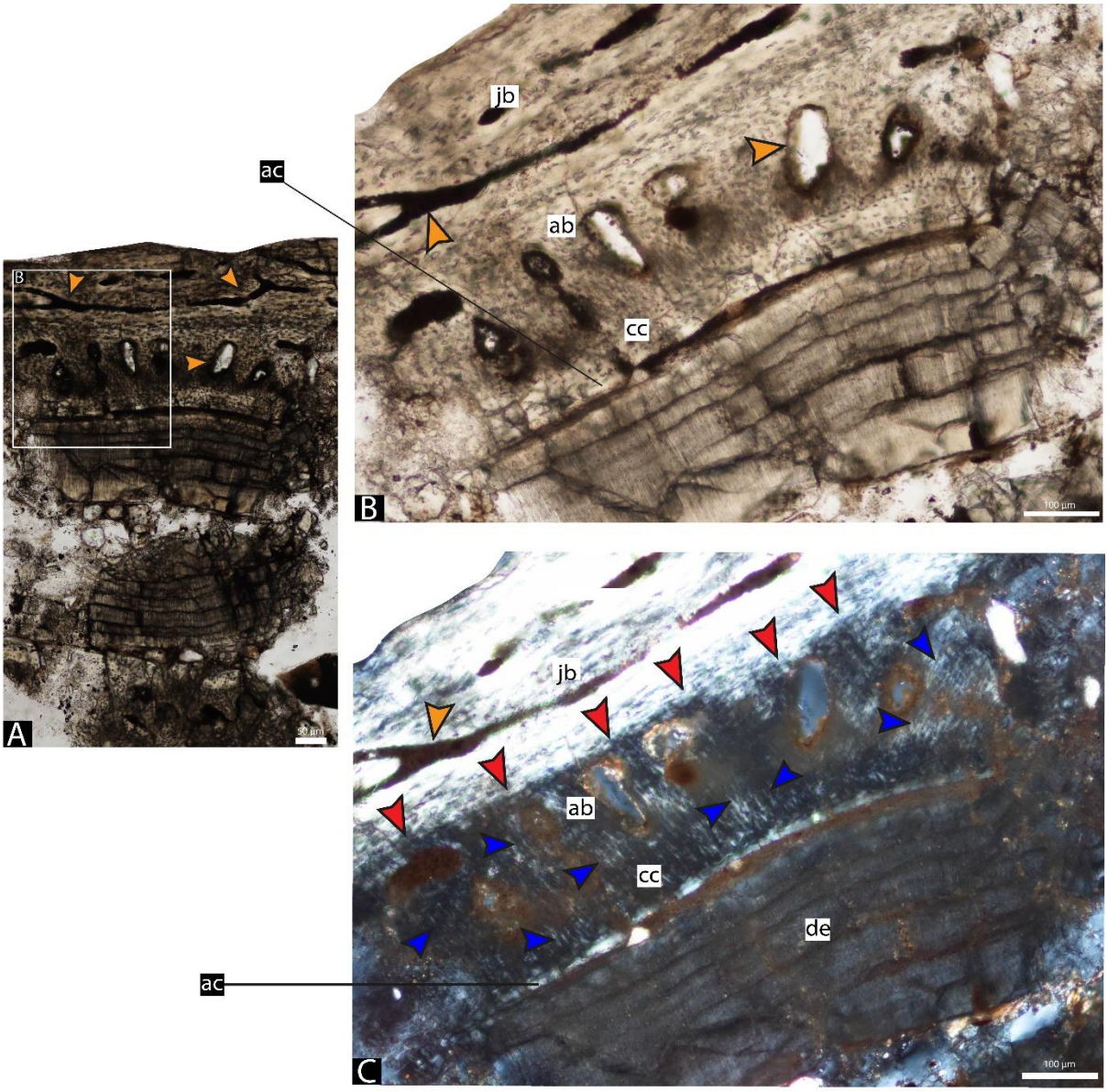

Figure 15. *Sacisaurus agudoensis* (MCN PV 10095) left dentary, dental tissues in coronal section at root level. **A.** Tooth of the fifth alveolus. **B.** Blood vessels (orange arrows) morphology and tooth attachment details. **C.** "B" under polarized light, showing the reversal line (red arrows), separating the alveolar bone from the jaw bone, and the presence of Sharpey's fibers across the cellular cementum and alveolar bone (blue arrows). Abbreviations: as in Fig.2.

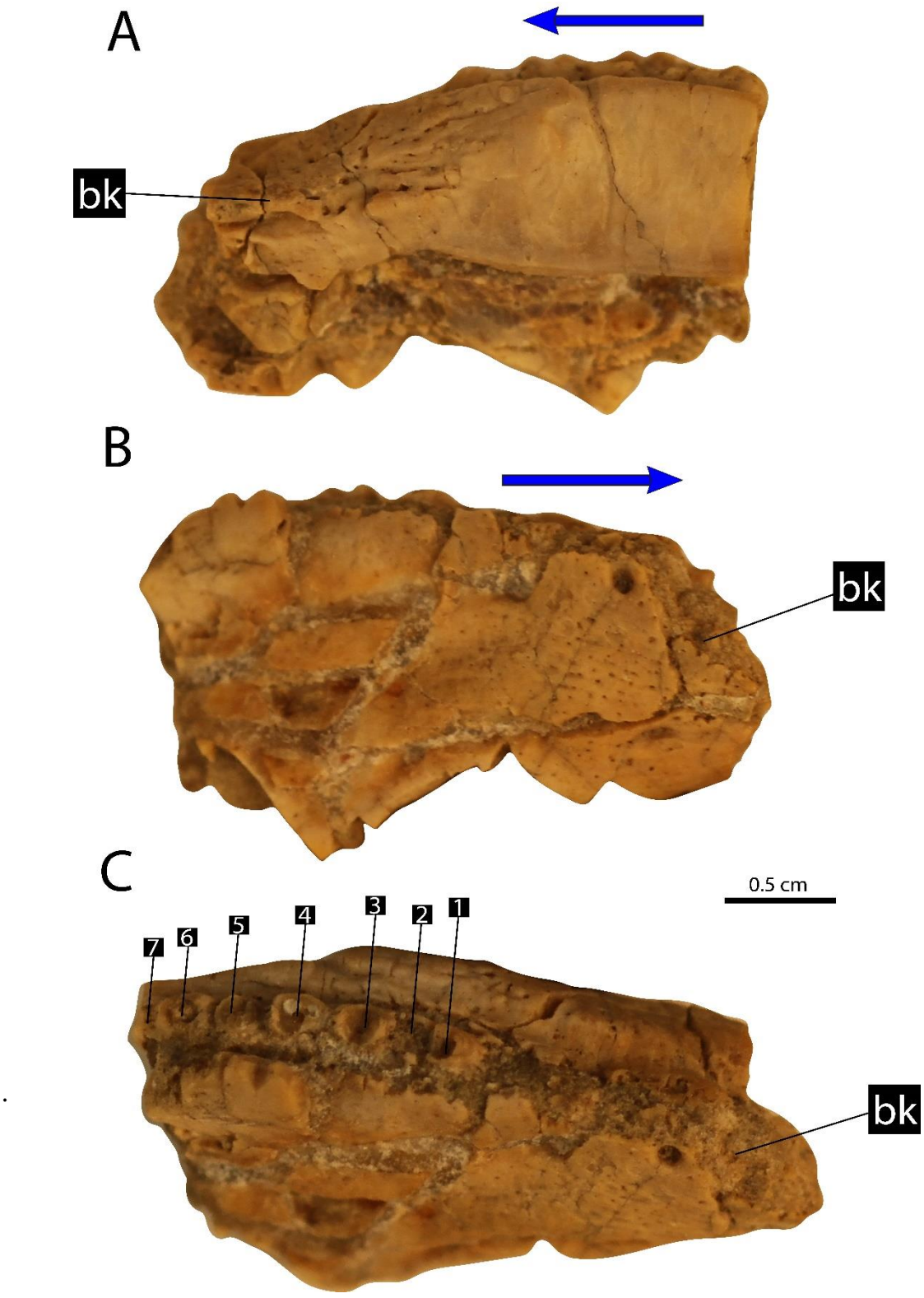

Figure 16. *Asilisaurus kongwe* (NMT RB 1086) right dentary fragment in lingual (A), labial (B), and dorsal (C) views prior to sectioning. Abbreviation: Bk = beak. Symbols as in Fig. 6.

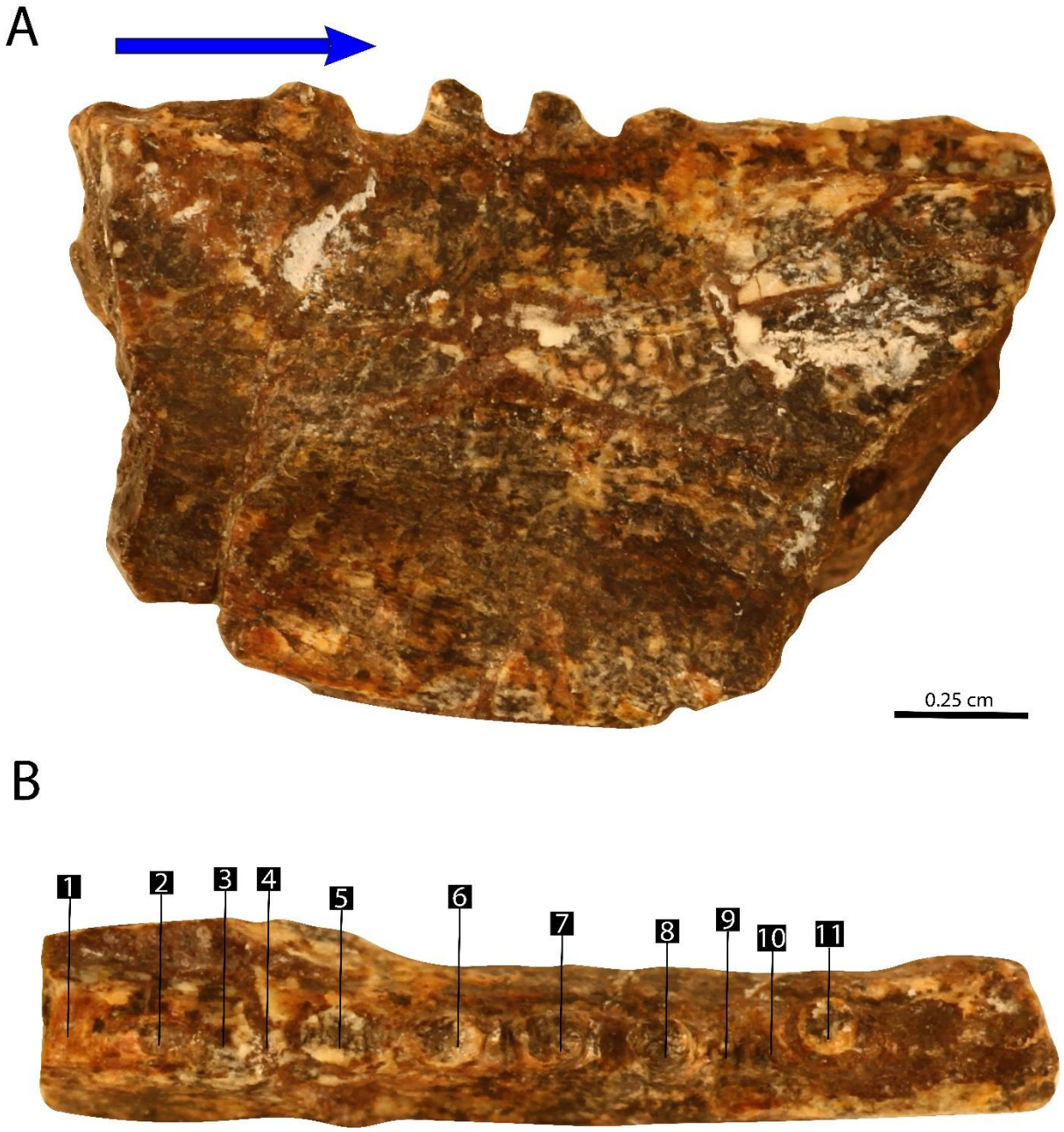

Figure 17. *Asilisaurus kongwe* (NMT RB 1087) lower jaw fragment in a lingual/labial? (A) and dorsal (C) views prior to sectioning. Symbols as in Fig. 6.

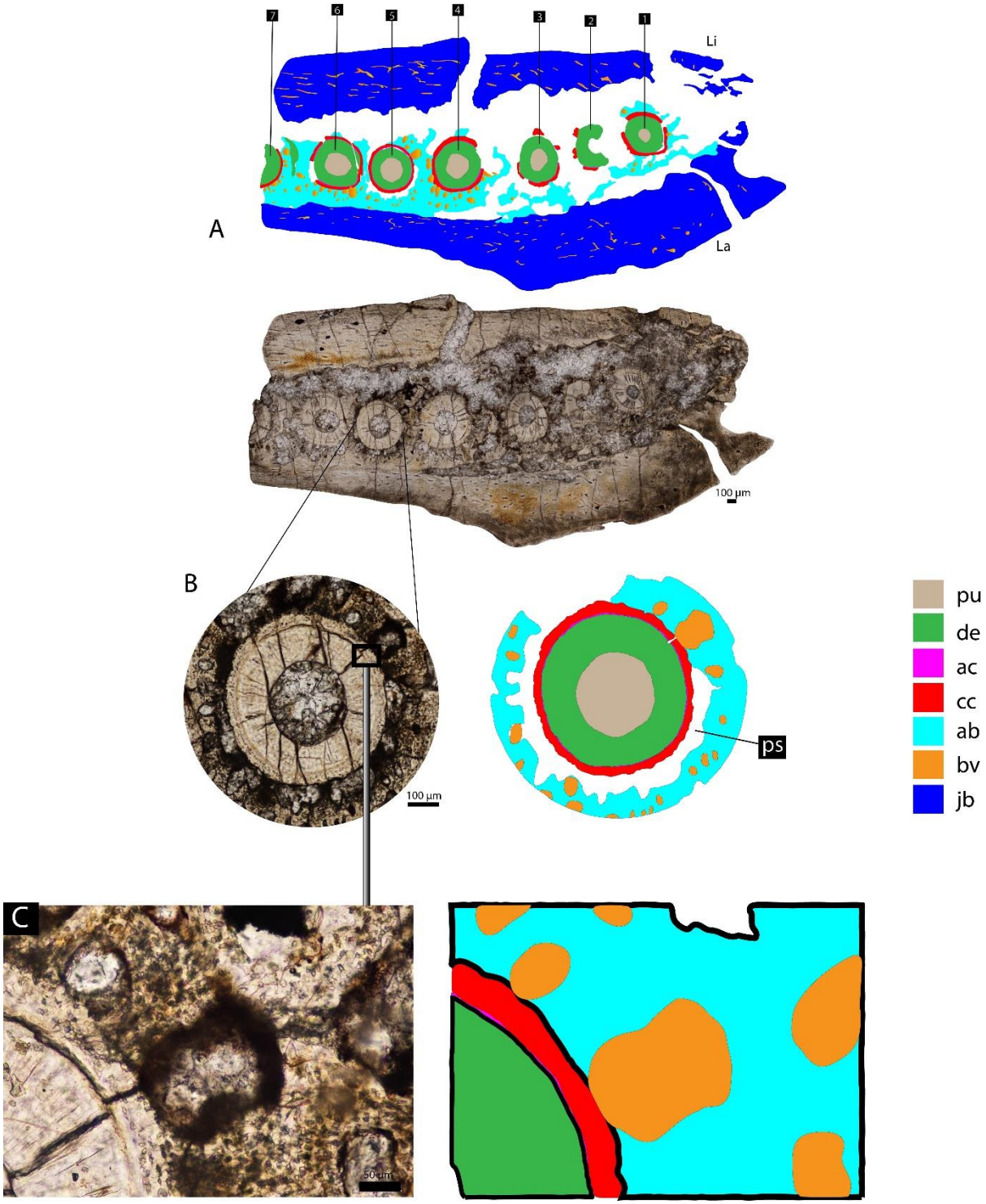

Figure 18. *Asilisaurus kongwe* (NMT RB 1086) right dentary, dental tissues in coronal section at root level, with diagrammatic illustrations. **A.** General view. **B.** Tooth of the fifth alveolus, showing the mineralization stage. **C.** Detail of "B", showing the contact between the alveolar bone and the cellular cementum. Abbreviations: as in Fig. 2

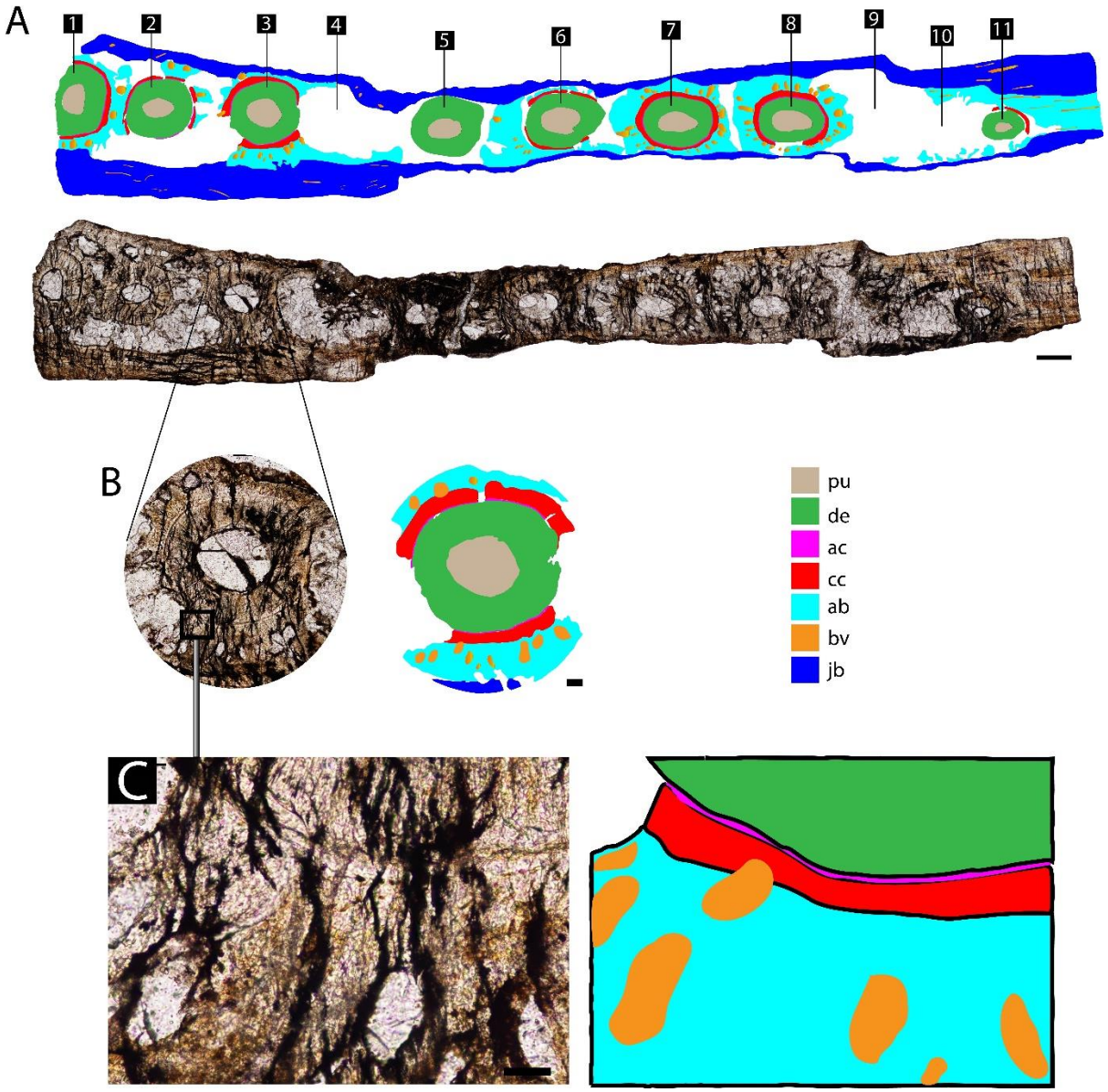

Figure 19. *Asilisaurus kongwe* (NMT RB 1087) dentary, dental tissues in coronal section at root level, with diagrammatic illustrations. **A.** General view. **B.** Tooth of the third alveolus. **C.** Detail of "B", showing the contact between the alveolar bone and the cellular cementum. Abbreviations: as in Fig. 2.

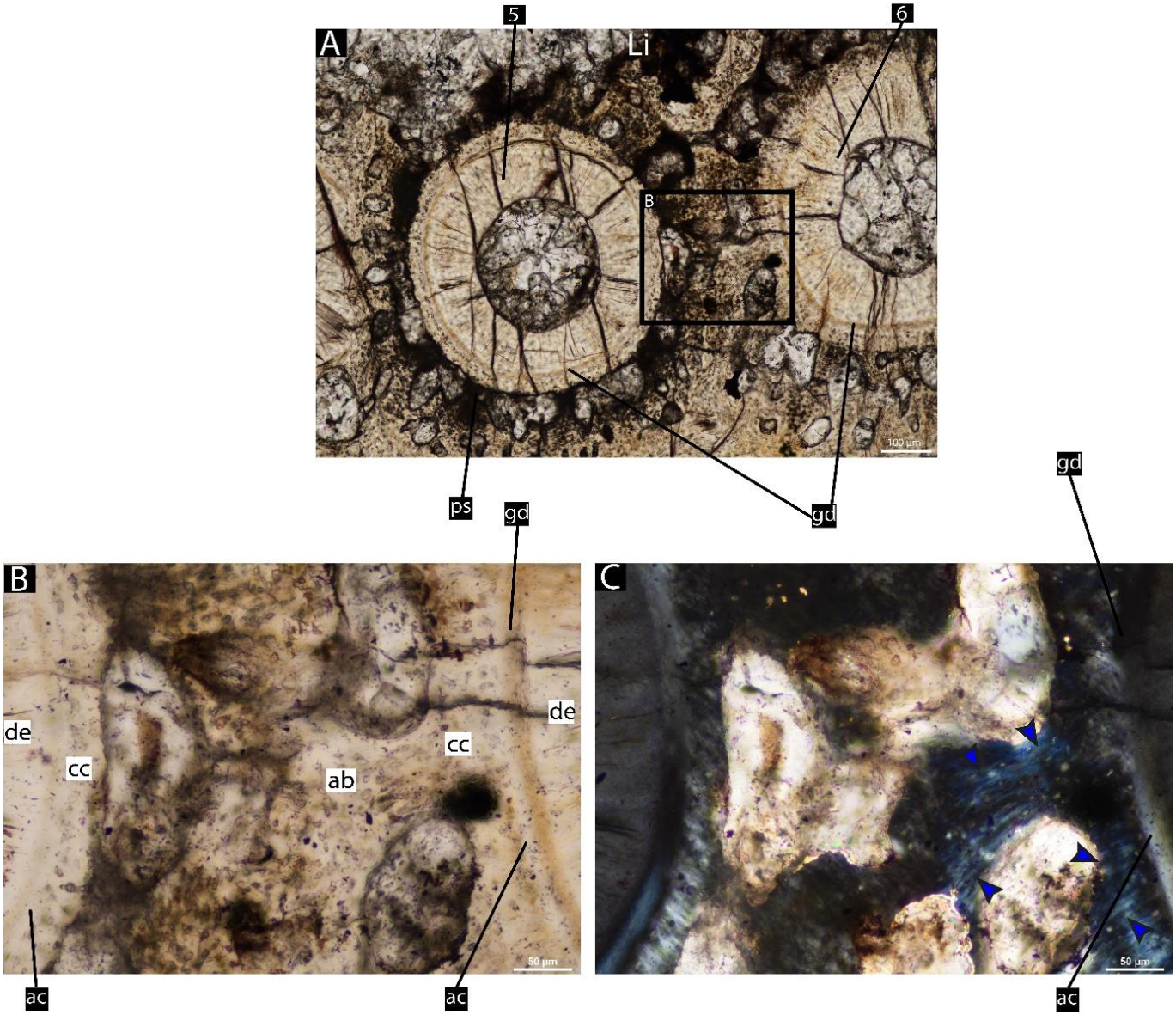

Figure 20. *Asilisaurus kongwe* (NMT RB 1086) dentary, dental tissues in coronal section at root level. **A.** Teeth of the fifth and sixth alveoli, showing the second on the mineralization stage. **B.** Tooth attachment details of an area in "A", showing the contact between the alveolar bone and cellular cementum. **C.** "B" under cross-polarized light, showing Sharpey's fibers across de cellular cementum and alveolar bone layers (blue arrows). Abbreviations: as in Fig. 2, plus gd = granular dentine.

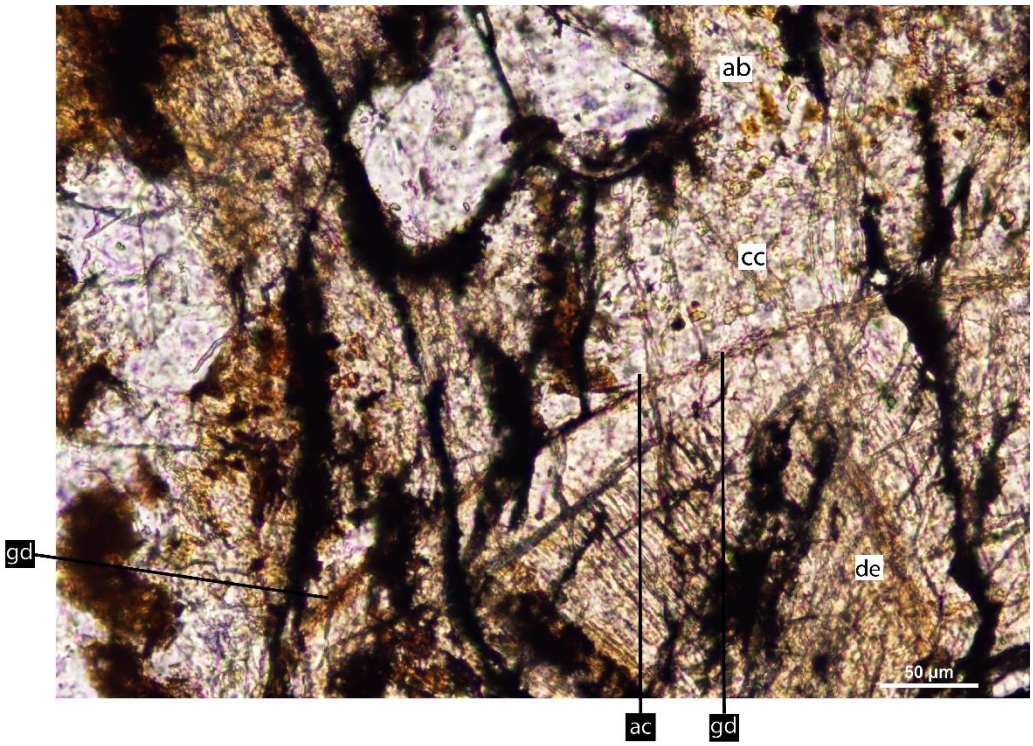

Figure 21. *Asilisaurus kongwe* (NMT RB 1087) dentary, dental tissues in coronal section at root level, showing details of the contact between the alveolar bone and the cellular cementum. Abbreviations: as in Fig. 20.

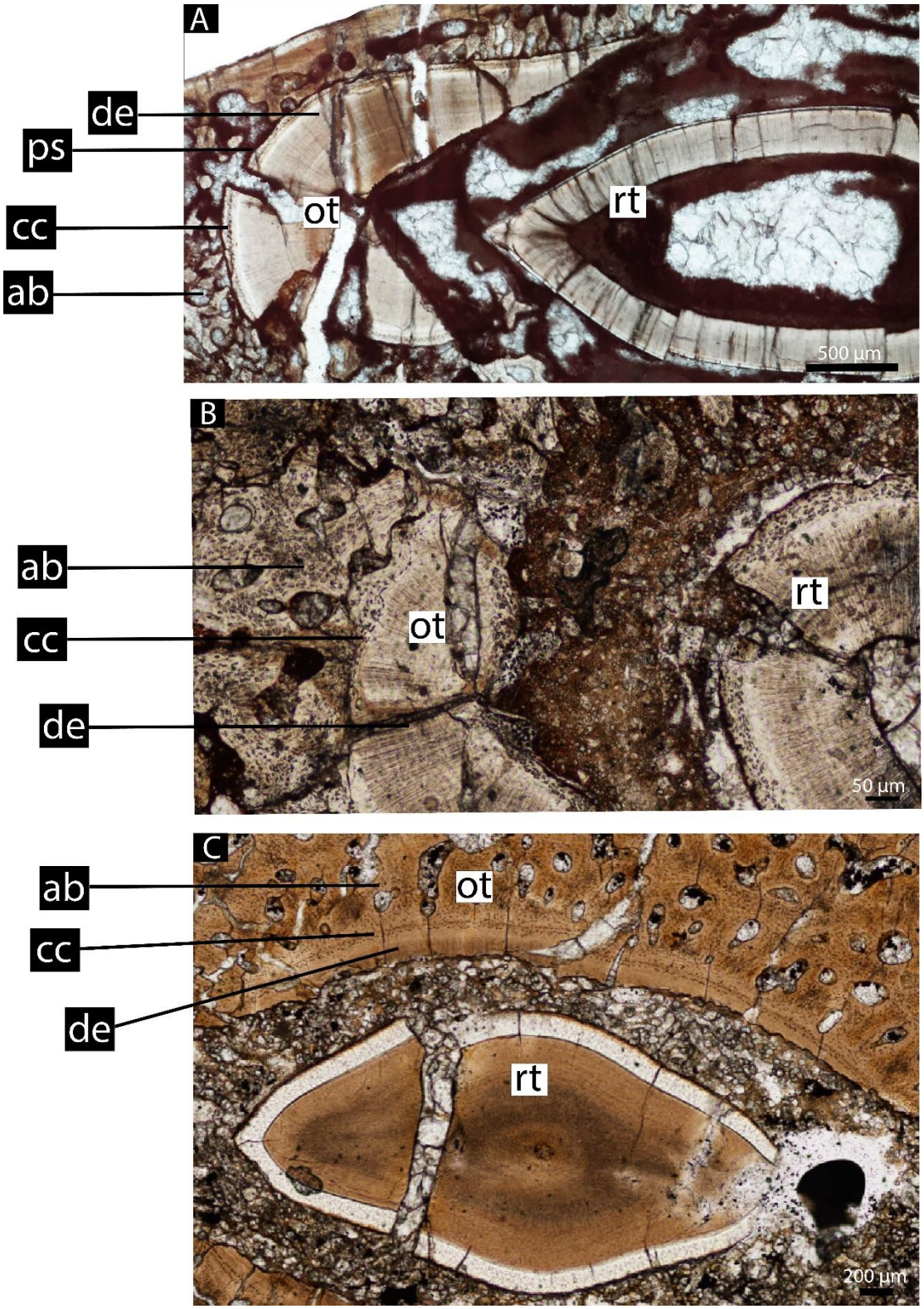

Figure 22. Dental tissues of the dentary of three different taxa with teeth at the same odontogenetic stage; i.e., replacement tooth being surrounded by a piece of the replaced tooth (old tooth generation). **A.** *Coelophysis bauri* (from LeBLanc et al., 2017). **B.** UFSM 1579 (Fig. 10 C, F). **C.** *Eucoelophysis baldwini* (Fig. 5) Abbreviations: as in Fig. 5.

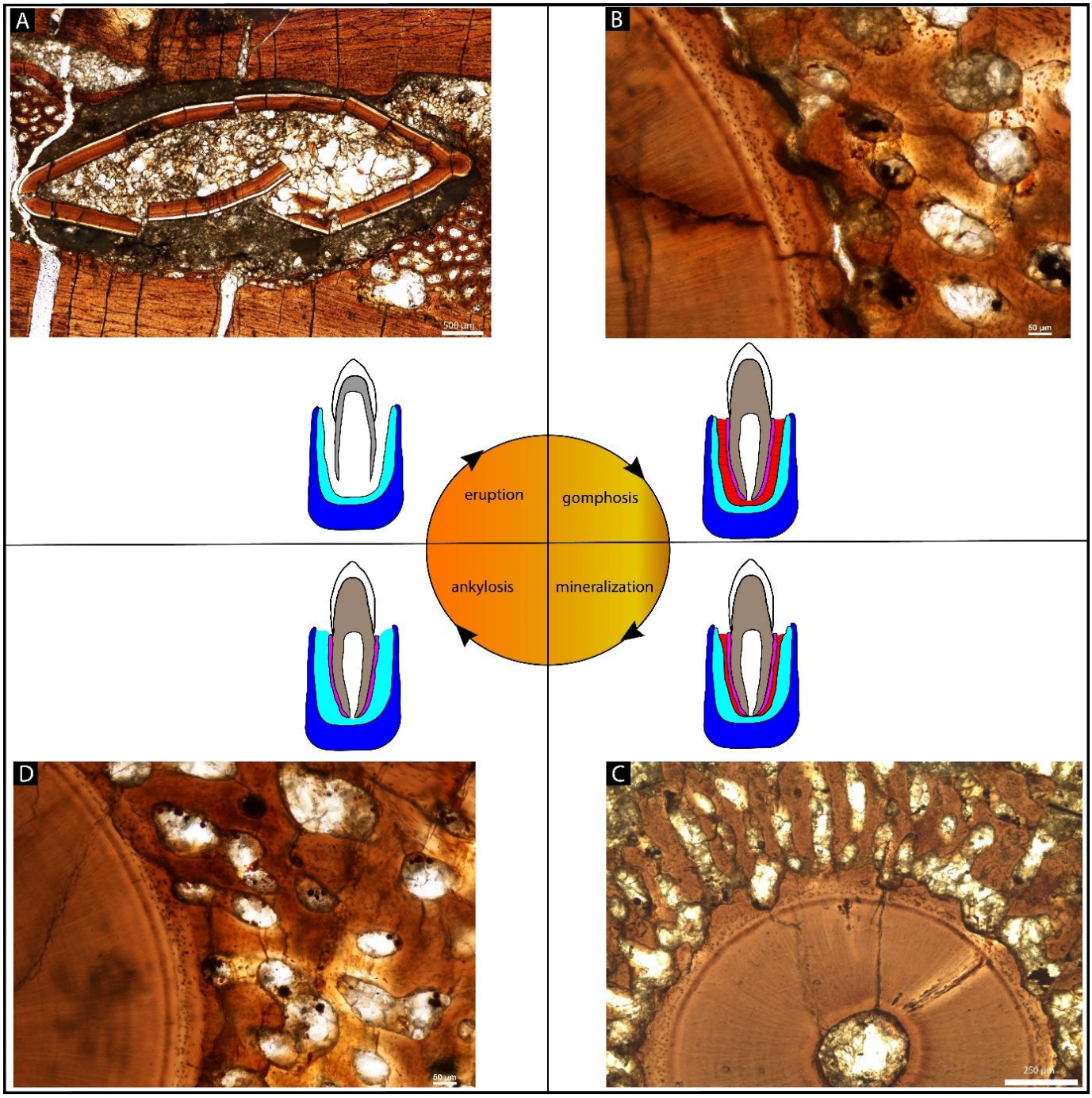

Figure 23. Four tooth ontogeny phases of *Eucoelophysis baldwini* (GR 1072). **A.** Eruption (fifth tooth): before the tooth is fully functional, beginning of tooth crown and early root tissues development. **B.** Gomphosis (first tooth): all three periodontal tissues (cellular cementum, periodontal ligament, and alveolar bone) are fully formed, with no contact between alveolar bone and cellular cementum. **C.** Mineralization (third tooth): alveolar bone calcifies centripetally toward cellular cementum, mineralizing periodontal space in some points. **D.** Ankylosis (third tooth): alveolar bone reaches cellular cementum layer, completely mineralizing periodontal ligament.

SUPPLEMENTARY ONLINE MATERIAL FOR

Tooth attachment in Silesauridae: understanding the ankylo-thecodont ontogenetic phase in the evolution of archosaur thecodonty

Gabriel Mestriner[1]; Aaron LeBlanc[2]; Sterling J. Nesbitt[3]; Júlio C. A. Marsola[4, 1]; Randall B. Irmis[5]; Átila da Rosa[6]; Ana Maria Ribeiro[7]; Jorge Ferigolo[7]; Max Langer[1]

[1]. Departamento de Biologia, Universidade de São Paulo, Avenida Bandeirantes 3900, Ribeirão Preto 14040-190, Brazil.

[2]. Department of Biological Sciences, University of Alberta, Edmonton, AB, Canada

[3]. Department of Geosciences, Virginia Tech, Blacksburg, Virginia, 24061, U.S.A.

[4].Programa de Pós-Graduação em Biologia Animal, Instituto de Biociências, Letras e Ciências Exatas – UNESP Campus de São José do Rio Preto

[5]. Utah Museum of Natural History and Department of Geology & Geophysics, University of Utah, 1390 E. Presidents Circle, Salt Lake City, UT 84112–0050, USA.

[6]. Laboratório de Estratigrafia e Paleobiologia, Departamento de Geociências, Universidade Federal de Santa Maria, Campus, Faixa de Camobi km 09, prédio 17, Santa Maria, Rio Grande do Sul, Brasil CEP 97105-900.

[7]. Museu de Ciências Naturais, Fundação Zoobotânica do rio Grande do Sul, Av. Salvador França, 1427, 90690-000 Porto Alegre, RS, Brasil.

The Anatomical Record

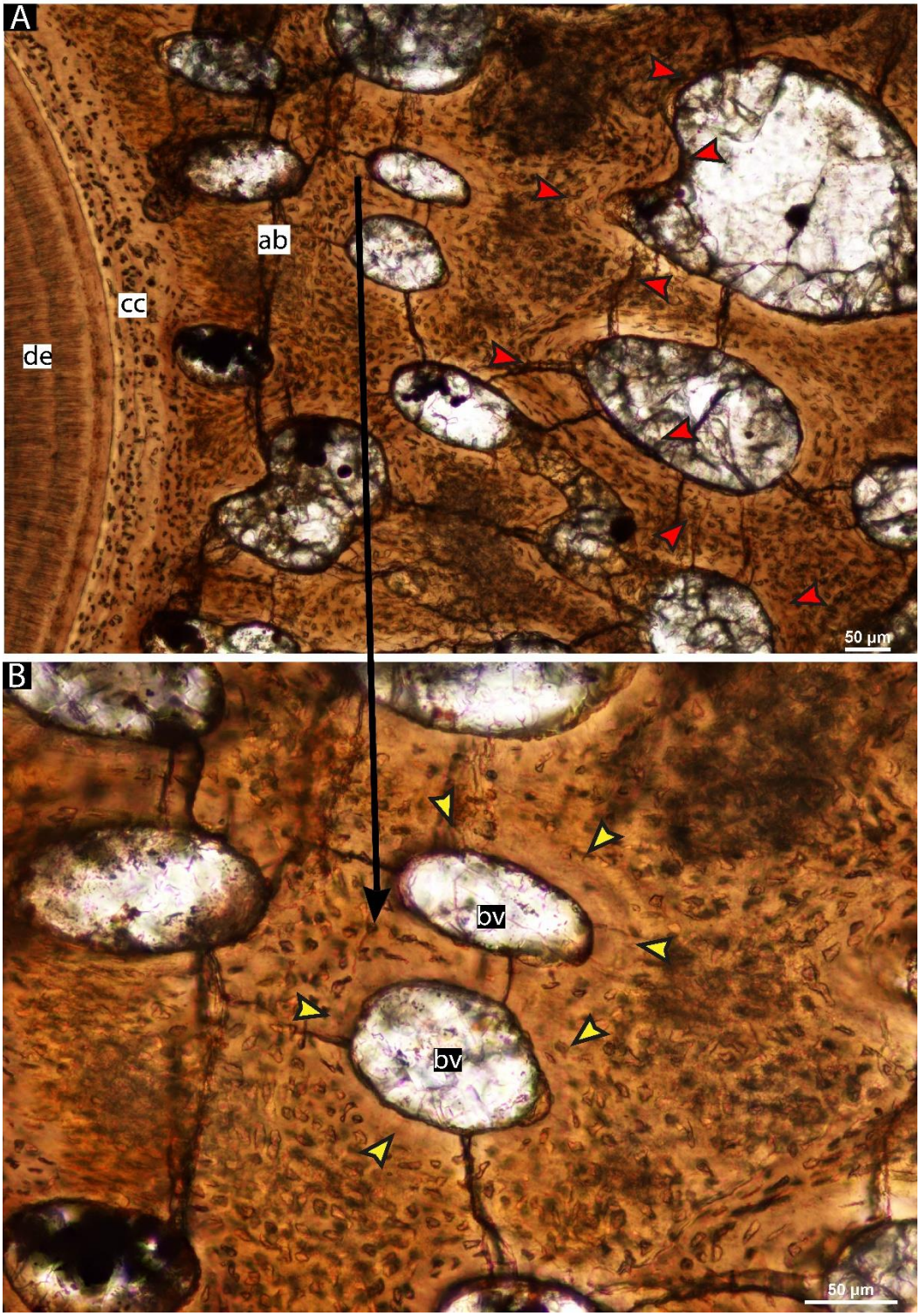

Figure 1. *Eucoelophysis baldwini* (GR 1072) right dentary, dental tissues in coronal section at root level. **A.** Interdental plate. Note the reversal line separating the alveolar bone corresponding to each alveolus. **B.** Zoom of an area of "A" showing lamellar bone tissue around blood vessels. Abbreviations: ab = alveolar bone; bv = blood vessel; cc = cellular cementum; de = dentine. Symbols: red arrow = reversal lines; yellow arrow = lamellar bone tissue.

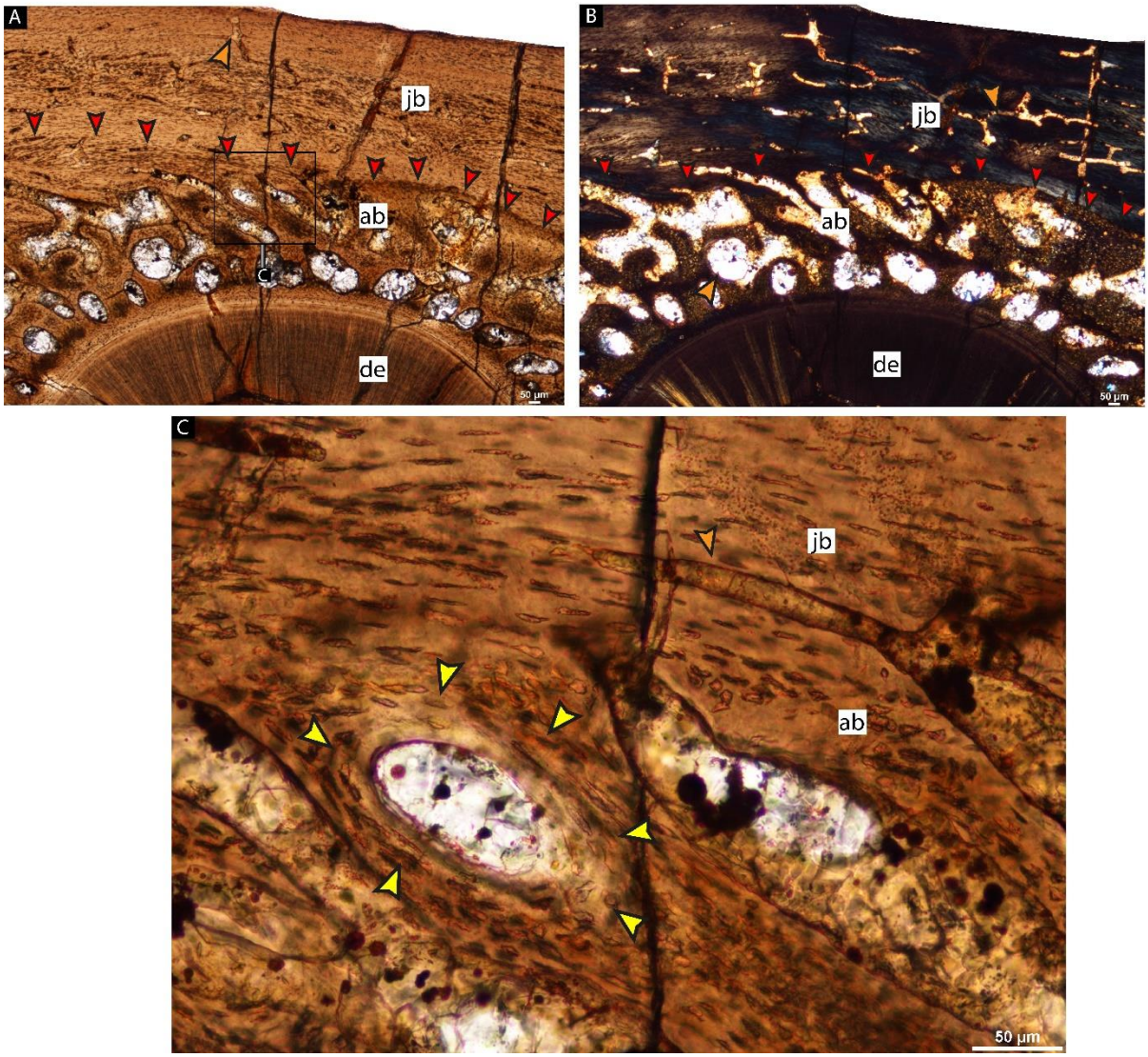

Figure 2. *Eucoelophysis baldwini* (GR 1072) right dentary, dental tissues in coronal section at root level. **A.** Alveolar bone/jaw bone contact, with reversal lines separating both tissues **B.** "A" under cross-polarized light. **C.** An area of "A" zoomed, showing lamellar bone tissue surrounding a blood vessel. Abbreviations and symbols: as in Fig.1, plus orange arrow = blood vessel.

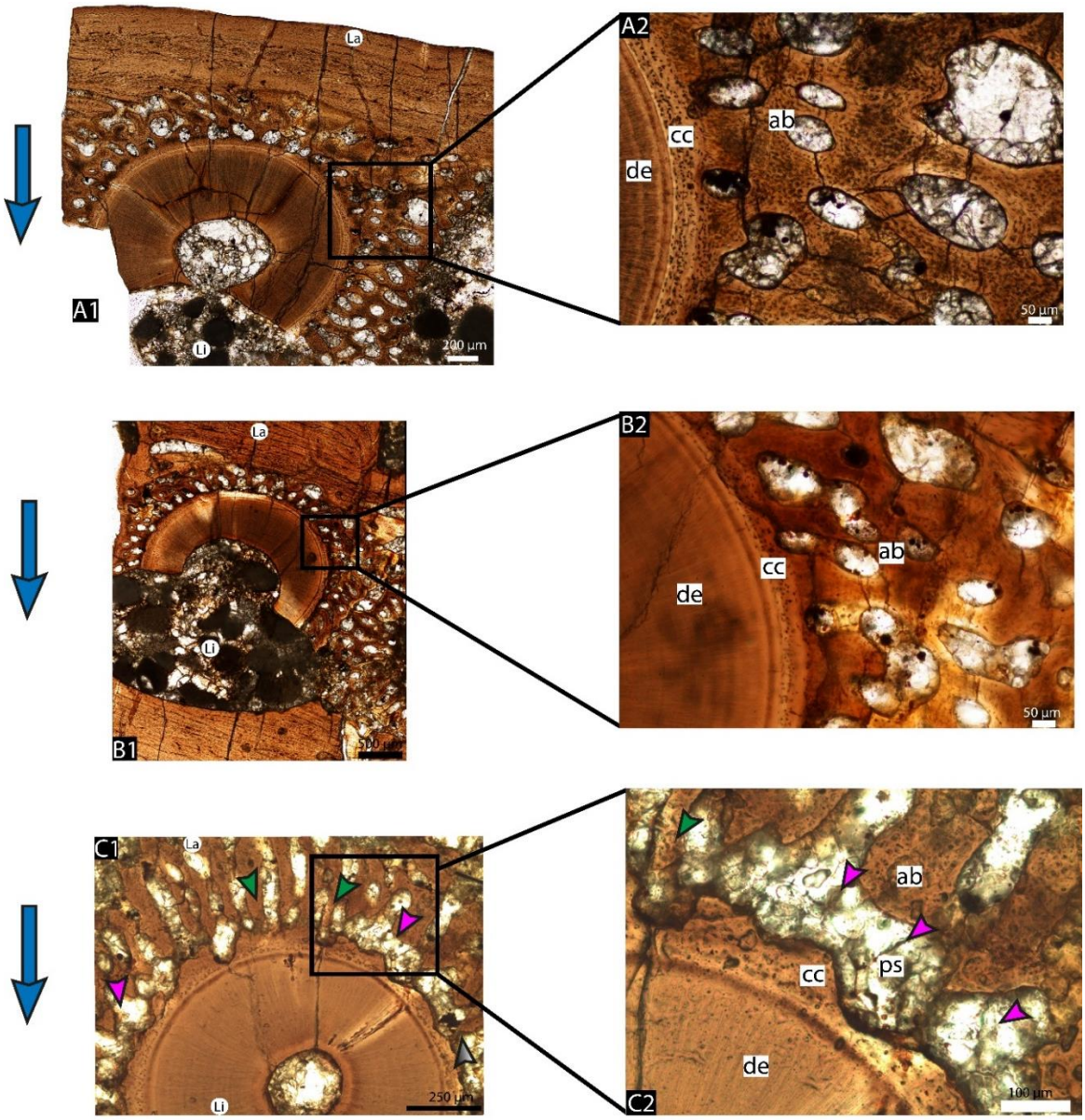

Figure 3. *Eucoelophysis baldwini* (GR 1072) right dentary, dental tissues of the tooth 3 in coronal section at root level, in different levels. **A1**. A more apical cross section showing the ankylosis stage. **A2**. "Detail of "A1", showing the contact between the alveolar bone and the cellular cementum. **B1**. A middle cross section showing the ankylosis. **B2**. "Detail of "B1", showing the contact between the alveolar bone and the cellular cementum. **C1**. A more basal cross section showing the mineralization stage. **C2**. Detail of "C1", showing unmineralized periodontal space in some points and the contact between the alveolar bone and cellular cementum in others. Abbreviations: as in Fig. 1, plus ps = periodontal space. Symbols: blue arrows = the dorso-ventral direction (from the most apical level to the most basal portion); pink arrow = periodontal space; green arrow = contact between the alveolar bone and cellular cementum.

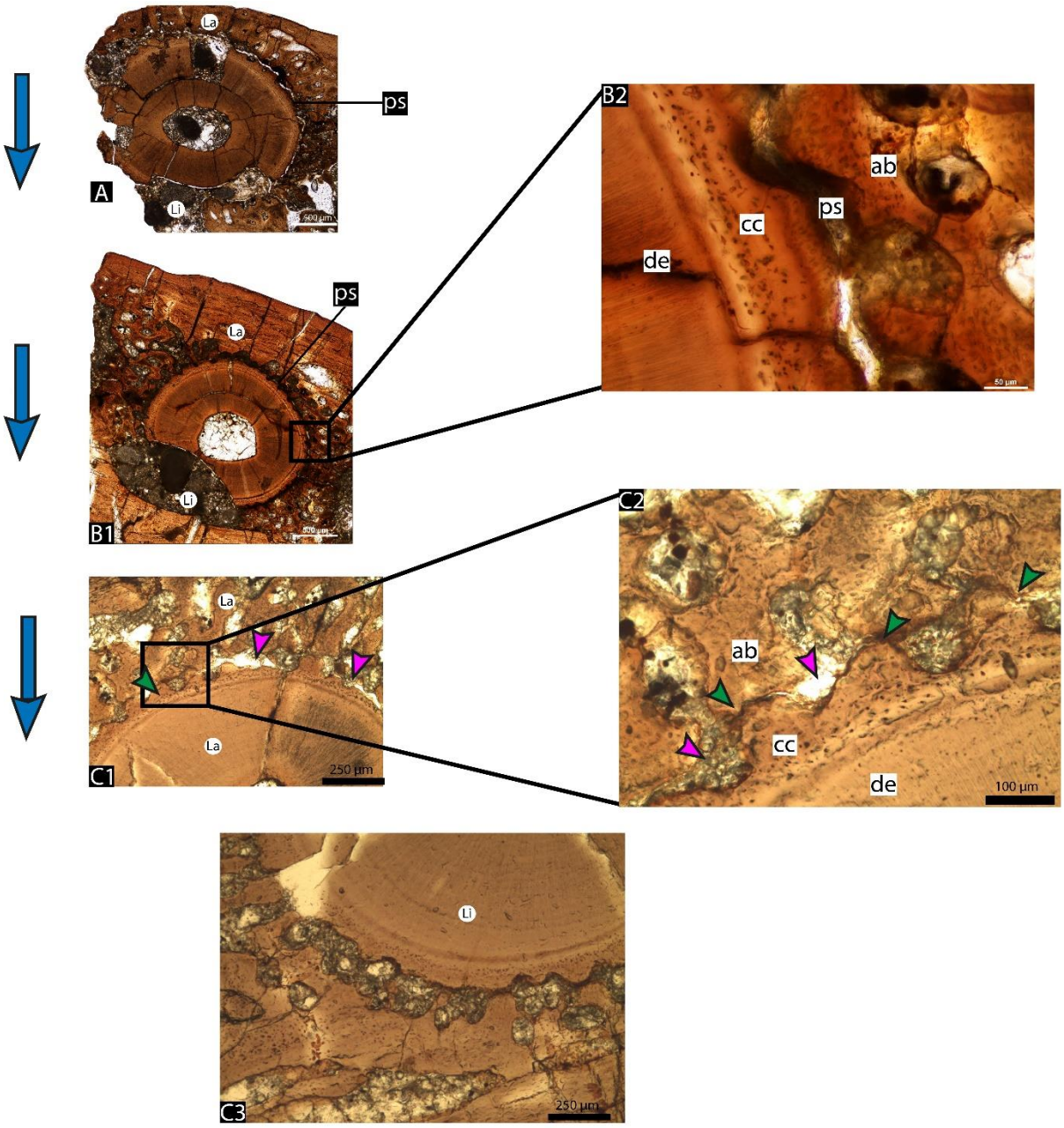

Figure 4. *Eucoelophysis baldwini* (GR 1072) right dentary, dental tissues of the tooth 1 in coronal section at root level, in different levels. **A1.** A more apical cross section showing the gomphosis. **B1.** A middle cross section also showing the gomphosis. **B2.** "Detail of "B1", showing unmineralized periodontal space **C1**. A more basal cross section showing the tooth the mineralization stage. **C2**. Detail of "C1", showing unmineralized periodontal space in some points and the contact between the alveolar bone and the cellular cementum in others. **C3.** Detail of the lingual side of the most basal cross section of the tooth 1, showing that at this level, the tooth is not being resorbed. Abbreviations: as in Fig. 1, plus ps = periodontal space. Symbols: as in Fig. 3.

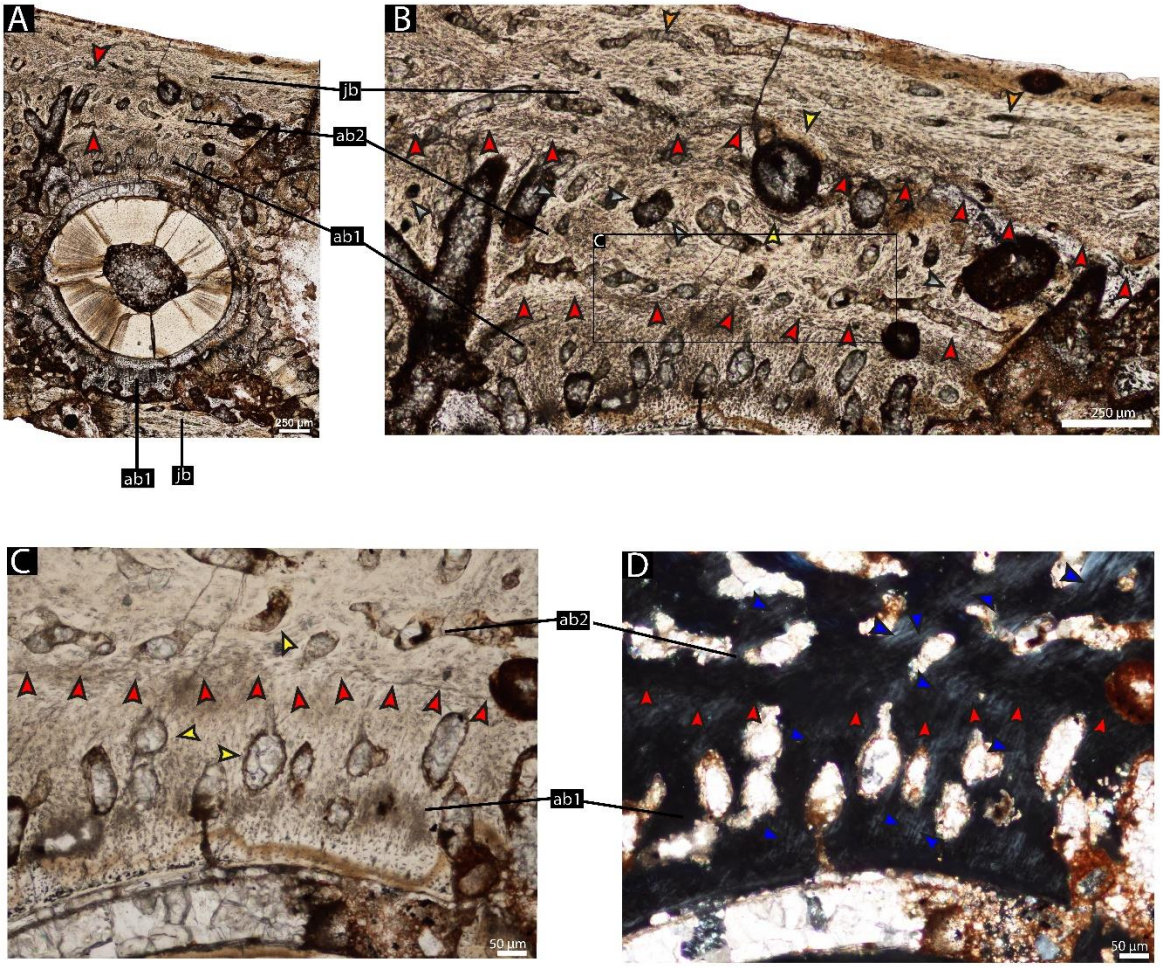

Figure 5. UFSM 1579 left maxilla, dental tissues in coronal section at root level. **A.** Tooth in the alveolus position 3, showing the primary/secondary alveolar bone contact and the secondary alveolar bone/jaw bone contact. **B.** Zoom of "A", showing details of the reversal line separating the layers. **C.** Zoom of an area of "B", focused in the contact between the primary alveolar bone and the secondary alveolar bone. **D.** "C" under cross-polarized light. Note the presence of Sharpey's fibers across both layers of alveolar bone. Abbreviations: ab1 = primary alveolar bone; ab2 = secondary alveolar bone; jb = jaw bone. Symbols: as in Fig. 2, plus: blue arrow = sharpey's fibers.

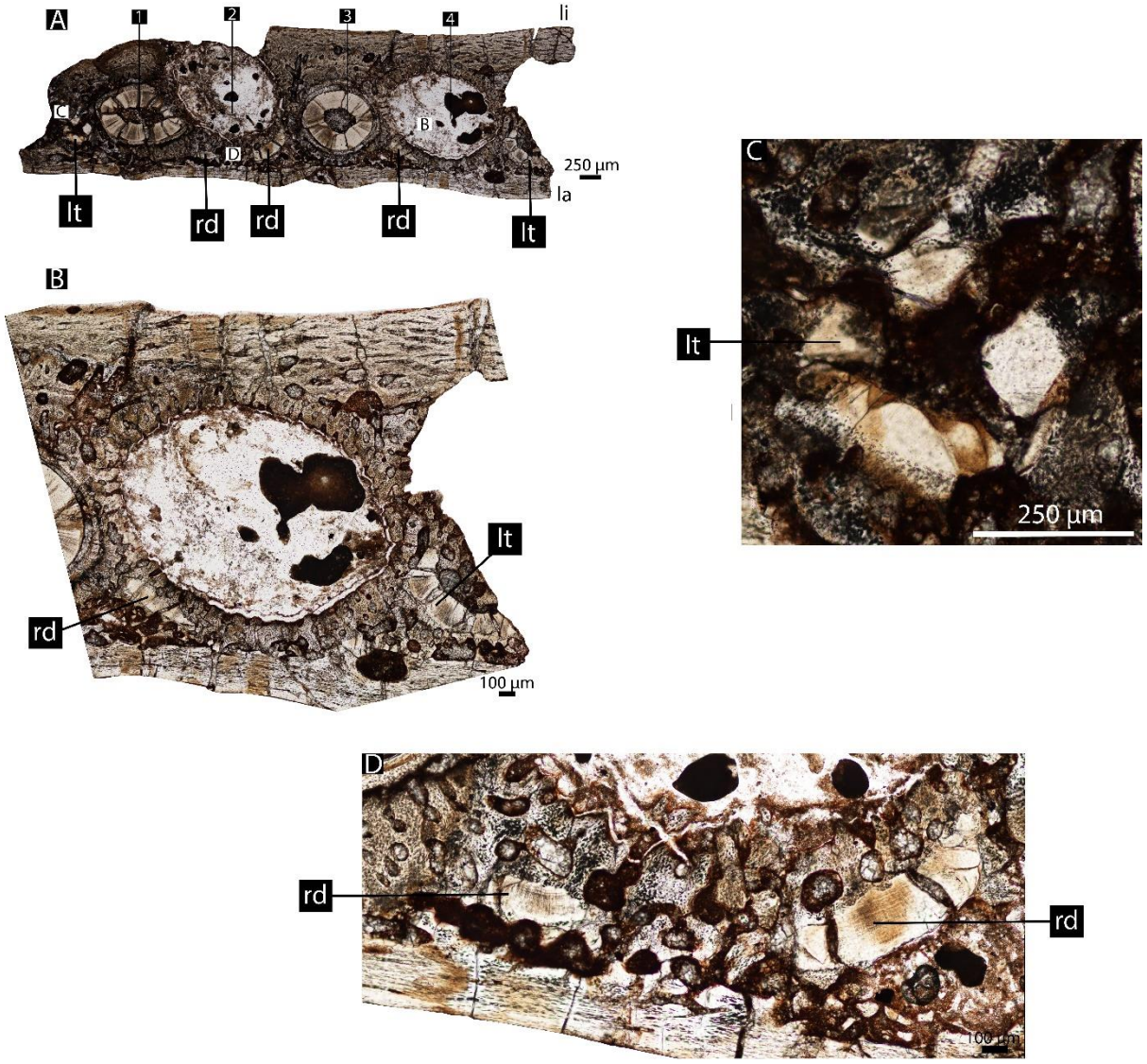

Figure 6. UFSM 1579 left maxilla, dental tissues in coronal section at root level. **A.** General view. **B.** Fourth alveolus zoomed. **C.** An area of "A" zoomed. **D.** An area of "A" zoomed. Abbreviations: la = labial; li = lingual; Lt = little tooth; rd = remnant of dentine.

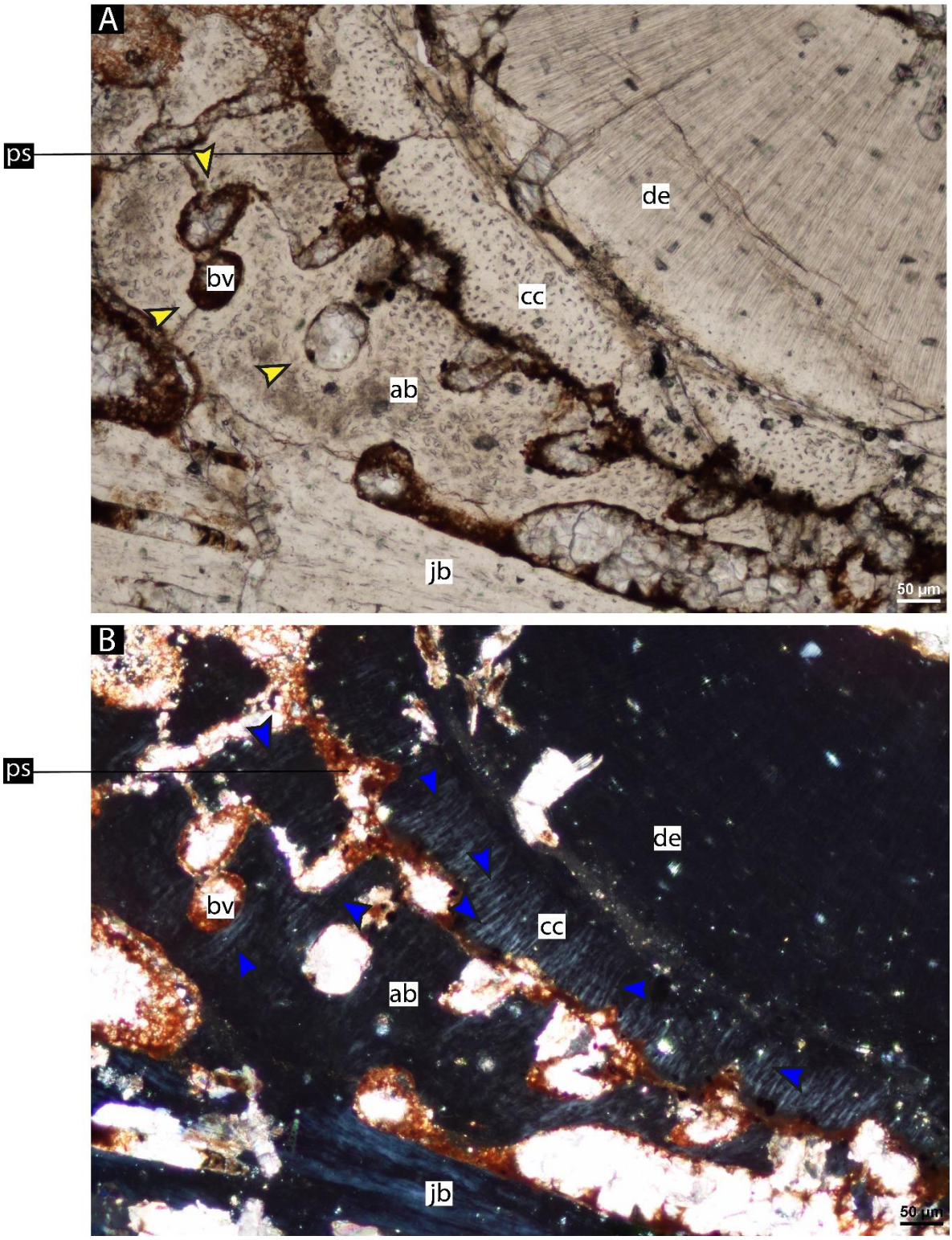

Figure 7. UFSM 1579 right dentary, dental tissues in coronal section at root level. **A.** Tooth attachment details of the fourth tooth. Note the presence of lamellar bone around the blood vessels. **B.** "A" under cross polarized light, showing Sharpey's fibers across de cellular cementum and alveolar bone layers. Abbreviations: as in Fig. 1, plus ps = periodontal space. Symbols: as in Fig. 5.

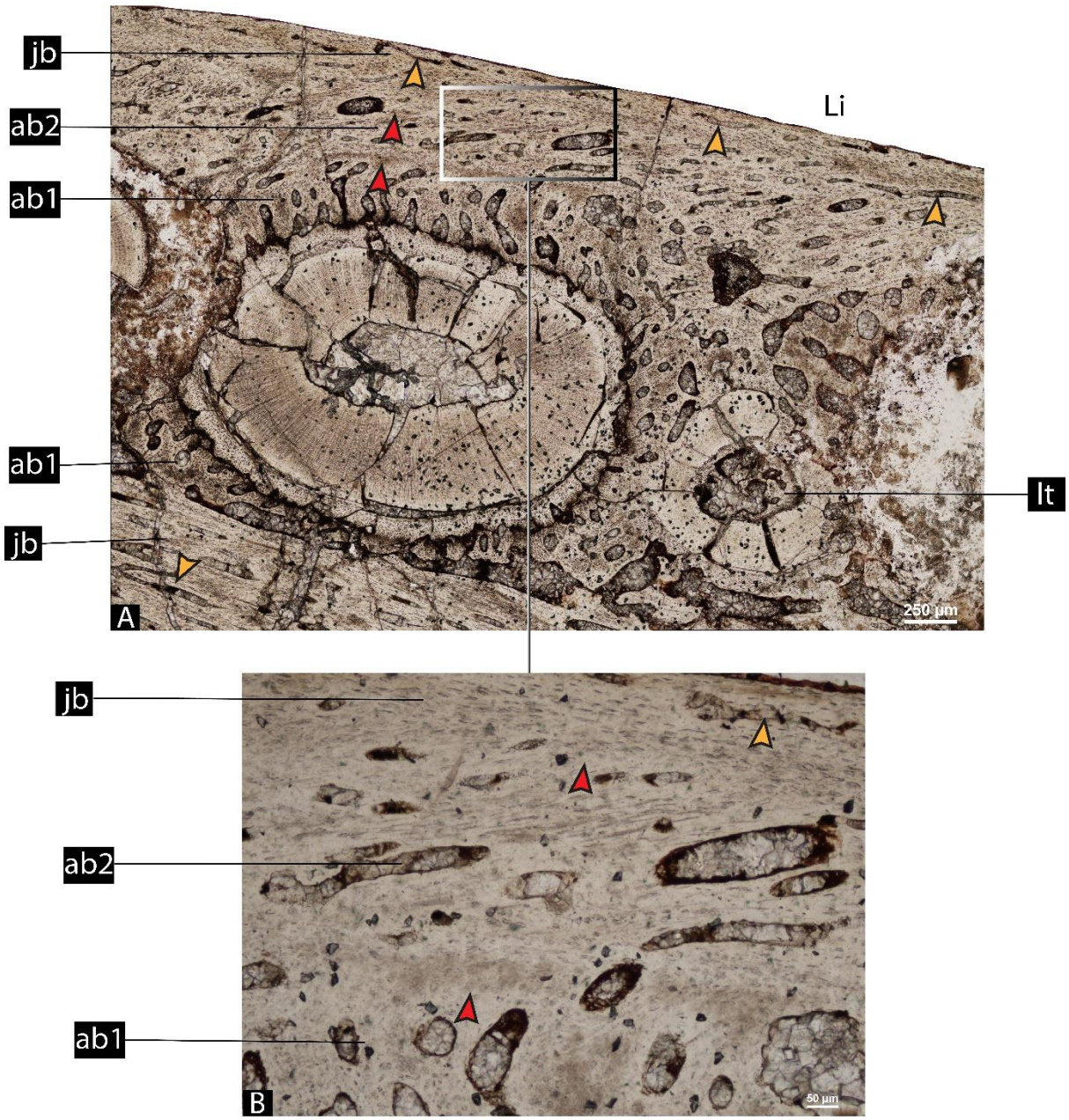

Figure 8. UFSM 1579 right dentary, dental tissues in coronal section at root level. **A.** Tooth in the alveolus position 4, showing reversal lines at the lingual side of the tooth separating the primary alveolar bone from the secondary alveolar bone layer, and separating the secondary alveolar bone layer from the jaw bone as well. Also note the presence of a little tooth posterior to the tooth. **B.** Zoom of an area of "A" where is possible to see details of the reversal line separating the primary alveolar bone from the secondary alveolar bone layer, and the secondary alveolar bone layer from the jaw bone. Abbreviations: ab1 = primary alveolar bone; ab2 = secondary alveolar bone; jb = jaw bone; Li = lingual; lt = little tooth. Symbols: as in Fig. 2.

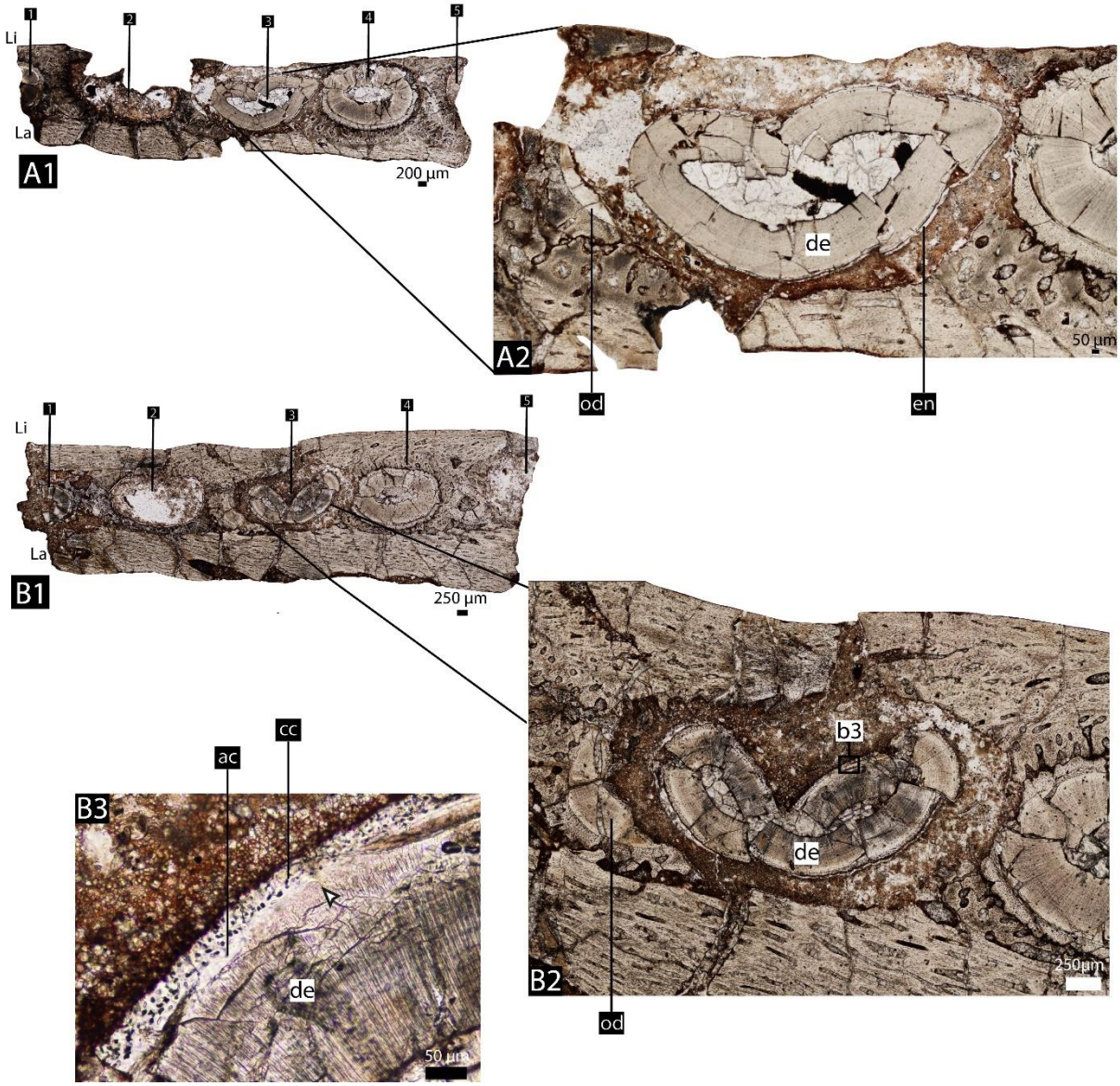

Figure 9. UFSM 1579 right dentary, dental tissues in coronal section at root level. **A1.** General view of a more apical cross section. **A2.** Details of the replacement tooth. Note the presence of enamel surrounding the dentine and a remaint of the replaced tooth (old tooth generation). **B1.** General view of a more basal cross section. **B2.** Details of the same replacement tooth. **B3.** Zoom of an area of "B" showing the tooth attachment tissues of the replacement tooth already present. Abbreviations: ac = acellular cementum; cc = cellular cementum; de = dentine; en = enamel; Li = lingual; ot = old tooth generation. White arrow = granular dentine.

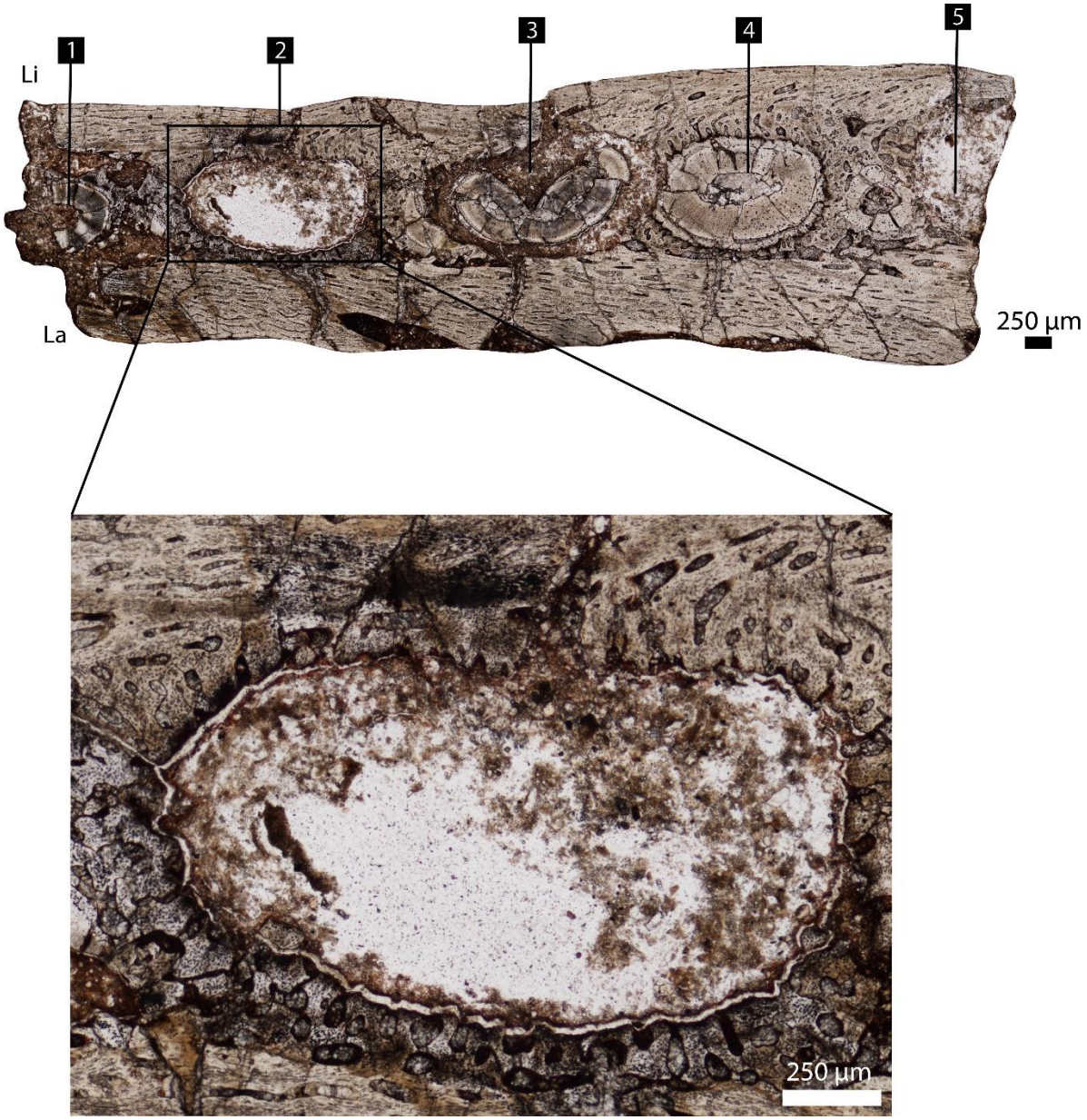

Figure 10. UFSM 1579 right dentary, dental tissues in coronal section at root level with a zoom at the second alveolus. La = labial; li = lingual.

Figure 11. *Asilisaurus kongwe* (NMT RB 1086) dentary, dental tissues in coronal section at root level showing a remnant of dentine belonging to an older tooth generation. Abbreviations: ab = alveolar bone; jb = jaw bone; rd = remnant of dentine. Symbols: Red arrows = reversal line. Numbers indicate the alveoli position.